T H E U N I V E R S I T Y O F A L B E R T A

RELEASE FORM

NAME OF AUTHOR: Thomas Marshall Newton

TITLE OF THESIS: A Study of the Gamma-Ray Angular Distributions from the $^{114,116}Cd$ and $^{146}Nd(n,n'\gamma)$ Reactions

DEGREE FOR WHICH THESIS IS PRESENTED: Master of Science

THE UNIVERSITY OF ALBERTA

A STUDY OF THE GAMMA-RAY ANGULAR DISTRIBUTIONS FROM THE $^{114,116}Cd$ AND $^{146}Nd(n,n'\gamma)$ Reactions

by

© Thomas Marshall Newton

A THESIS

SUBMITTED TO THE FACULTY OF GRADUATE STUDIES AND RESEARCH

IN PARTIAL FULFILMENT OF THE REQUIREMENTS FOR THE DEGREE

OF MASTER OF SCIENCE

DEPARTMENT OF PHYSICS

EDMONTON, ALBERTA

SPRING, 1979

THE UNIVERSITY OF ALBERTA

FACULTY OF GRADUATE STUDIES AND RESEARCH

The undersigned certify that they have read, and recommend to the Faculty of Graduate Studies and Research, for acceptance, a thesis entitled A Study of the Gamma-Ray Angular Distributions from the ^{114,116}Cd and ^{146}Nd(n,n'γ) Reactions

submitted by Thomas Marshall Newton

in partial fulfilment of the requirements of the degree of Master of Science.

ABSTRACT

Energy levels below 2.2 Mev excitation in $^{114,116}Cd$ and ^{146}Nd have been investigated using the $(n,n'\gamma)$ reaction. Gamma-ray angular distributions were measured, and energy levels, spins and gamma-ray multipole mixing ratios deduced. Spin assignments and gamma-ray multipole mixing ratios were determined by comparing the experimental data to the predictions of the Statistical Compound Nuclear Model.

For ^{114}Cd, levels and their spins have been confirmed at 1134(0^+), 1210(2^+), 1283(4^+), 1365(2^+), 1733(4^+) and 1843(2^+) keV. New spin assignments have been made for the levels at 1861(3^+) and 2049(3^+). The state at 1959 keV has been shown to be consistent with a spin assignment of 3^-.

For ^{116}Cd, levels and their spins have been confirmed at 1213(2^+), 1220(4^+) and 1381(0^+) keV. New spin assignments have been made for the levels at 1644(2^+) and 1917(3^+) keV. The state at 1923 keV has been shown to be consistent with a spin-parity assignment of 3^-.

For ^{146}Nd, levels and their spins have been confirmed at 1043(4^+) and 1189(3^-) keV. A new spin assignment has been made for the level at 1376(1) keV. A state at 1787 keV has been proposed.

ACKNOWLEDGEMENTS

I would like to express my appreciation to my supervisors, Drs. D. M. Sheppard and W. J. McDonald, for their assistance and encouragement.

I am most grateful to Dr. P. W. Green for his help throughout all parts of this work. His enlightening discussions were a boon to me.

I am very grateful to Dr. J. M. Davidson, who was the driving force behind the initial stages of this work.

I would like to express my appreciation to Dr. H. S. Sherif for many interesting and helpful discussions.

I would also like to thank all of my colleagues who helped with the data collection: H. R. Hooper, S. W. L. (Seven Fingers of Death) Leung, and Dr. H. S. Seifken.

A special thanks goes to R. Sloboda for his talent in making collision theory come to life.

Also, I am grateful to "Jock" Elliot for his help and the use of his Van de Graaff. Thanks also goes to the entire technical and secretarial staff at NRC. I am indebted to Dr. W. K. Dawson for the use of his "golf clubs" and Dr. G. C. Neilson for his brilliant over the shoulder caddying ability.

The financial assistance of the University of Alberta is gratefully acknowledged.

To my parents, July, 1978

TABLE OF CONTENTS

LIST OF TABLES

LIST OF FIGURES

CHAPTER 1

INTRODUCTION

Several years ago Scharff, Goldhaber and Weneser (Sc55) pointed out that certain regularities exhibited by the first and second excited states of even-even medium weight nuclei could be described by a collective vibrational model of the nucleus. The ^{114,116}Cd isotopes is in the transition zone of vibrational to rotational nuclei. If these nuclei are well described by the collective vibrational model, their low-lying energy level scheme should have the spin sequence 0^+, 2^+, $(0^+2^+4^+)$, 3^-, $(0^+2^+3^+4^+6^+)$. At the time of the Scharff, Goldhaber and Weneser paper, however, little information about the levels above the second excited state was known. As a result, several experimental techniques have been used in the past few years to study these nuclei.

For ^{114,116}Cd, the results from (p,p') and (α,α') experiments (St68, Ko69, Ha63, Co65, De72) established the level scheme up to 3.0 MeV. The one and two phonon states of these isotopes were identified through the measurement of the charged particle angular distributions. The γ-ray decay scheme of the ^{114}Cd levels was first established through the ^{113}Cd(n,γ) work of Groshev *et al.* (Gr62). Bäcklin *et al.* (Ba66) repeated the neutron capture

work while also measuring the internal conversion spectrum. This resulted in a spin-parity assignment of 0^+ to the ^{114}Cd level at 1306 keV excitation. As ^{115}Cd has a lifetime of only 53 hours, no neutron capture work has been done to investigate the γ-ray decay scheme of ^{116}Cd.

Angular distribution measurements of γ-rays from the ^{114,116}Cd(p,p'γ) [Mi69, De73], ^{114,116}Cd(α,α'γ) [Mi69, Ha63], and ^{114,116}Cd(^{16}O,^{16}O'γ) [Mc65] reactions corroborated the earlier spin-parity assignments for the one and two phonon states. In addition, single particle states [1306 (0^+) and 1365 (2^+) keV in ^{114}Cd and 1280 (2^+) keV in ^{116}Cd] were observed at approximately the same energies as the two phonon states.

Investigations of the excitation functions of γ-rays following the ^{114,116}Cd(n,n'γ) reactions (Gi74) revealed further features of the level structures of these two nuclei. The states at approximately 1860 keV in ^{114}Cd and 1920 keV in ^{116}Cd were found to be a doublet and triplet respectively. Also, the previously proposed levels at 1644 keV excitation in ^{114}Cd and 1733 keV excitation in ^{116}Cd were confirmed. The previous 3^- assignments to the ^{114,116}Cd states near 1960 keV and 1920 keV were, however, disputed. Their results, together with the results from previous works are listed in Tables I and II.

The earliest works resulting in spin-parity assignments for the excited states of ^{146}Nd involved Coulomb

Table I. A Summary of the Results of Previous Investigations of ^{114}Cd.

Level Energy (keV)	(p,p') [a]	(n,γ) [b]	$(n,n'\gamma)$ [d]
558	2^+	2^+	2
1134	0^+	0^+	0
1210	2^+	2^+	2
1283	4^+	4^+	4
1306		0^+ [c]	0
1365	2^+	2^+	2
1733		4^+	4
1843		2	1
1861			(0)
1865		(0^+)	1
1959	3^-	(2^-)	(1)
2049		1^+	(4)

a) Ref. Ko69

b) Ref. Gr68

c) Ref. Ba65

d) Ref. Gi74

Table II. A Summary of the Results of Previous Investigations of ^{116}Cd.

Level Energy (keV)	$(n,n'\gamma)$ [a] Excitation	Previous Results
513	2	2^{+} [d]
1213	2	2 [b]
1220	4	4 [b]
1283	0	2 [c]
1381	0	0 [d]
1644	(2,3)	
1917	(0)	
1923		$3^{-}(\simeq 1920)$ [d]
1930		
2120		$(3^{-},5^{-})$ $(\simeq 2115)$ [d]

a) Ref. Gi74

b) Ref. De73

c) Ref. De72

d) See Table 1 of Ref. De72 and references therein.

excitation (Ha62, Be67, Bu67). Spin-parities of 2^+, 4^+, and 3^- were assigned to the levels at 453, 1043 and 1189 keV excitation on the basis of γ-ray angular distribution measurements. The γ-ray decay scheme for higher levels was established through (n,γ) work, as compiled by Groshev *et al.* (Gr68). The level scheme of ^{146}Nd was also investigated by the (d,d') work of Christensen *et al.* (Ch70) and the (t,p) work of Chapman *et al.* (Ch72). In those works, spin-parity assignments made on the basis of the angular distributions of the outgoing charged particles were consistent with those of earlier works. These results are listed in Table III.

Although many experiments have been carried out in an effort to investigate the structures of these three nuclei, a few uncertainties remain. The situation regarding spin assignments for the levels above 1300 keV excitation, and the multipole mixing ratios for the γ-ray decays is still uncertain.

Neutron scattering reactions represent a valuable technique for such investigations since the absence of a Coulomb barrier allows the levels of interest to be excited close to threshold, thereby eliminating complications due to cascade feeding. In this work γ-ray angular distributions from the ^{114,116}Cd(n,n'γ) reactions have been studied, providing further information about the spins and parities of the low-lying levels.

Table III. A Summary of the Results of Previous Investigations of ^{146}Nd.

Level Energy (keV)	$(^{16}O,^{16}O'\gamma)$ [a]	(d,d') [b]	(t,p) [c]
454	2^+	2^+	(2^+)
1043	4^+	4^+	
1189	3^-	3^-	
1377		$(1^-) \simeq 1373$	
1471		$(2^+) \simeq 1468$	
1515		(5^-)	
1680			$0^+ \simeq 1693$
1740		4^+	

a) Ref. Bu67

b) Ref. Ch70

c) Ref. Ch72

Multipole mixing ratios for the reported transitions were also deduced. This technique has the following additional advantages:

1. The three phonon states near 1900 keV can be investigated, which was not possible using Coulomb excitation (5-9).
2. There is no necessity of detecting all of the γ-decay modes from a given level.
3. The systematic error associated with γ-ray excitation functions due to the angular dependence of the γ-ray is avoided.
4. The sensitivity of the angular distribution calculations to the optical model parameters is much smaller than it is for excitation functions.

These last three points were a source of error in the $(n,n'\gamma)$ excitation work of Gill *et al.*

CHAPTER 2

THEORY

In the compound nucleus picture of a nuclear reaction, the energy carried into the target by the projectile is shared with all of the nucleons shortly after contact. Once the energy is shared, a large number of energy exchanges are required for one, or a system of particles to acquire enough energy so that it can be emitted by the compound nucleus. Because of the energy sharing, the disintegration of the compound system does not depend on the method by which it has been formed. The mode of decay does, however, depend on the constants of motion: energy, angular momentum, and parity. As a result, it is possible to separate a nuclear reaction into two separate events; one, the formation of the compound nucleus, and two, the disintegration of the system into the products of the reaction. This is the basis of the compound nucleus model.

To determine the cross section for the formation of the compound nucleus, all possible two-body interactions between the projectile and the nucleons of the target should be considered. However, this approach is much too complicated except for the simplest reactions. Consequently, a model in which the many body problem is reduced to that of two structureless bodies acting through an average potential

is adopted. This approximation is known as the optical model.

In the optical model, the incident particle is influenced by a potential of the form

$$U(r) = V_c(r) - V_o f(r,R_o,a_o) - i(W - 4a_i W_D \frac{\partial}{\partial r}) f(r,R_k,a_i) + 2(V_{so} + iW_{so}) \frac{1}{r} \frac{\partial}{\partial r} f(r,R_{so},a_{so}) \vec{\sigma} \cdot \vec{L} \qquad (1)$$

where V_o is the real well depth, W and W_D are the volume and surface imaginary well depths, and V_{so} and W_{so} are the real and imaginary parts of the spin-orbit well depths. The functions $f(r,R_x,a_x)$ have the form

$$f(r,R_x,a_x) = (1 + \exp(\frac{r-R_x}{a_x}))^{-1} \qquad (2)$$

where R_x and a_x are the corresponding radii and well diffuseness parameters. $V_c(r)$ is the Coulomb potential which is taken to be that due to a charge of Ze uniformly distributed over a sphere of radius R_c. The real and imaginary potentials account for refraction and absorption of the incident particle whereas the spin-orbit potential term takes into account their polarization.

Once formed, the compound nucleus can decay to a final state through what is called a reaction channel. The final states of the nuclear reaction can be linked to the initial state by a collision matrix U. The collision matrix is composed of elements which relate the

amplitudes of the various partial waves of the reaction channels to the partial waves of the incident channel. This can easily be seen if one considers the total wave function of the nuclear reaction Ψ. It can be written as

$$\Psi = \sum_c v_c^{-1/2} (A_c I_c - B_c O_v) \psi_c \qquad (3)$$

where the summation is over all allowed channels. The parameters I_c and O_c represent the incoming and outgoing waves, having amplitudes of A_c and B_c respectively. The factor $v_c^{-1/2}$ is used as $v_c^{-1/2} I_c$ corresponds to the incoming flux. ψ_c is the channel wave function, which contains the quantum description of the channel. For a single entrance channel c, the relationship between the amplitude coefficients is given by

$$B_{c'} = U_{c'c} A_c \qquad (4)$$

where $U_{c'c}$ is an element of the collision matrix. U, although it is expressed through the asymptotic behavior of the wave functions, does, however, contain the inherent physics of the collision interaction. By hypothesis, each matrix element can be decomposed into a weakly energy dependent $\bar{U}_{c'c}$ and a rapidly fluctuating term $\tilde{U}_{c'c}$ that averages to zero over a large enough energy interval. That is,

$$U_{c'c} = \bar{U}_{c'c} + \tilde{U}_{c'c}$$

where $\bar{U}_{c'c} = \langle U_{c'c} \rangle = \text{const}$

and $\tilde{U}_{c'c} \neq \text{const but } \langle \tilde{U}_{c'c} \rangle = 0$

Using this notation, the formation of the compound nucleus through channel c can be written

$$\begin{aligned} \bar{\sigma}_c &= \frac{\pi}{k_c^2} \sum_{c'} \langle |\tilde{U}_{c'c}|^2 \rangle \\ &= \frac{\pi}{k_c^2} (1 - \sum_{c'} |U_{c'c}|^2) \\ &= \frac{\pi}{k_c^2} T_c \end{aligned} \tag{5}$$

where T_c is the transmission coefficient for channel c, and k_c is the wave number for the relative motion of the particles in channel c. The transmission coefficient expresses the flux associated with the compound nucleus component of the reaction. The total cross section for a reaction channel c' is the product of the factor $\bar{\sigma}_c$ that expresses the cross-section for formation through channel c and a branching ratio for the decay of the compound system into exit channel c'. Through time reversal invariance and conservation of flux, the problem of the decay of the compound nucleus through channel c' can be related to the situation where the compound nucleus is formed through channel c'. That is,

$$k_c^2 \, \bar{\sigma}_{cc'} = k_{c'}^2 \, \bar{\sigma}_{c'c} \tag{6}$$

Use of the principle of detailed balance allows the average cross section to be expressed as a function of the transmission coefficients.

$$\bar{\sigma}_{c'c} = \frac{\pi}{k_c^2} \frac{T_c T_{c'}}{\sum_{c''} T_{c''}} \tag{7}$$

where the summation is over all possible exit channels c''. The labels c, c', and c'' characterize the quantum description of the respective channels, and thus contain a prescription of the various angular momenta and parities involved. When this dependence is explicitly taken into account, one finds (Vo73) that when a compound nucleus is formed through channel c, the average cross section for the decay through channel c' is

$$\bar{\sigma}_{c'c} = \frac{\pi}{k_c^2} \sum_{J\pi} \frac{2J+1}{(2I+1)(2i+1)} \{ \sum_{j\ell} T_{\ell j}(c) \} \times \{ \sum_{j'\ell'} T_{\ell'j'}(c') \} / \{ \sum_{c''} \sum_{j''\ell''} T_{\ell''j''}(c'') \} \tag{8}$$

where I and i are the respective spins of the target and projectile. This is the basis of the statistical theory of nuclear reactions.

The exit channels under consideration in this work are those that involve gamma radiation. For the gamma decay from the initial state $|J_1 M_1\rangle$ of the residual nucleus to the final state $|J_2 M_2\rangle$, the probability amplitude is given by (Ro67)

$$A^{q}_{M_1M_2}(\vec{k}) = \left\{ \frac{k}{2\pi h} \right\}^{1/2} \sum_{LM\pi} q^{\pi} \langle J_1M_1 | T^{<\pi>}_{LM} | J_2M_2 \rangle \; D^{L}_{Mq}(R) \quad (9)$$

where $T^{<\pi>}_{LM}$ represents the interaction in terms of the electromagnetic operators; $<\pi = 0>$ denoting the electric operators and $<\pi = 1>$ the magnetic operators. The quantity q takes on the values of ± 1 for right-handed and left-handed circular polarization respectively. The rotation matrix $D^{L}_{Mq}(R)$ describes a rotation that projects the propogation vector $\vec{k}$ onto the z-axis. When the spin orientation of the final state is not observed, the transition probability $P^{q}_{M_1}(k)$ for a gamma emission from the initial state is an incoherent sum over the possible values of M_2. The total transition probability for photons with the momentum $\vec{k}$ is then obtained by weighting each $P^{q}_{M_1}(k)$ with the relative population parameters $w(M_1)$ of the substate M_1.

$$\begin{aligned} p^{q}(k) &= \sum_{M_1} w(M_1) \; P^{q}_{M_1}(k) \\ &= \sum_{M_1} w(M_1) \sum_{M_2} |A^{q}_{M_1M_2}(\vec{k})|^2 \end{aligned} \quad (10)$$

The angular distribution for the emission of photons from the state J_1 to the state J_2 is obtained by an expansion of (10)

$$w(\theta) = p^{q}(k) = \frac{k}{2\pi h} \sum_{LL'K} \sum_{\pi\pi'} B_K(J_1) \; R^{q}_{K}(LL'J_1J_2) \; P_K(\cos\theta) \; x$$

$$q^{\pi+\pi'} \; x \; \frac{\langle J_1 || T^{<\pi>}_{L} || J_2 \rangle}{(2L+1)^{1/2}} \; \frac{\langle J_1 || T^{<\pi>}_{L'} || J_2 \rangle^{*}}{(2L'+1)^{1/2}} \quad (11)$$

where

$$B_K(J_1) = \sum_{M_1} w(M_1)(-1)^{J_1-M_1} (2J_1+1)^{1/2} (J_1 J_1 M_1 -M_1 | KO),$$

and

$$R_k^q(LL'J_1J_2) = (-1)^{q+J_1-J_2+L'-L-K} (2J_1+1)^{1/2} (2L+1)^{1/2}$$
$$x(2L'+1)^{1/2} (LL'q-q|KO) W(J_1J_1L';KJ_2).$$

The $P_k(\cos\theta)$ are the Legendre Polynomials. As the B_k coefficients are functions of the population parameters, they describe the effects due to nuclear alignment. The $R_k^q(LL'J_1J_2)$ coefficients depend only on the quantities that characterize the gamma transition. The reduced matrix elements, divided by factors of $(2L+1)^{1/2}$, are proportional to the square root of the partial gamma width due to the multipole transition (π,L). That is;

$$\Gamma_{\pi L} = \frac{4k}{h^2} |\langle J_1||T_L^{<\pi>}||J_2\rangle|^2/(2L+1) \qquad (12)$$

The reduced matrix elements contain the nuclear information. Experimentally, the sum of their square moduli can be obtained by lifetime information $(1/\tau = (1/h) \sum_{\pi L} \Gamma_{\pi L})$. Consequently, for angular distribution measurements, one is interested in determining only the ratios of the reduced matrix elements. To further this end, the multipole mixing ratios are introduced.

$$\delta_L^{<\pi>} = \frac{\langle J_1||T_L^{<\pi>}||J_2\rangle/(2L+1)^{1/2}}{\langle J_1||T_{\bar{L}}^{<\bar{\pi}>}||J_2\rangle/(2\bar{L}+1)^{1/2}} \qquad (13)$$

where $\bar{L}\ \bar{\pi}$ represents the lowest possible multipolarity involved in the gamma decay. Using the mixing ratio, and summing over q, as polarization was not observed in this work, Eq. (11) becomes

$$W(\theta) = \sum_{LL'K\pi\pi'} \{B_K(J_1)\ R_K(LL'J_1J_2)\ P_K(\cos\theta)\}$$
$$x\ \{\ 1+(-1)^{L+L'+\pi+\pi'-K}\ \}\ \delta_L^{<\pi>}\ \delta_{L'}^{<\pi'>} \Big/ \sum_{L\pi} |\delta_L^{<\pi>}|^2 \qquad (14)$$

The summation is over only K=even terms when the nucleus is in an aligned condition [$w(M_1) = w(-M_1)$]; therefore $B_{K=odd} = 0$). This same condition holds true even when the initial state is not aligned, if J_1 and J_2 have definite parity. As electromagnetic operators conserve parity, there are selection rules for the type of radiation that can occur for a gamma transition between states of parity Π_1 and Π_2. They are

$(\Pi_1)(\Pi_2)$	Type of radiation	
	π=0 (electric)	π=1 (magnetic)
1	even	odd
-1	odd	even

Hence, all terms in Eq. (14) have $L+L'+\pi+\pi'$=even, and the factor $(1 + (-1)^{L+L'+\pi+\pi'-K})$ are zero if K is odd, and 2 if K is even. If only two multipoles contribute to the transition, the theoretical angular distribution becomes

$$W(\theta) = \sum_{K=\text{even}} B_K(J_1)\, P_K(\cos(\theta) \times \{R_K(\bar{L}\bar{L}J_1J_2) + 2\delta R_K(\bar{L}LJ_1J_2) + \delta^2 R_K(LLJ_1J_2)\}/(1+\delta^2) \quad (15)$$

This equation is valid when the two states have definite spins and parities and when circular polarization is not observed. An experimental angular distribution from an aligned nucleus has the form

$$W_{exp}(\theta) = \sum_{K=\text{even}} a_K\, P_K(\cos\theta) \quad (16)$$

To facilitate the comparison of the experimental data to the theoretical angular distribution, Green *et al.* (Gr72) have rewritten Eq. (15) in the form of Eq. (16) with the transformation

$$a_K' = \alpha_K + \beta_K \sin 2(\rho - \rho_{K0})$$

$$\text{where} \quad \rho = \arctan\delta \quad (17)$$

The coefficients α_K, β_K, and ρ_{KO} are functions of the B_K and R_K coefficients.

In principle, if the B_K coefficients are known, it is possible to extract the multipole mixing ratio δ from an experimental γ-ray angular distribution. The mixing ratios are defined in terms of the reduced matrix elements, which in turn are functions of the matrix elements $\langle J_1 M_1 | T_{LM}^{<\pi>} | J_2 M_2 \rangle$. Therefore, by deducing the value of δ, information about the initial and final state nuclear wave functions can be obtained.

CHAPTER 3

EXPERIMENTAL PROCEDURE

3.1 Data Analysis

The $(n,n'\gamma)$ reaction is useful in nuclear physics as it enables one to investigate the structure of a heavy target nucleus at a low energy. Reactions initiated with charged particles are not feasible at these low energies because of the large Coulomb barrier. Ideally, a neutron scattering experiment would utilize a small sample situated at a large distance from the neutron production source. This would guarantee that all reactions in the scatter would be initiated by monoenergetic neutrons colinear with the beam axis. However, this is not feasible because of the difficulty in obtaining a high flux neutron beam. To reduce the time involved in obtaining a reasonable amount of data, the large sample method (Di72 and references therein) was formulated (see fig. 1). It required a large amount of scatterer material (approximately one mole) being placed at a large distance away from the neutron production source. This had the effect of maximizing the number of reactions while restricting the energy spread of the neutron beam to an acceptable level. For most samples however, the target cost is prohibitively high. This resulted in the

Figure 1.

Two types of large sample experiments: a) The pulsed beam time-of-flight method as used by Cranberg and Levin (Cr56). The scatterer used was a cylinder of approximately one mole of ^{56}Fe. b) The ring shaped scatterer method as used by Nishimura *et al*. (Ni65). The scatterer was composed of 346.6 gm of ^{56}Fe.

a)

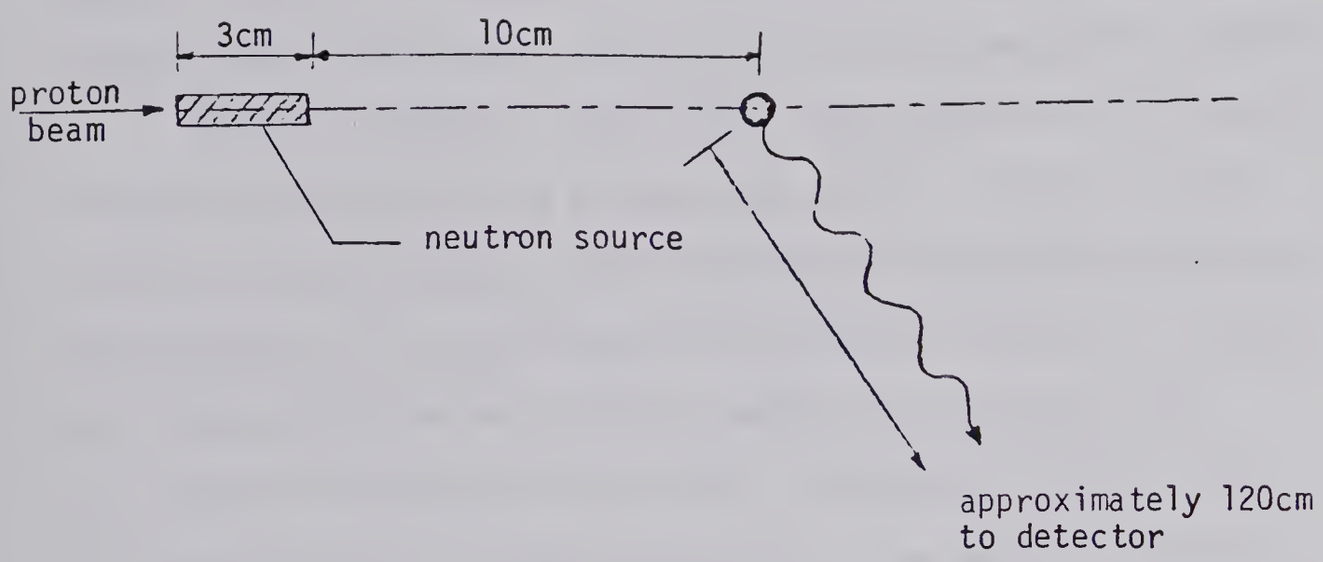
3cm
10cm
proton
beam
neutron source
approximately 120cm
to detector

b)

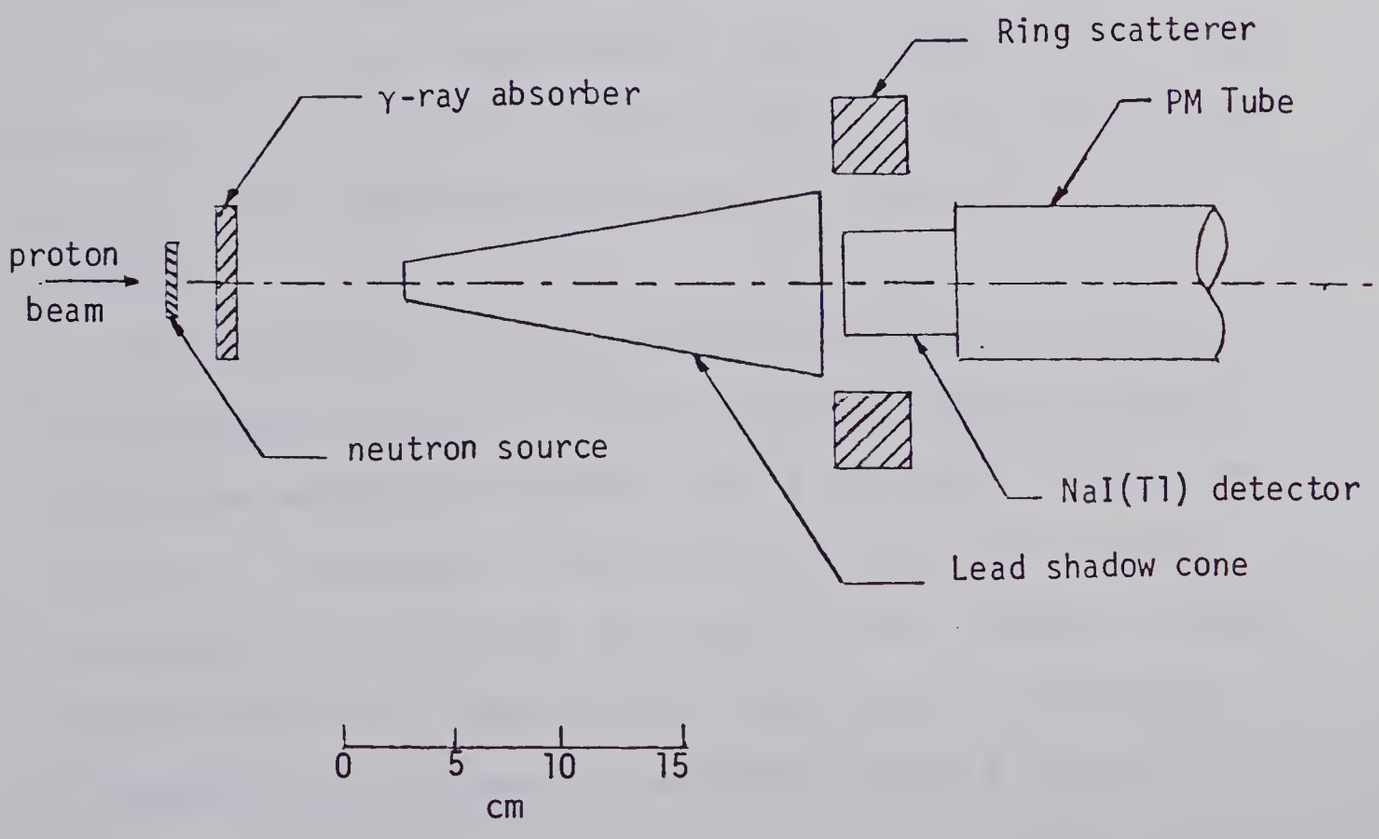
Ring scatterer
γ-ray absorber
PM Tube
proton
beam
neutron source
NaI(Tl) detector
Lead shadow cone
0
5
10
15
cm

development of the small sample method (E171) for studying nuclei. The small sample technique relied on a close scatterer-neutron source geometry. Although this geometry gave rise to a high neutron flux, there was a large spread in neutron energy, corresponding to the differing angles with which the neutrons left the production source.

Another inherent difficulty involved with the close geometry method is the distorting effect of the finite sizes of the scatterer and the neutron production source. Corrections to γ-ray angular distribution data to account for these effects can only be made if the spins and parities of the states involved, and the multipole mixing ratio of the γ decay are known. As this is usually the information that is desired, the distorting effects must be folded into the theoretical angular distributions. The distorted theoretical angular distributions can then be compared to the experimental data to deduce the γ-ray multipole mixing ratio, and the initial state's spin and parity. This method was developed by Davidson *et al.* (Da76a).

The geometry of the experiment is shown in figure 2. The incident proton of energy E reacts with the neutron production source at a point P on a circular beamspot of radius r. A neutron of energy E_n is produced, leaving the production source at an angle θ_n with respect to the proton beam axis. The neutron then travels a distance ℓ_n inside the scatterer to reach the point P' where it

Figure 2.

a) The geometry of the beam, target and detector for a small sample experiment. Two different types of γ-ray experiments have been done using this geometry.
b) The angular distribution for the 1220→513 keV transition in ^{116}Cd, as measured in this work. The two curves are the distorted theoretical distributions for different neutron energies. The $E_n = \infty$ curve corresponds to a non-aligned initial state. The energy dependence of the theoretical distribution is a function of the B_k coefficients. For example, the $E_n = \infty$ angular distribution is a factor of 1.25 higher than the E_n = 1.7 MeV distribution at $\theta_\gamma = 90°$. This factor decreases to 1.15 for the E_n = 2.8 MeV distribution.
c) The excitation functions for the 1220 keV state. The experimental data is that of Gill et al (6:74) which was taken at $\theta_\gamma = 90°$. An isotropic γ-ray angular distribution was assumed in this work. The corresponding theoretical excitation function is denoted by the solid curve. The dashed curve, which includes angular distribution effects, was obtained by the use of a correction factor, as described above. The correction of excitation curves due to angular distribution effects is straight forward when there is only one γ-decay mode available. This procedure is complicated when there is more than one γ-decay mode, as one needs to know not only the spins and parities of the states involved, but the branching and multipole mixing ratios of the γ-decays. This is self defeating, as this is usually the information that is being deduced.

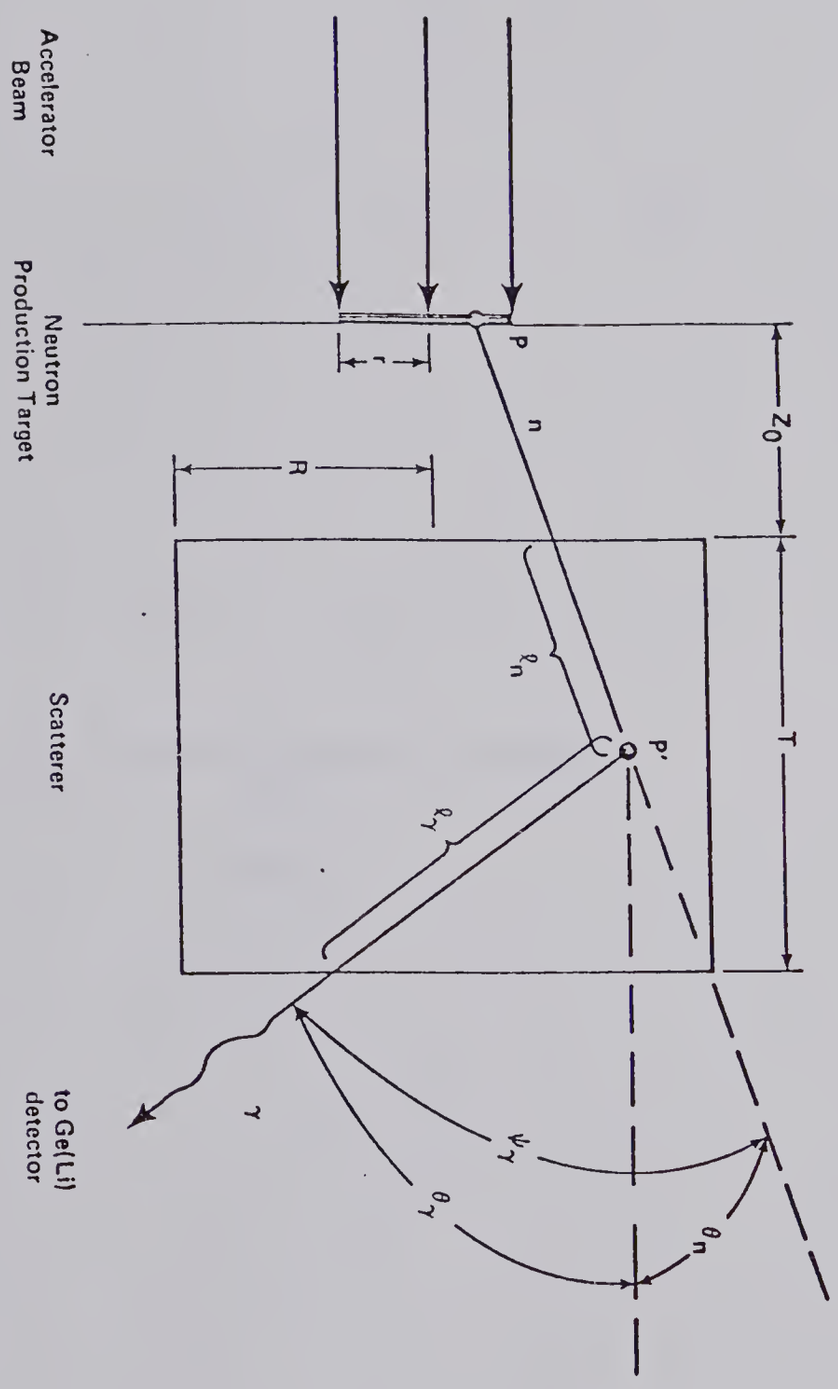
Accelerator Beam
Neutron Production Target
Scatterer
to Ge(Li) detector
P
r
n
R
Z_0
T
ℓ_n
P'
ℓ_γ
γ
ψ_γ
θ_γ
θ_n

2b)

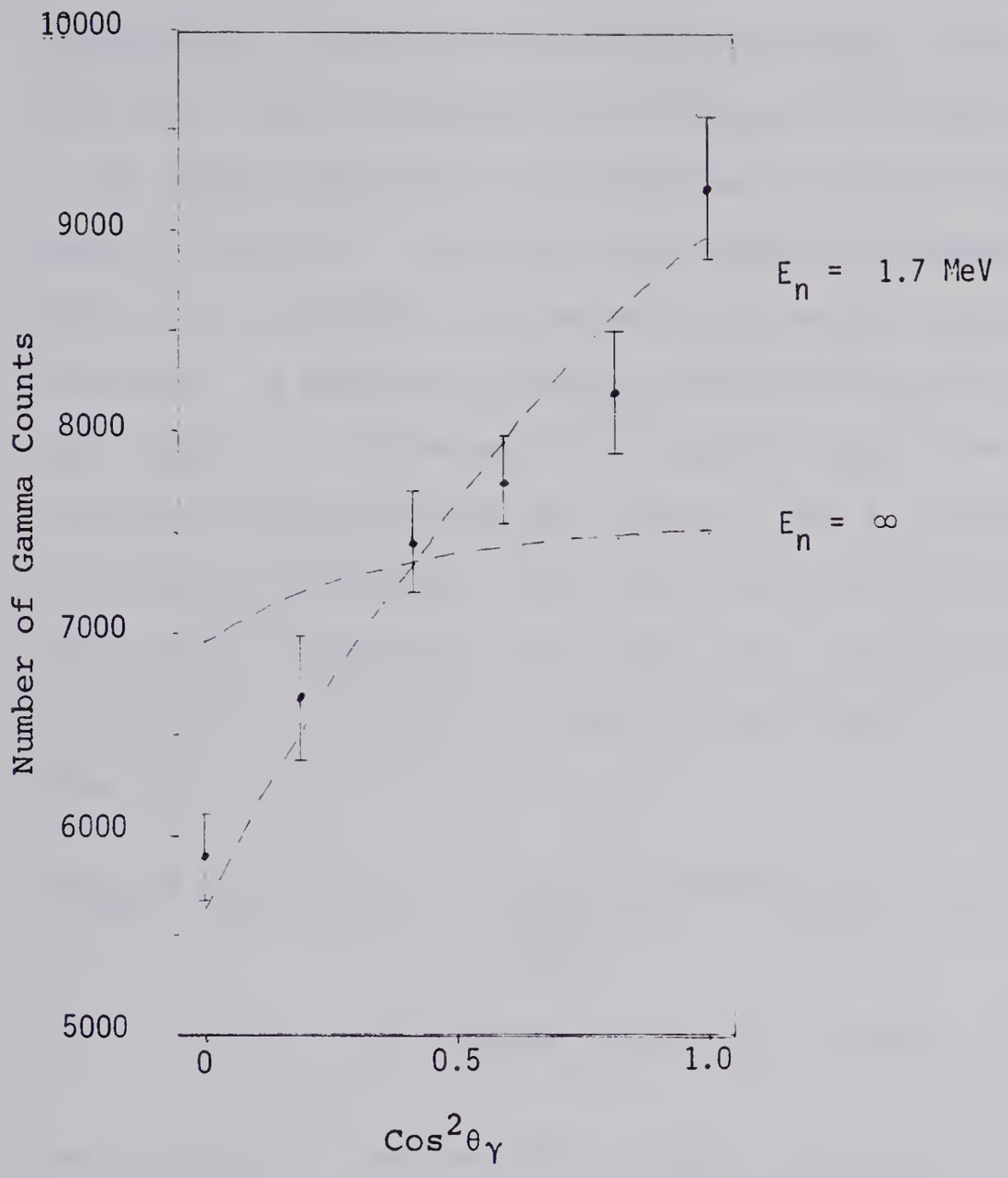
10000
9000
8000
7000
6000
5000
Number of Gamma Counts
0
0.5
1.0
$\cos^2\theta_\gamma$
E_n = 1.7 MeV
E_n = ∞

2c)

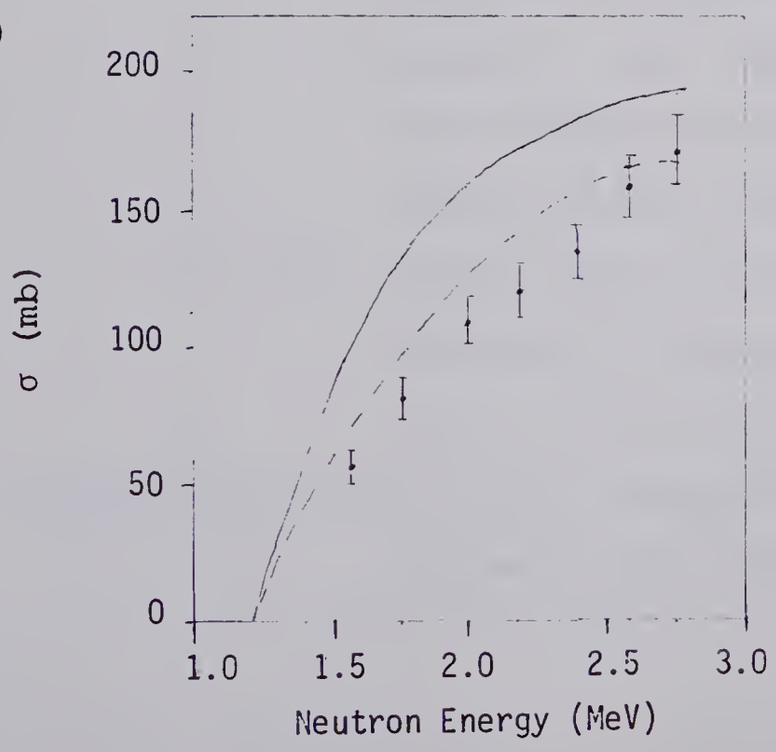
200
150
100
50
0
σ (mb)
1.0
1.5
2.0
2.5
3.0
Neutron Energy (MeV)

inelastically scatters from a target nucleus. The resulting γ-ray is emitted in a direction θ_γ with respect to the proton beam and ψ_γ with respect to the incident neutron direction. If the γ-ray is not scattered or absorbed, it travels a distance of ℓ_γ before leaving the scatterer. A detector placed in the direction of Θ_γ with respect to the beam line detects γ-rays from all possible combinations of the points P and P' for which the process is allowed. The total observed intensity is then equal to the sum of all such γ-ray contributions. The distorted theoretical angular distribution is then given by

$$W_{dis}(\theta,J_i,J_f,\delta) = I \frac{\sigma_n(E,\theta_n)}{r^2_{PP'}} \exp(-\mu_n \ell_n)\, \sigma_{nn'}(E_n) \times W_{th}(E_n,\psi_\gamma,J_i,J_f,\delta) \exp(-\mu_\gamma \ell_\gamma)\, dE\,dV\,dA \quad (18)$$

where $\sigma_n(E,\theta_n)$ is the differential cross section for the neutron production reaction at an angle θ_n, for incident proton energy E.

I is a normalizing function.

μ_n is the neutron attenuation coefficient.

$\sigma_{nn'}(E_n)$ is the total cross section for the (n,n') reaction for neutrons of energy E_n.

μ_γ is the γ-ray attenuation coefficient.

$W_{th}(E_n,\psi_\gamma,J_i,J_f,\delta)$ is the theoretical angular distribution of gamma rays from the $J_i \rightarrow J_f$ transition,

having a mixing ratio δ, for incident neutron energy E_n, where the outgoing γ-ray makes an angle of ψ_γ with respect to the incident neutron direction.

dEdVdA are the integration variables over the proton energy, the scatterer volume, and the area of the beamspot.

The differential cross sections for the $^{3}H(p,n)^{3}He$ reaction used were those of Perry *et al.* (Pe60). The neutron and γ-ray attentuation coefficients were taken from standard compilations of neutron and photon cross sections (Go56, St67). The total (n,n') inelastic cross section was taken to be proportional to the square root of the difference between the neutron energy and the threshold energy (Bl52).

The theoretical angular distributions were calculated by using a series of computer programs. First, the transmission coefficients for the $^{114,116}Cd$ and ^{146}Nd nuclei were calculated by the computer program TRANCO, written by H. S. Sherif (Sh76). The transmission coefficients are given in terms of the optical model phase shifts $\delta_{\ell j}$ by the relation

$$T_{\ell j} = 1 - |\exp(2i\delta_{\ell j})|^2 \qquad (19)$$

The phase shifts were determined by matching the internal and external wave functions at a point where the nuclear

potential is zero. The potential used was the optical model, with the parameters of Wilmore and Hodgson (Wi64).

The transmission coefficients generated by TRANCO were used as input by the program AK, written by P. W. Green (Gr71). This program calculated the relative population parameters of the magnetic substates $w(M_1)$ from the Compound Nucleus Statistical Model. Tables of B_K coefficients, as a function of neutron energy and the initial state's spin and parity, were generated for each level studied. A test was carried out to determine the dependence of B_K coefficients on the magnitude of the transmission coefficients. In this test, the optical model parameters of Wilmore and Hodgson (Wi64), Perey and Buck (Pe62), Rosen *et al.* (Ro65), and Bjorklund and Fernbach (Bj58) were used to calculate transmission coefficients for levels in ^{114}Cd. It was found that, whereas the transmission coefficients generated by the different sets of optical model parameters differed by as much as 70%, the angular distribution coefficients varied by only about 3%. These results are in agreement with those of Pilt *et al.* (Pi70), who carried out a similar test for the $^{55}Mn(p,n)$ reaction.

The B_K coefficients were used as input for the computer program EVA, written by J. M. Davidson (Da76b). EVA numerically integrated Eq. (18) to find the distorted theoretical angular distributions for specified values of J_1, π_1, J_2, and δ. These were then compared to the

experimental data by means of the χ^2 test. Plots of χ^2 as a function of the multipole mixing ratio ($-90° \leq \arctan\delta \leq 90°$) were generated for all possible values of the initial state's spin-parity consistent with dipole and quadrupole radiation. The 0.1% confidence level (En74) was taken as the criterion for rejecting a spin assignment.

3.2 Experimental Setup and Apparatus

The experimental setup is shown in fig. 3. Protons were used to produce neutrons via the $^3H(p,n)^3He$ reaction. The tritium targets consisted of a 3.27 mg/cm^2 layer of metallic erbium deposited on a tantalum backing, with tritium absorbed in the erbium layer at an atomic ratio of 1:1. A 10 nsec pulsed beam with a repitition rate of 1 MHz and an average current of .7 μA was provided by the University of Alberta Van de Graaff accelerator. Time-of-flight gating of the signals from each of two Ge(Li) detectors reduced the background from the $(n,n'\gamma)$ reaction in the detectors and gave an upper limit of approximately 20 nsec for the lifetimes of the observed states. The accumulated charge per angle for the six hour runs was typically 15 mC.

A tantalum collimator with an aperture of 0.24 cm diameter was placed approximately 1 cm from the neutron production target. The cylindrical scatterer was placed

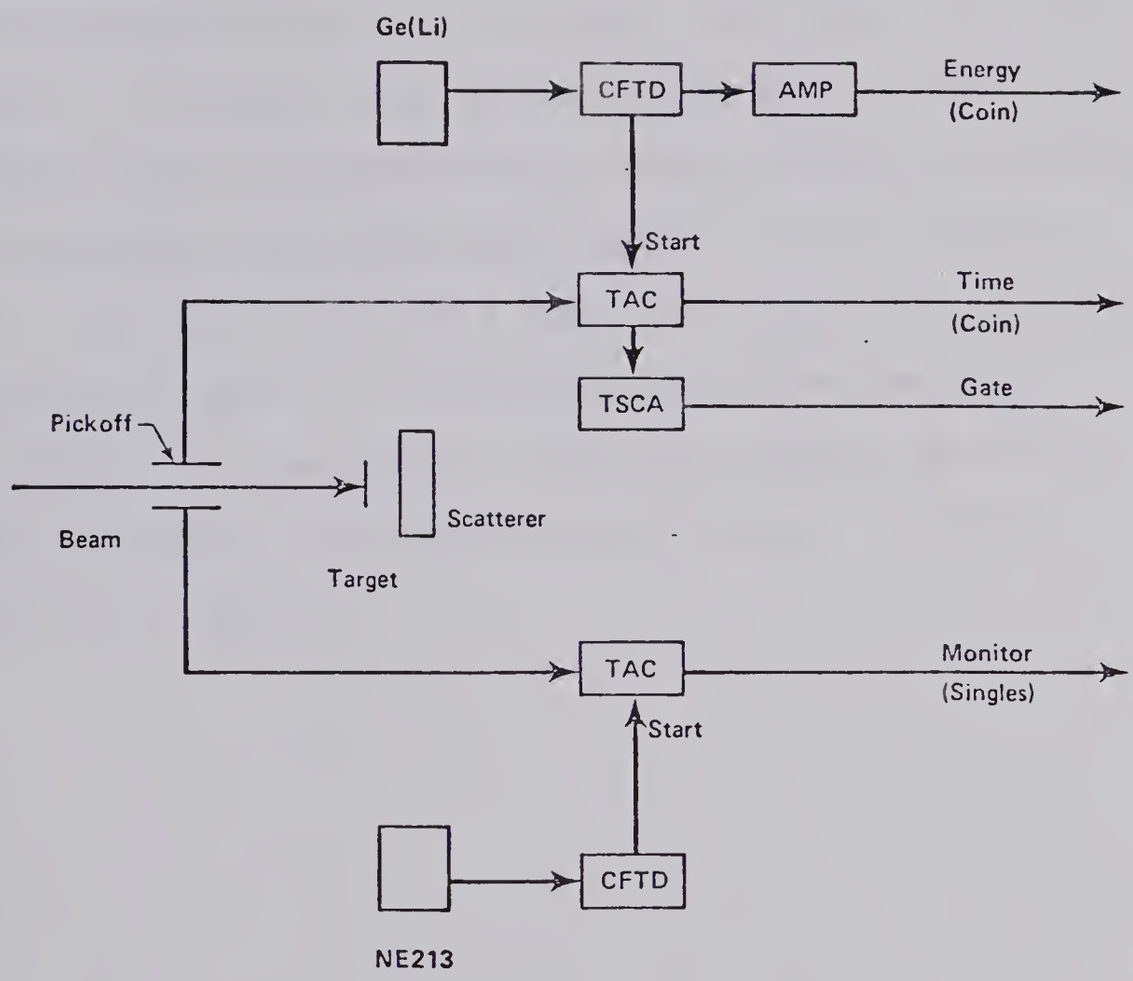

Figure 3. Experimental set-up and electronics.

a distance of 0.5 cm from the neutron production target. It's axis and the beam axis were colinear. Angular distributions were recorded for all nuclei at two different proton energies. These energies, along with the scatterer characteristics, are listed in Table IV.

Two Ge(Li) detectors placed about 50 cm from the scatterer, detected the γ-ray radiation. The angles θ_γ at which data was taken were 90°, 65°, 50°, 40°, 25°, and 0°. Neutron flux was monitored using a stationary NE213 liquid scintillation detector placed at a distance of several meters from the target. A ^{137}Cs source, E_γ = 661 keV, was placed above the Ge(Li) detectors to provide a means of calibrating dead time and gain stability of the system. Signals from the detectors were analyzed and stored on line using a Honeywell DDP-516 computer.

Table IV. Scatterer Characteristics.

Nucleus	Proton energy (in MeV)	Neutron energy (maximum, in MeV)	Scatterer material	% of isotope	Size	
					r(cm)	h(cm)
^{114}Cd	2.60	1.67	CdO	98.5		
	3.60	2.67			.79	.48
^{116}Cd	2.60	1.67	CdO	94.3		
	3.60	2.67			.79	.48
^{146}Nd	2.90	1.97	Nd_2O_3	85.0		
	3.60	2.67			.79	.49

CHAPTER 4

RESULTS

The properties of the low-lying states of the ^{114,116}Cd and ^{146}Nd nuclei were determined by measuring the angular distributions of γ-ray transitions. The experimental data was then compared to the theoretical angular distributions, which were generated for all values of the initial state's spin and parity such that the γ-ray transition was consistent with dipole and quadrupole radiation. The sensitivity of the angular distribution to parity is due to the dependence of the B_K coefficients on the initial state's alignment. For all transitions studied in this work, calculations were done for both parity assignments. In no case was it possible to exclude one parity assignment on the basis of the 0.1% confidence level. Since the differences are usually small, all results shown in this section, except where noted, are for positive parity assignments. Parity assignments were made on the basis of the $\chi^2_{min} + 1$ per degree of freedom rule and a consideration of lifetimes.

4.1 Results for ^{114}Cd.

A typical γ-ray spectrum for ^{114}Cd, taken at a proton bombarding energy of 3.60 Mev, is shown in fig. 4a. The numbers above each peak denote the energies, in keV, of the γ-ray transitions between levels in ^{114}Cd. The deduced level and decay scheme, as shown in fig. 5, is in good agreement with the level and decay scheme proposed by Gill *et al.* (Gi74). Table V summarizes the mixing ratios and spin-parity assignments determined in this work. The errors on the mixing ratios were determined by the χ^2_{min} + 1 rule (Ro75). As the first excited state of ^{114}Cd has been extensively investigated in previous works, it has not been studied here.

4.1.1 The 1134, 1210, and 1283 keV levels.

These three levels have previously been shown in several experiments (Ki75) to be the triplet of two phonon states, having spin-parities of 0^+, 2^+, and 4^+. The results for the 1134 → 558 keV transition are shown in fig. 6. As the plot of χ^2 versus arctanδ shows, the results are consistent with a spin-parity assignment of 0^+ for the 1134 keV state. The level at 1210 keV was seen to decay *via* γ-rays of 651 and 1210 keV to the first excited and ground states. The 1210 → 0 keV transition, however, was seen in sufficient strength only during the $E_n \leq 2.67$ MeV runs, when this state was

Figure 4.

Typical γ-ray spectra for the Cd isotopes. a) ^{114}Cd. The numbers above each peak refer to the energies, in keV, of the γ-ray transitions between the Cd levels. Background peaks are denoted by B. b) ^{116}Cd. The inset shows the γ-ray decays of the triplet of states near 1920 keV.

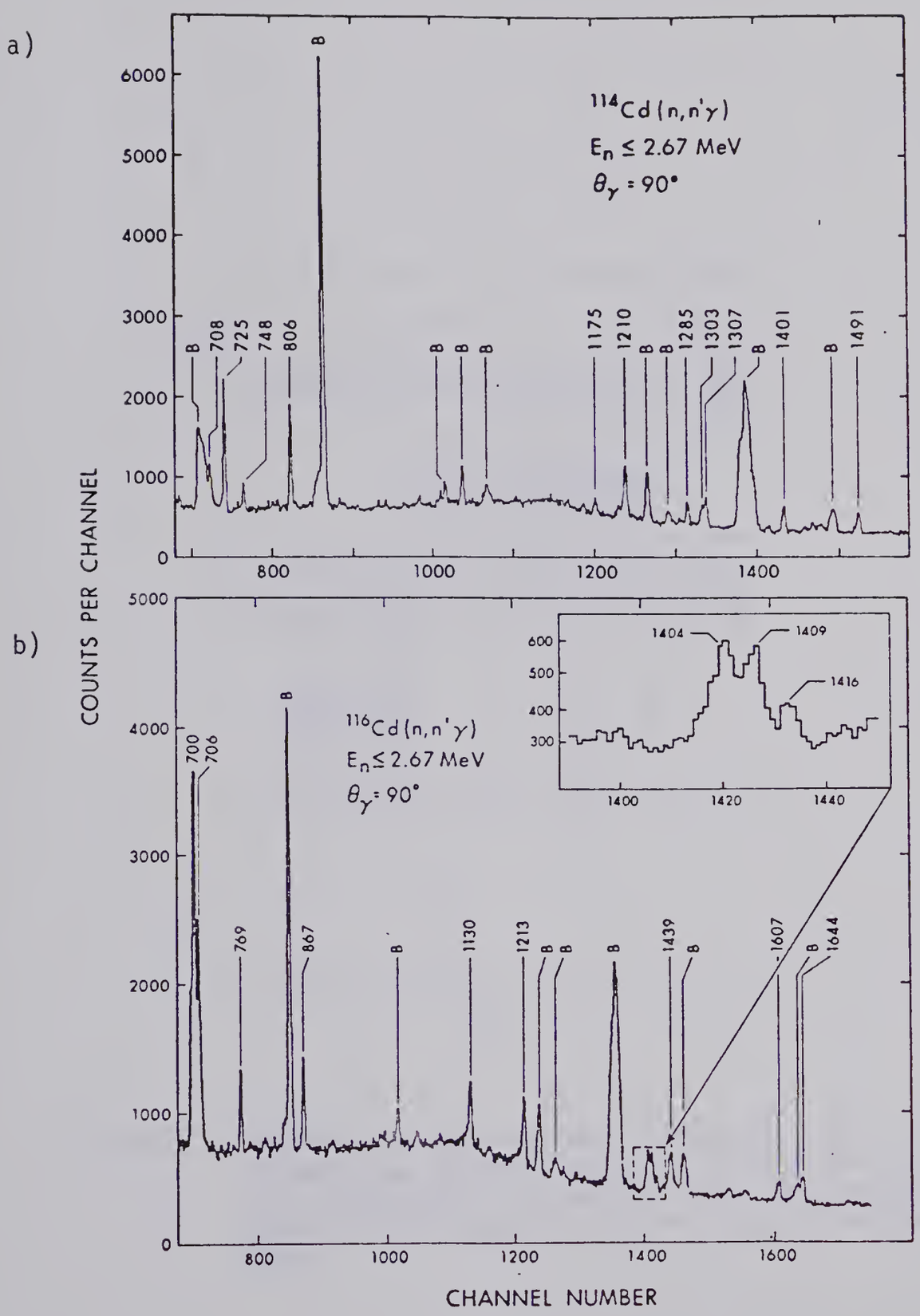
a)
b)
^{114}Cd(n,n'γ)
$E_n \leq 2.67$ MeV
$\theta_\gamma = 90°$
^{116}Cd(n,n'γ)
$E_n \leq 2.67$ MeV
$\theta_\gamma = 90°$
COUNTS PER CHANNEL
CHANNEL NUMBER
B
708
725
748
806
1175
1210
1285
1303
1307
1401
1491
700
706
769
867
1130
1213
1439
1607
1644
1404
1409
1416

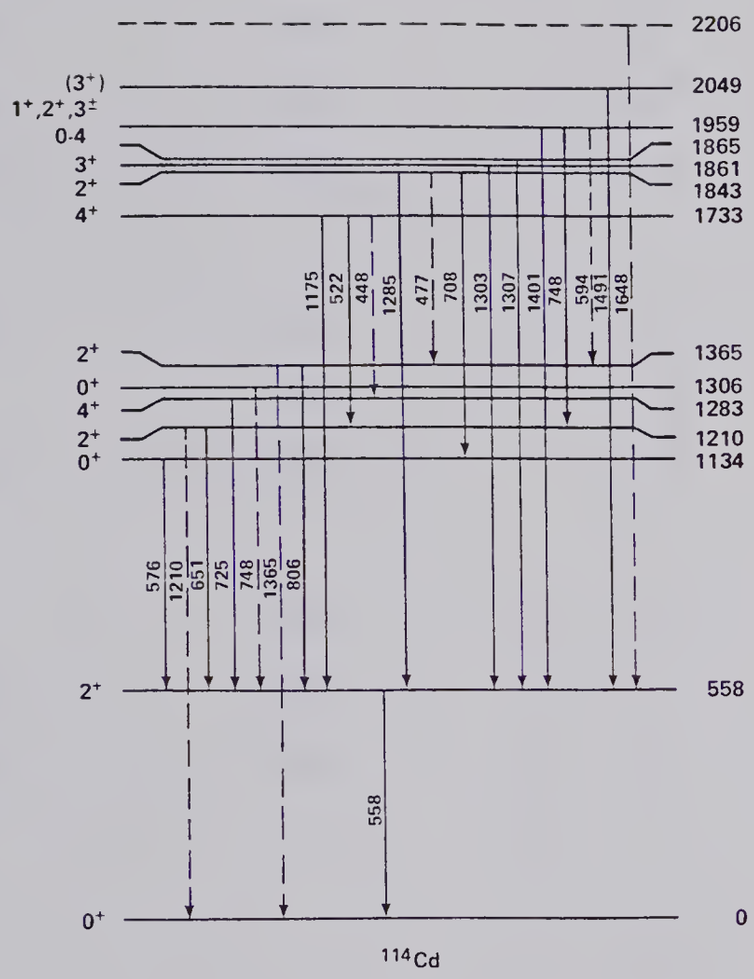

Figure 5. The deduced level and decay scheme for ^{114}Cd. The dotted lines refer to transitions that were too weak to provide useful information. The spin-parity assignments are the result of the present and previous works.

Table V. The Gamma Ray Mixing Ratios and Spin-Parity Assignments for ^{114}Cd Determined in This Work.

Level Energy[a]	γ-ray Energy	$J_i^\pi \rightarrow J_f^\pi$	Arctanδ
1134	576	$0^+ \rightarrow 2^+$	0
1210	651	$2^+ \rightarrow 2^+$	58 13
1283	725	$4^+ \rightarrow 2^+$	0[b]
1365	806	$2^+ \rightarrow 2^+$	-80 5
			16 5
1733	1175	$4^+ \rightarrow 2^+$	0[b]
	552	$4^+ \rightarrow 2^+$	0[b]
1843	1285	$2^+ \rightarrow 2^+$	-80 10
			21 15
	708	$2^+ \rightarrow 0^+$	0
1861	1303	$3^+ \rightarrow 2^+$	62 → 16
1865	1307	$0 \rightarrow 2^+$	0
		$1 \rightarrow 2^+$	all values
		$2 \rightarrow 2^+$	5 → 90
		$3 \rightarrow 2^+$	-15 → 20
			55 → 90
		$4^+ \rightarrow 2^+$	0[b]
1959	1401	$1^+ \rightarrow 2^+$	-50 35
		$2^+ \rightarrow 2^+$	52 14
		$3^+ \rightarrow 2^+$	72 12

(continued....)

Table V (continued)

		$3^- \rightarrow 2^+$	9 9
	748	$1^+ \rightarrow 2^+$	-50 35
		$2^+ \rightarrow 2^+$	53 20
		$3^+ \rightarrow 2^+$	71 10
		$3^- \rightarrow 2^+$	6 11
2049	1491	$3^+ \rightarrow 2^+$	76 10

a) The energies are in keV. The uncertainties are ±1 keV.

b) The radiation was assumed to be pure quadrupole.

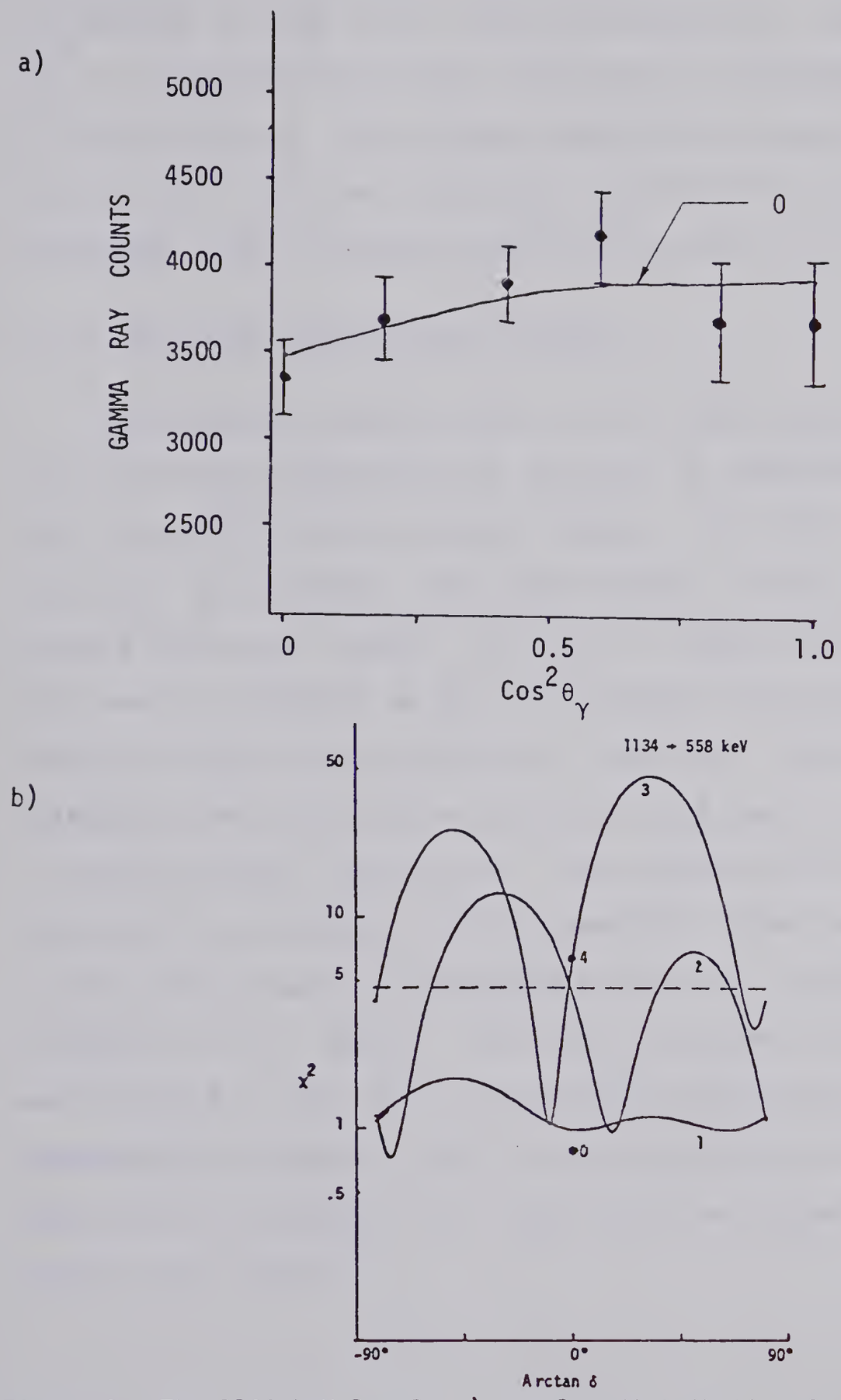

Figure 6. The 1134 keV level: a) angular distribution for the 576 keV γ-ray, and b) χ^2 curves.

fed through γ-ray cascades from higher excited states. The results for the 1210 → 558 keV transition, shown in fig. 7, are consistent with a spin-parity assignment of 2^+ for this level. The angular distribution measurements for the 1283 → 558 keV transition, shown in fig. 8, are consistent with an initial state spin parity of 4^+.

4.1.2 The 1306 and 1365 keV levels.

The nature of these states is not very well known, but it has been proposed that they may be considered as quasi (single) particle states (Sa64a). The 1306 keV level has two reported γ-ray decay modes, to the 1210 and 558 keV levels (Bä66). The 1306 → 1210 keV transition was not observed as the γ-ray energy spectrum had a cutoff of approximately 250 keV. The 1306 → 558 keV transition was observed in this work, but was too weak to provide useful information. The weakness of this transition is probably due to competition from the decay to the ground state *via* internal conversion, as observed by Bäcklin *et al.* (Bä66). The 1365 → 558 keV transition was observed in this work. The angular distribution measurements, shown in fig. 9, are consistent with a spin-parity assignment of 2^+ that has been suggested by earlier work (Ki75).

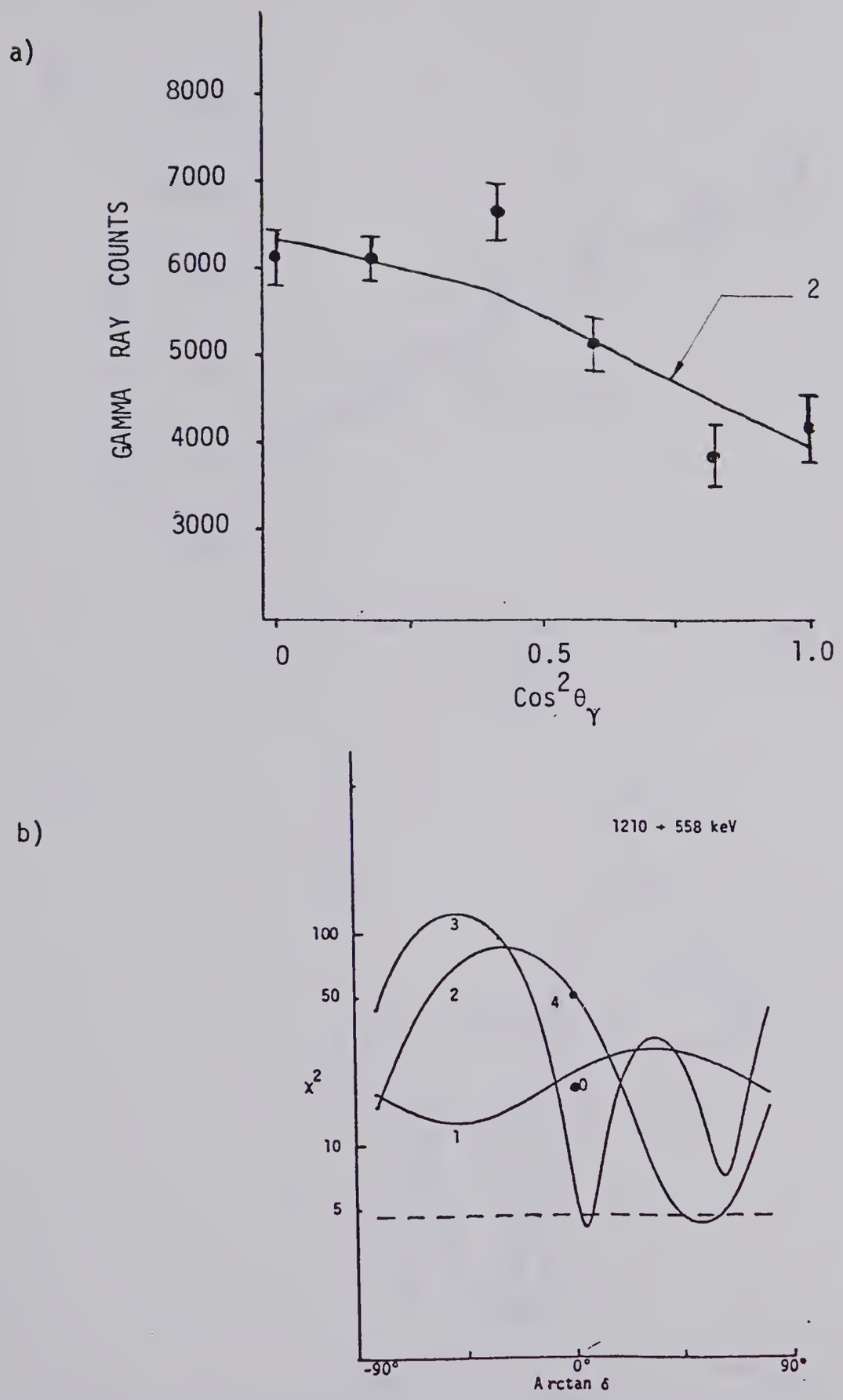

Figure 7. The 1210 keV level: a) angular distribution for the 651 keV γ-ray, and b) χ^2 curves.

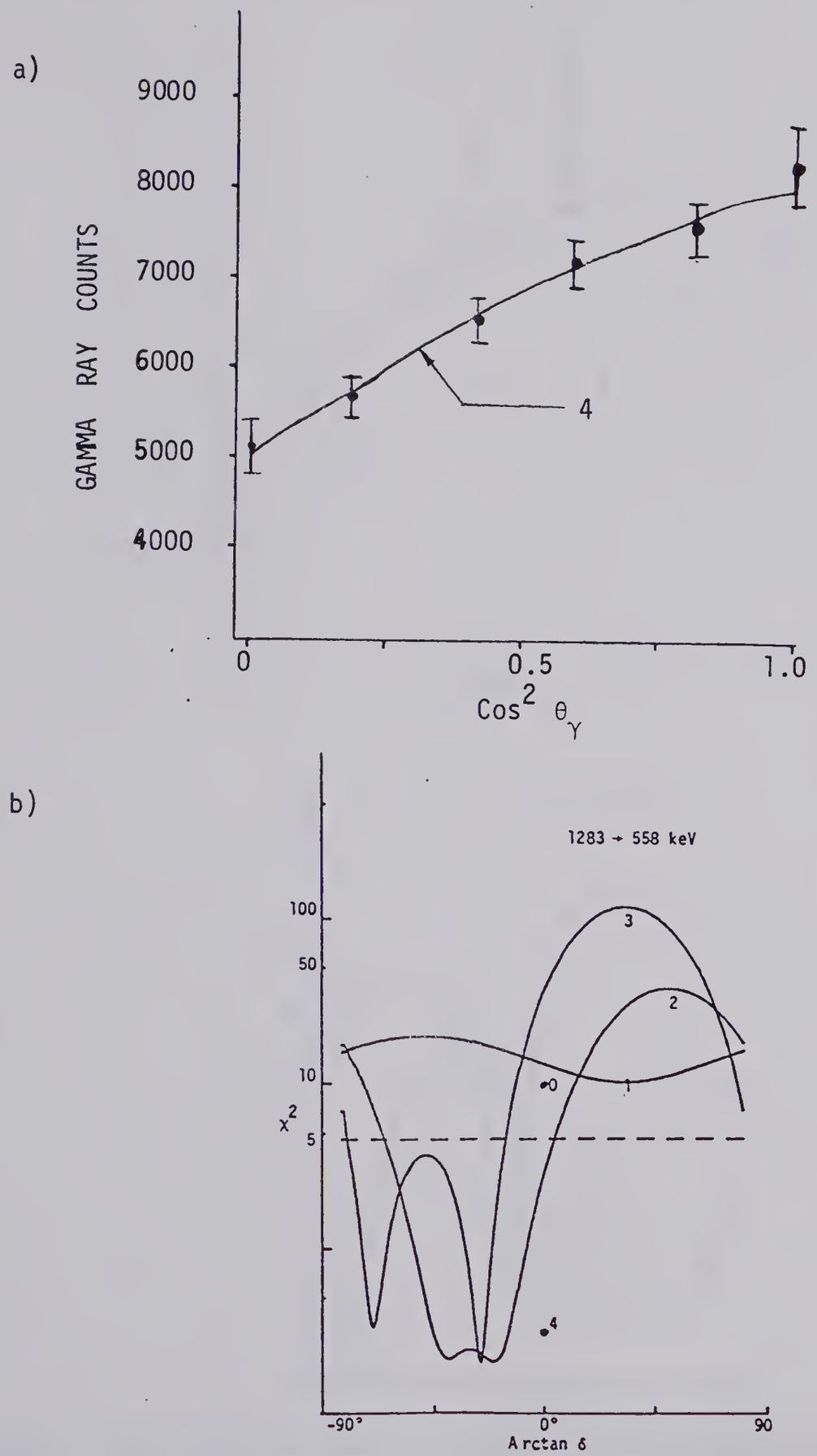

Figure 8. The 1283 keV level: a) angular distribution for the 725 keV γ-ray, and b) χ^2 curves.

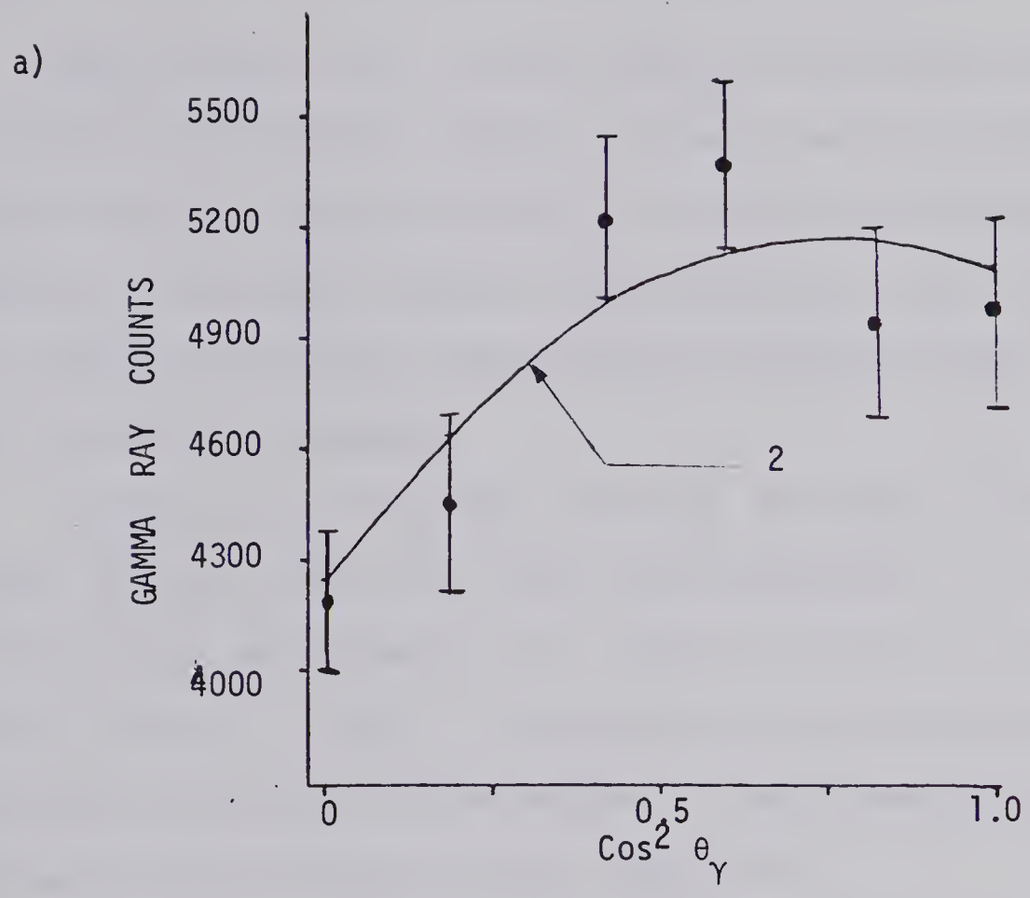

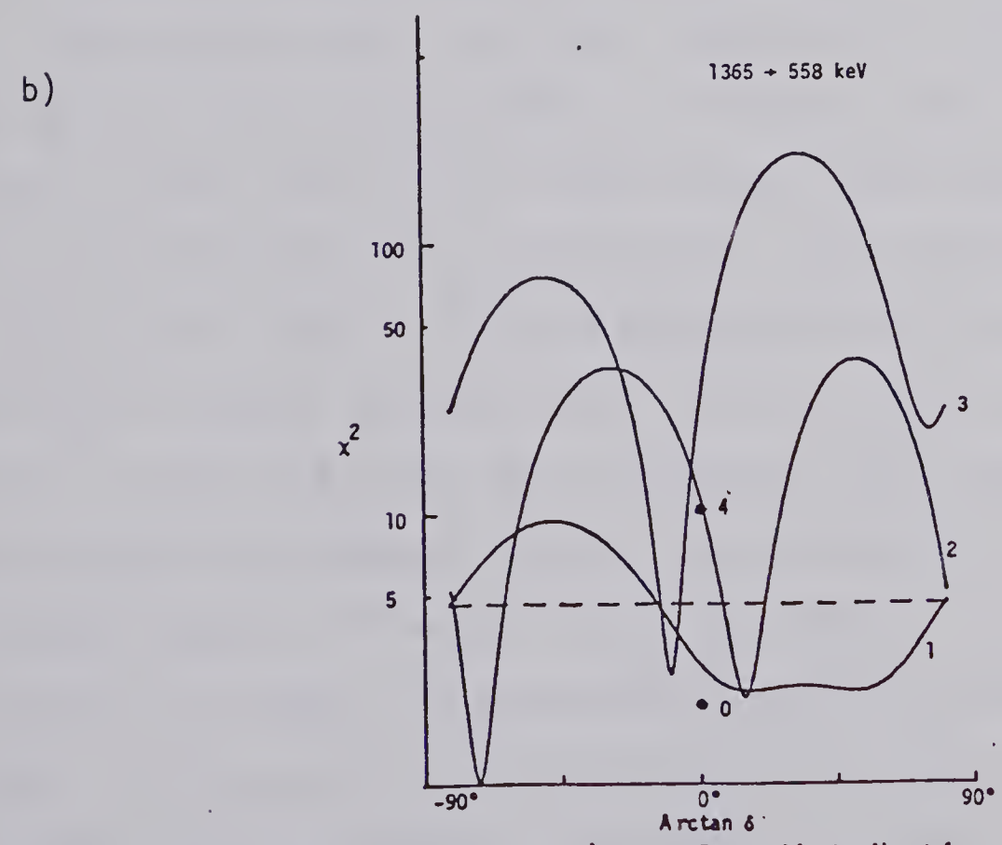

Figure 9. The 1365 keV level: a) angular distribution for the 806 keV γ-ray, and b) χ^2 curves.

4.1.3 The 1733, 1843, 1861, and 1865 keV levels.

These states all lie well above the triplet of two-phonon quadrupole states, and well below the quadrupole-octupole states suggested by Sakai and Tamura (Sa64a). Curiously, these states were not observed in in Coulomb excitation, which should preferentially excite collective states.

The state at 1733 keV was seen to decay to the levels at 558, 1210, and 1306 keV excitation. The angular distribution measurements for the two stronger transitions, shown in figs. 10 and 11, placed no restrictions on the value of the spin of this state. A spin assignment of 4^+ has previously been made (Gr68,Gi74).

Four decay modes have been reported for the level at 1843 keV excitation (Bä66). Of these, only the transitions to the levels at 1134 and 558 keV were seen. As the 1134 keV state has a spin of 0^+, the multipole mixing ratio for the 1843 → 1134 keV transition must be zero. As fig. 12 shows, the only spin for which the value of $\chi^2(\delta = 0)$ was below the 0.1% confidence limit was 2. If this state has negative parity, the transition to the 558 keV level, a 2^+ state, would be almost pure E1, giving a δ of zero. The deduced values of arctanδ of $\pm(80° \pm 10°)$ and $21° \pm 12°$ from the plot of χ^2 versus arctanδ, shown in fig. 13, make this assignment relatively

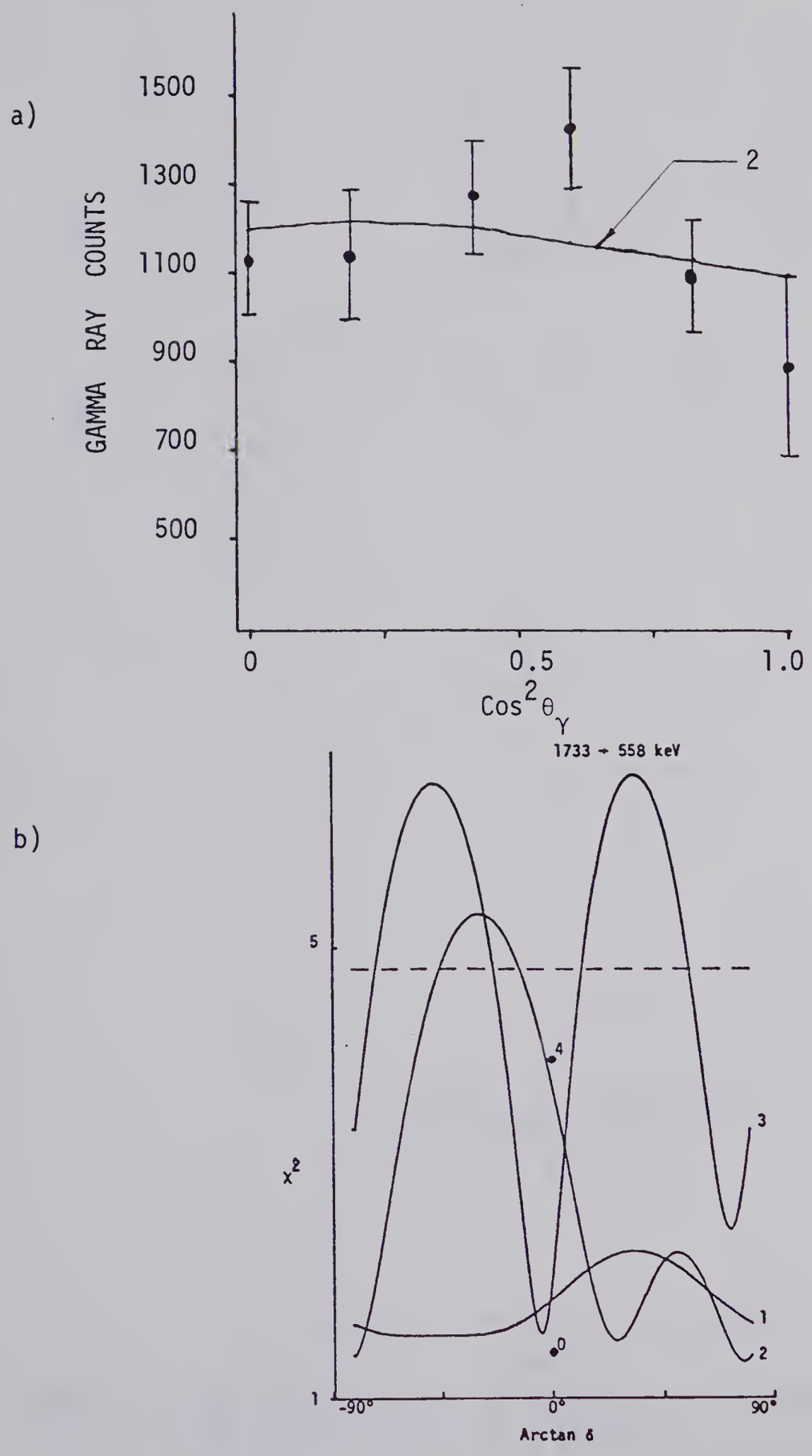

Figure 10. The 1733 keV level: a) angular distribution for the 1175 keV γ-ray, and b) χ^2 curves.

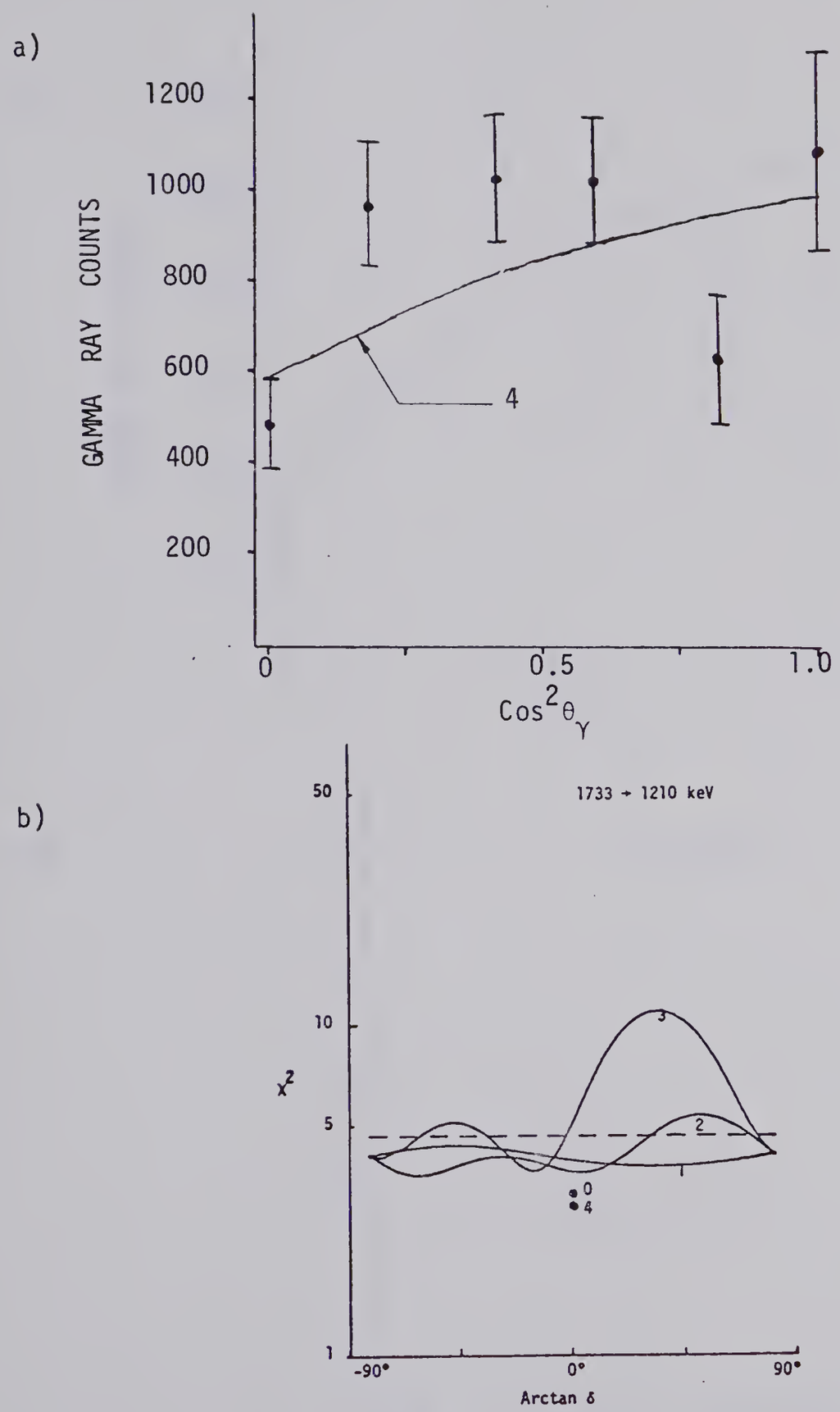

Figure 11. The 1733 keV level: a) angular distribution for the 522 keV γ-ray, and b) χ^2 curves.

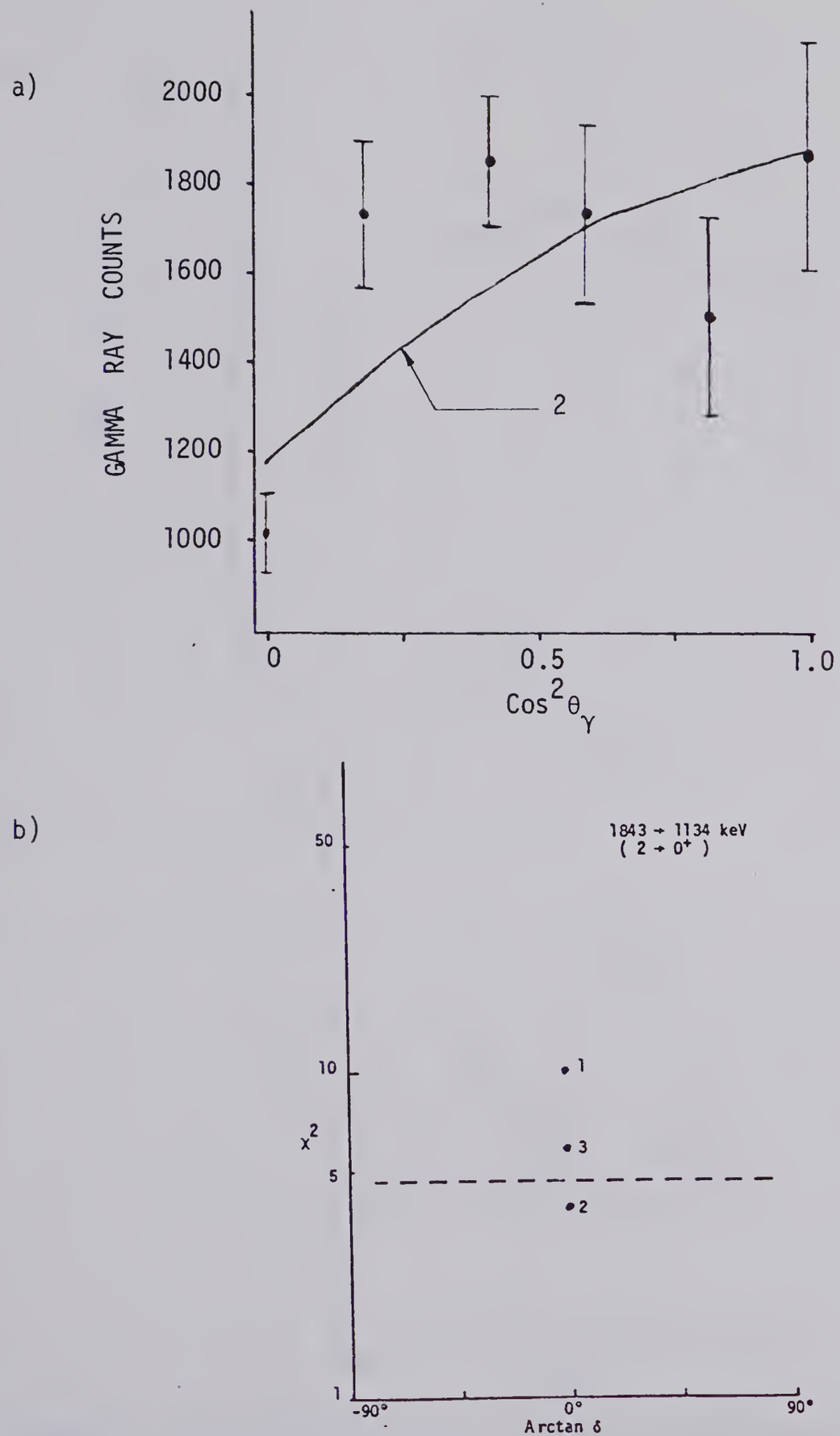

Figure 12. The 1843 keV level: a) angular distribution for the 708 keV γ-ray, and b) $\chi^2(\delta=0)$.

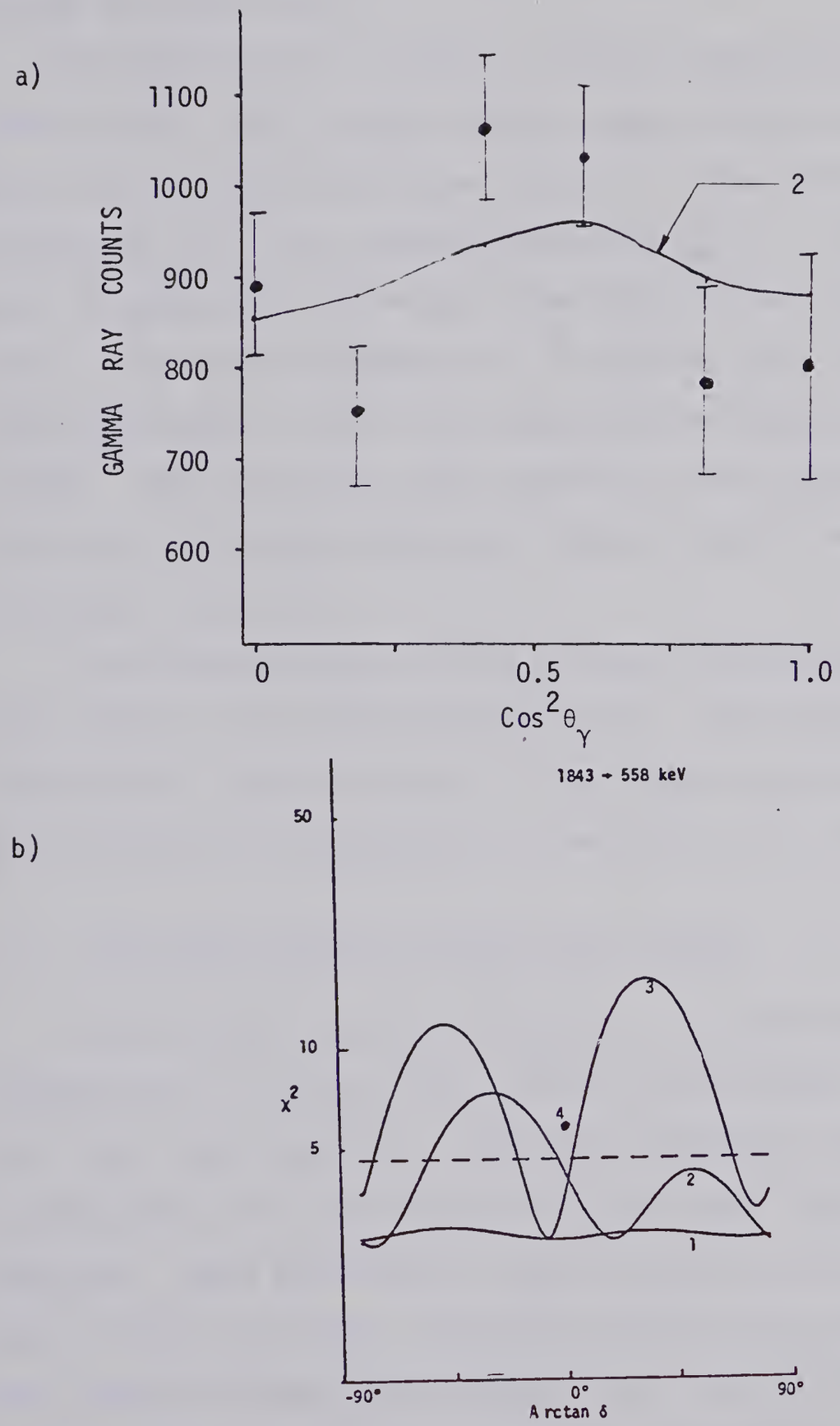

Figure 13. The 1843 keV level: a) angular distribution for the 1285 keV γ-ray, and b) χ^2 curves.

improbable. Therefore, we assign a spin-parity of 2^+ to the 1843 keV state.

The results for the 1861 → 558 keV transition are shown in fig. 14. As this figure shows, minima in $\chi^2(\delta)$ permit only an initial state spin of 3. The values of arctan δ of 16° → 62° obtained from the χ^2_{min} + 1 rule make it relatively improbable that this is the octupole state. The spin assignment of 3^+ suggests that the 1861 keV state is one of the three-phonon quadrupole states. This state has been observed in the study of Cd(n,n'γ) excitation functions (Gi74), and was tentatively assigned a spin of 1.

The excited state at 1865 keV has one reported decay mode; to the first excited state. The angular distribution, shown in fig. 15, was found to be isotropic, which placed no restriction on the spin of this state.

4.1.4 The 1959, 2049, and 2206 keV levels.

The 1959 keV state has reported γ-ray branches to the established 2^+ states at 558, 1210, and 1365 keV. The 594 keV γ-ray from the 1959 → 1365 keV transition could not be resolved due to a background peak from the ^{74}Ge(n,n'γ) reaction. This was also the case in the (n,n'γ) excitation work of Gill *et al.*(4) Although the 748 keV γ-ray has also been placed in the decay scheme as the 1306 → 558 keV transition, it has previously been shown (4) that the 1959 → 1210

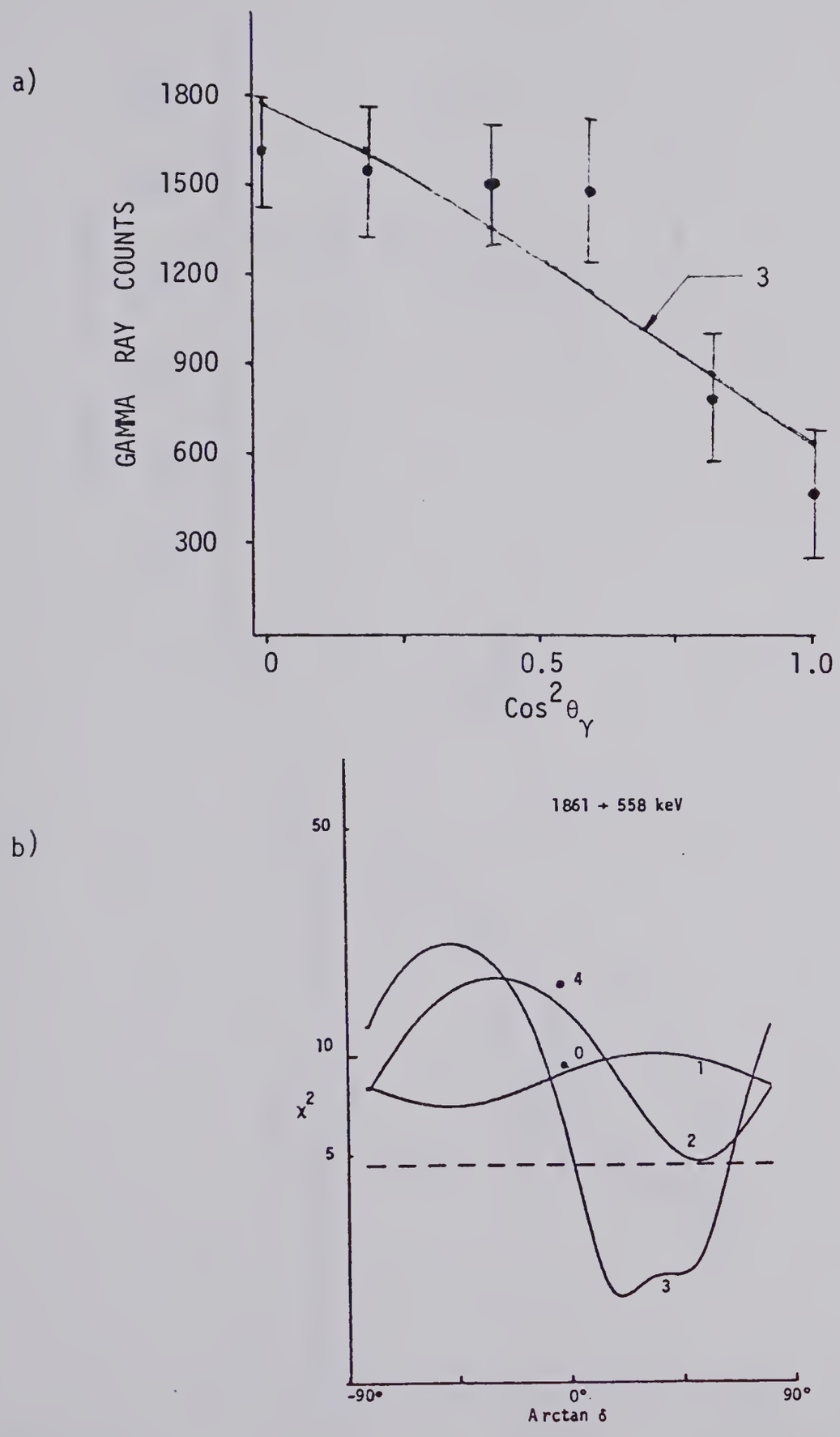

Figure 14. The 1861 keV level: a) angular distribution for the 1303 keV γ-ray, and b) χ^2 curves.

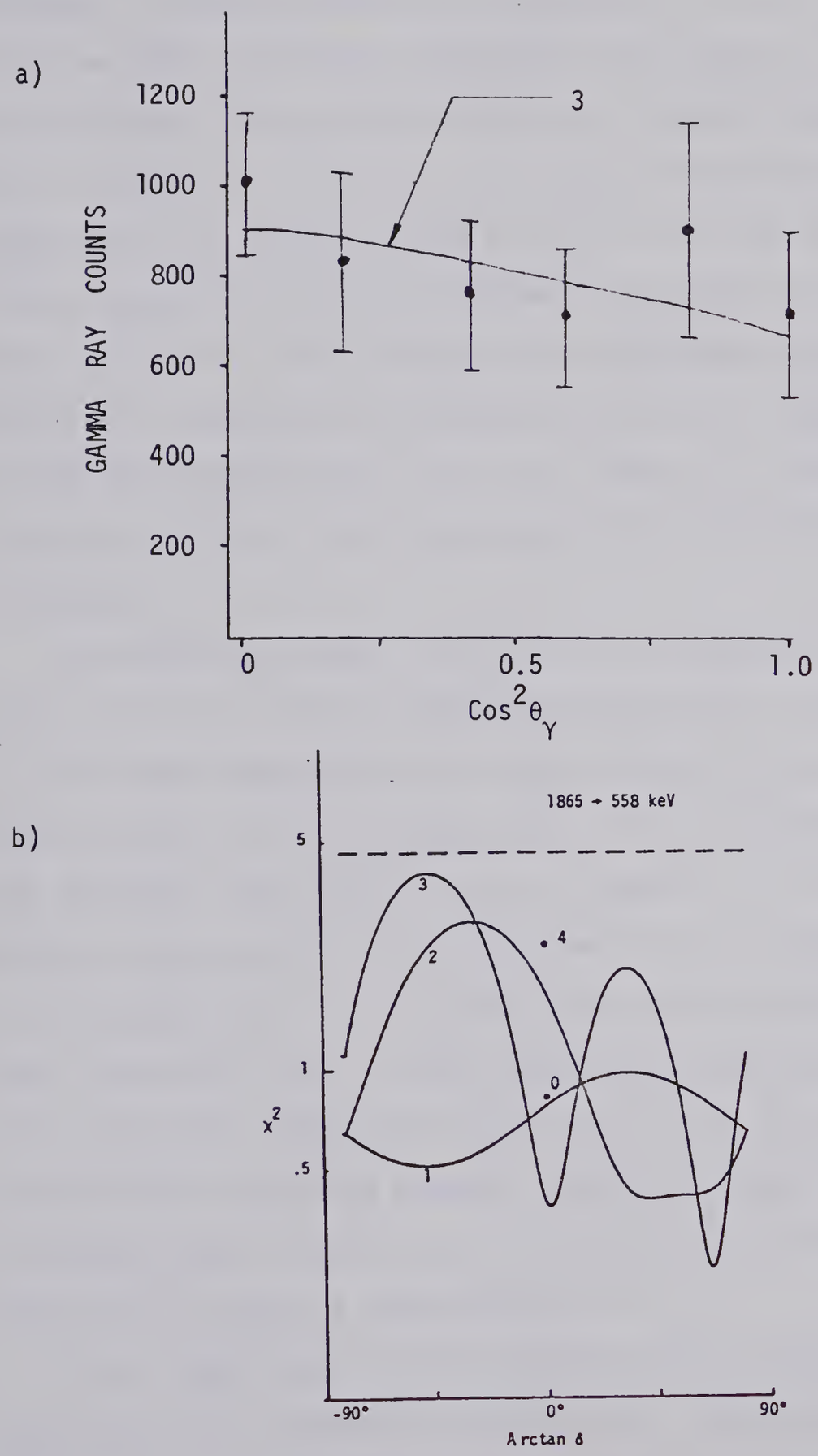

Figure 15. The 1865 keV level: a) angular distribution for the 1307 keV γ-ray, and b) χ^2 curves.

keV transition is mainly responsible for the observed strength. Sample angular distributions for the 1959 → 1210 and 1959 → 558 keV transitions and plots of χ^2 versus arctan δ are shown in Fig. 6. As this Figure shows, minima in χ^2 occur below the 0.1% confidence level only for initial spins of 1,2,3 for both transitions. The minimum χ^2 per degree of freedom for the spin assignment 1 corresponds to a confidence level of only 0.5%, making that assignment relatively improbable. It should also be noted that for a spin of 3, the deduced values of arctan δ are consistent with a negative parity assignment.

The 1959 keV state was originally assigned a spin-parity of 3^- in the Coulomb excitation work of Sakai *et al.*(7) This assignment was later disputed by the (n,n'γ) work of Gill *et al* (4) whose measured cross section for the 1959 keV state was too low to support a 3^- assignment. The fact that the 594 keV γ-ray could not be resolved made the assignment of J = 1 in that work for the 1959 keV level tentative only. This, taken in conjunction with the 0.5% confidence level for a spin of 1, and the fact that the 1959 keV state was observed through Coulomb excitation, a reaction that should favor a single phonon transition, leads us to assign a spin-parity of 3^-.

The γ-ray decay of the 2049 keV state to the first excited state was observed in this work. The angular distri-

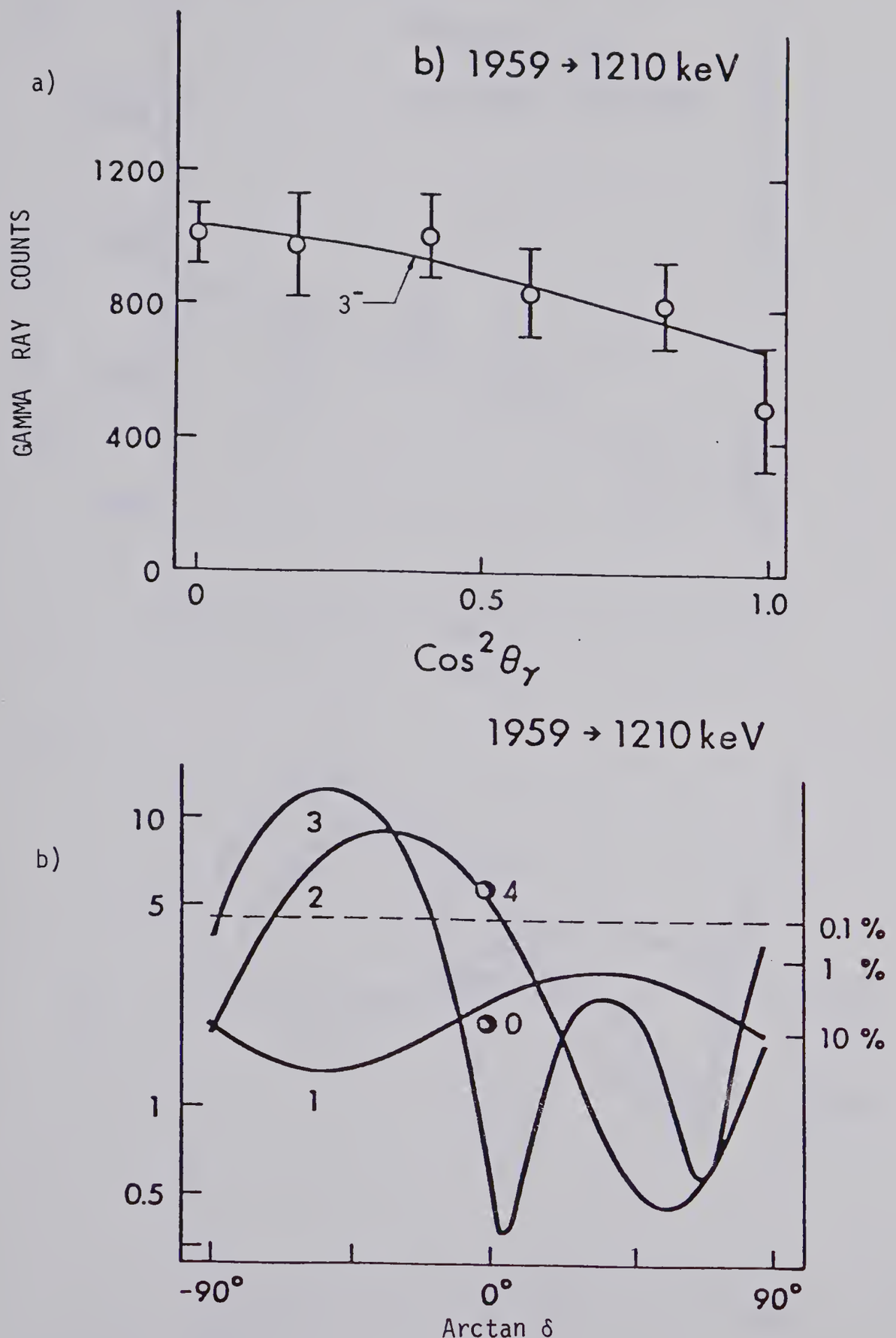

Figure 16. The 1959 keV level: a) angular distribution for the 748 keV γ-ray, and b) χ^2 curves.

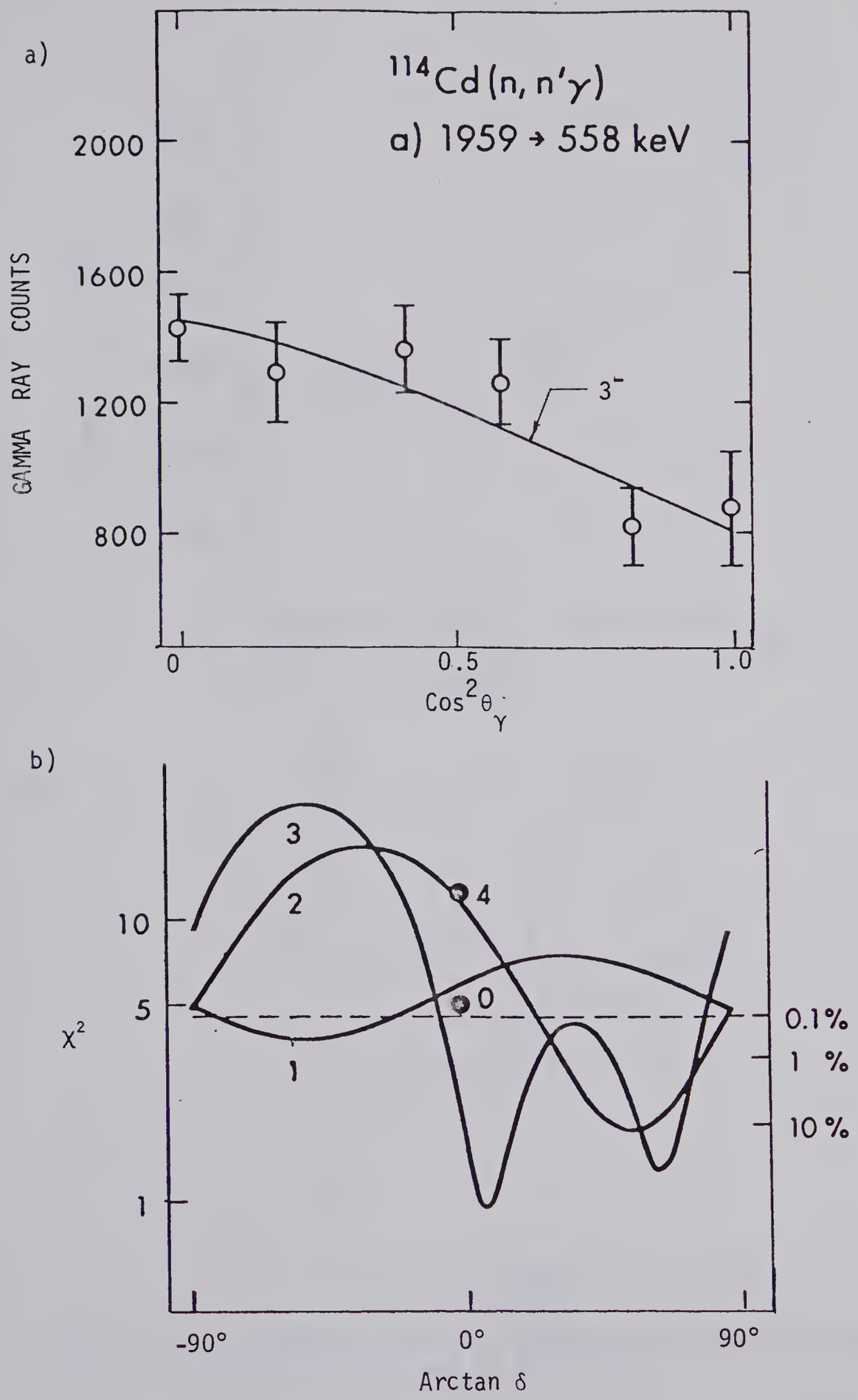

Figure 17. The 1959 keV level: a) angular distribution for the 1401 keV γ-ray, and b) χ^2 curves.

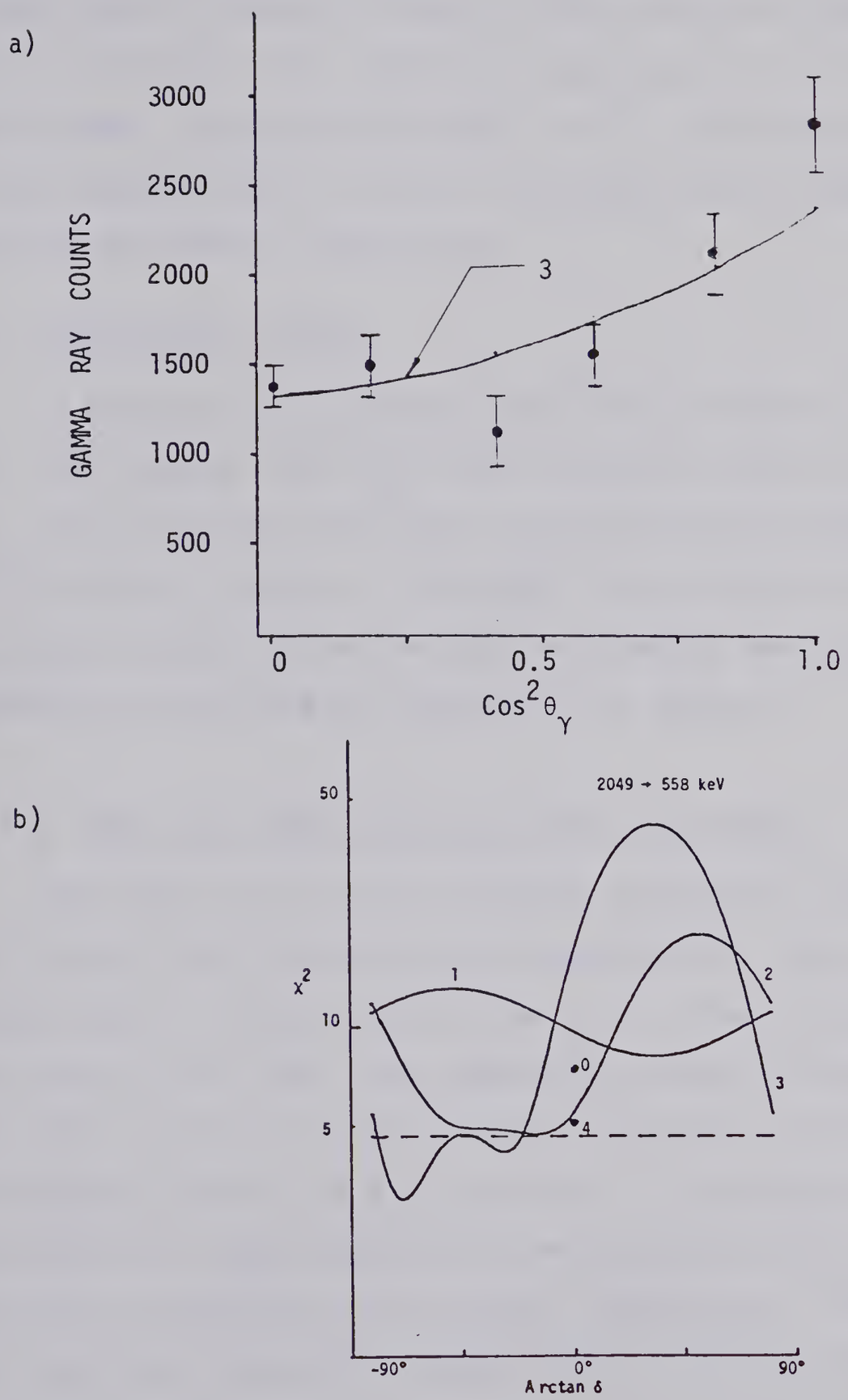

Figure 18. The 2049 keV level: a) angular distribution for the 1491 keV γ-ray, and b) χ^2 curves.

bution measurements, shown in fig. 18, allowed an initial state spin of 3 with an arctan of the multipole mixing ratio δ of 70° ± 10°, implying a spin-parity of 3^+ for this level. Thus the assignment is 3^+. The 1648 keV γ-ray from the 2206 → 558 keV transition was too weak to provide any useful information.

4.2 Results for ^{116}Cd.

A typical γ-ray spectrum for ^{116}Cd is shown in fig. 4b. The deduced level and decay scheme is shown in fig. 19. As in the case of ^{114}Cd, the first excited state of ^{116}Cd was not studied in this work. The values of the multipole mixing ratios and the spin-parity assignments deduced in this work are summarized in Table VI.

4.2.1 The 1213, 1220, 1283, and 1381 keV levels.

The first two of the two-phonon quadrupole states are at 1213 and 1220 keV excitation respectively. The primary decay mode for these states is by γ-ray de-excitation to the level at 513 keV. The observed branching ratios for the 1213 keV level are 56 ± 7% for the 1213 → 513 keV transition and 44 ± 7% for the 1213 → 0 keV transition. The error for these results is associated with the non-isotropic weighting of the angular distribution. The 1220 keV state was observed to decay only to the 513 keV state.

The angular distribution measurements for the 1213 →

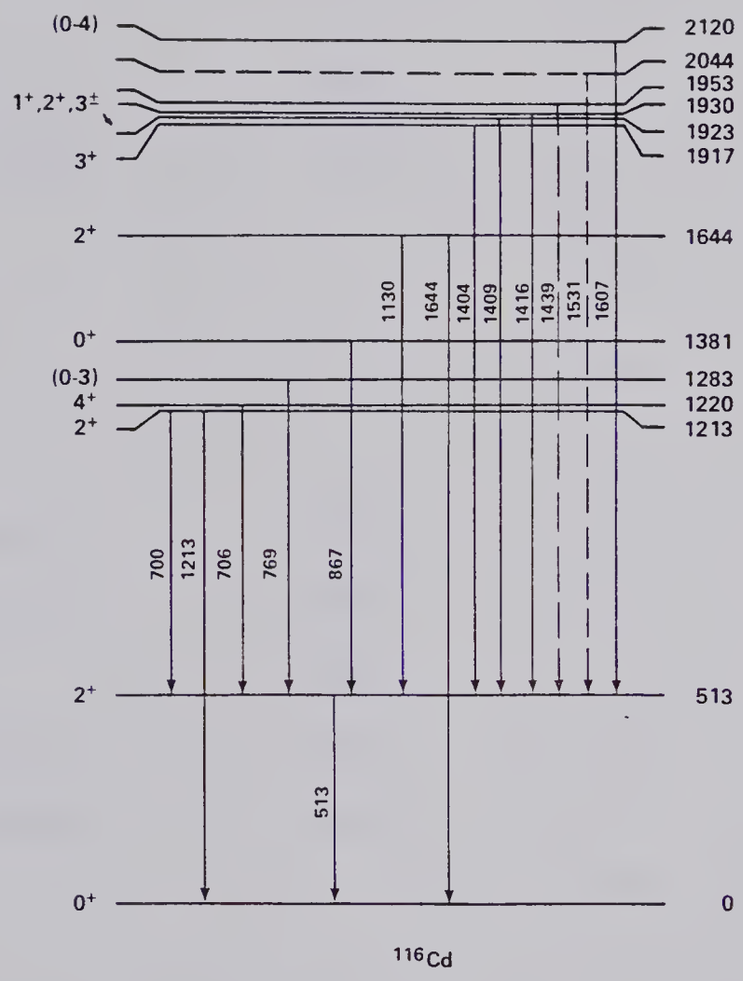

Figure 19. The deduced level and decay scheme of ^{116}Cd. The dotted lines refer to those transitions that were observed, but were too weak to provide useful information. The spin-parity assignments are the result of the present and previous works.

Table VI. The Gamma Ray Mixing Ratios and Spin-Parity Assignments for ^{116}Cd Determined in This Work.

Level Energy[a]	γ-ray Energy	$J_i^\pi \rightarrow J_f^\pi$	Arctanδ
1213	1213	$2^+ \rightarrow 0^+$	0
	700	$2^+ \rightarrow 2^+$	57 13
1220	706	$4^+ \rightarrow 2^+$	0[b]
1283	769	$0^+ \rightarrow 2^+$	0
		$1^\pm \rightarrow 2^+$	all values
		$2^+ \rightarrow 2^+$	28 → 90
		$3^+ \rightarrow 2^+$	78 8
		$3^- \rightarrow 2^+$	-2 7
1381	867	$0^+ \rightarrow 2^+$	0
1644	1644	$2^+ \rightarrow 0^+$	0
	1130	$2^+ \rightarrow 2^+$	-32 19
1917	1404	$3^+ \rightarrow 2^+$	38 20
1923	1409	$1^+ \rightarrow 2^+$	-51 25
		$2^+ \rightarrow 2^+$	63 18
		$3^+ \rightarrow 2^+$	75 9
		$3^- \rightarrow 2^+$	8 8
1930	1416	$0^+ \rightarrow 2^+$	0
		$1^+ \rightarrow 2^+$	all values
		$2^\pm \rightarrow 2^+$	-90 → -52; -7 → 90
		$3^\pm \rightarrow 2^+$	-11 16

(continued....)

Table VI (continued)

		$4^+ \rightarrow 2^+$	$0^{b)}$
2120	1607	$0^+ \rightarrow 2^+$	0
		$1^\pm \rightarrow 2^+$	4 → 69
		$2^\pm \rightarrow 2^+$	1 $\underline{16}$
		$3^\pm \rightarrow 2^+$	-19 $\underline{8}$
		$4^+ \rightarrow 2^+$	$0^{b)}$

a), b) The notation is as in Table V.

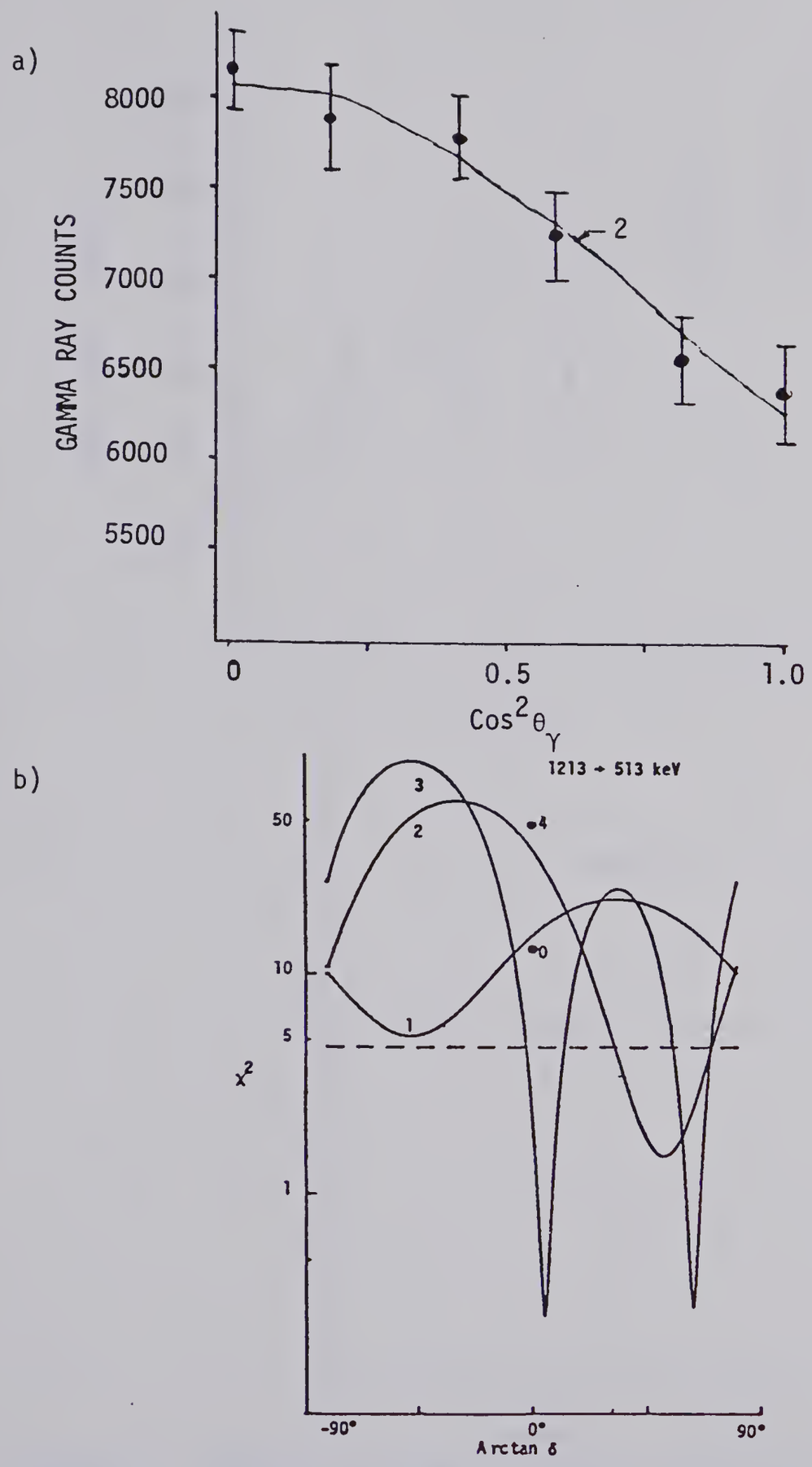

Figure 20. The 1213 keV level: a) angular distribution for the 700 keV γ-ray, and b) χ^2 curves.

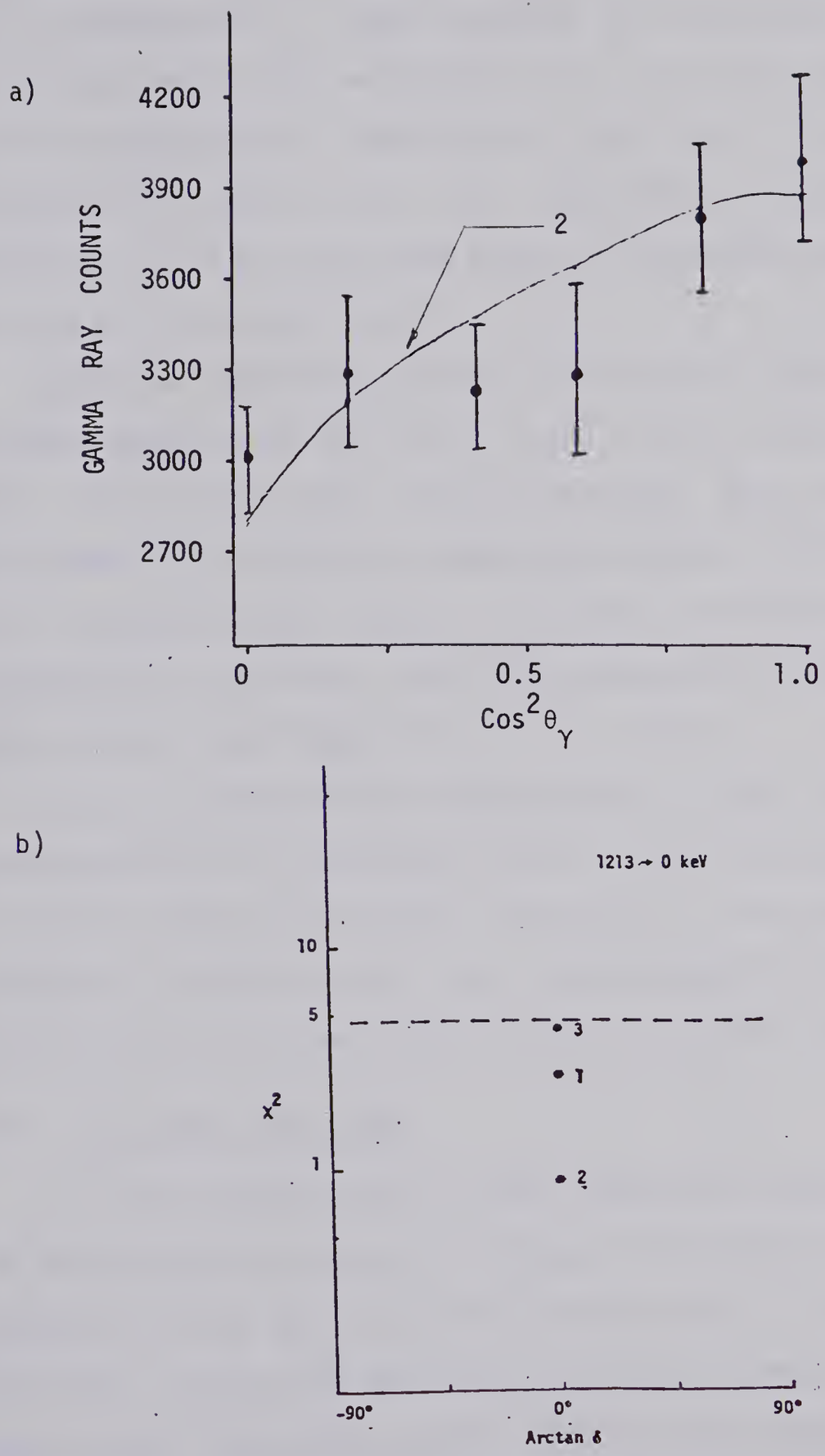

Figure 21. The 1213 keV level: a) angular distribution for the 1213 keV γ-ray, and b) $\chi^2(\delta)$.

513 and 1213 → 0 keV transitions are shown in figs. 20 and 21 respectively. These results are consistent with an initial state spin and parity of 2^+ for the level at 1213 keV excitation. The data for the 1220 → 513 keV transition is shown in fig. 22. The previous assignment (Ca75) of 4^+ to the 1220 keV state is consistent with the results of the present work.

Previous information about the level at 1283 keV excitation comes from the (p,p') |ref. De72|, (p,p'γ) |ref. De73|, and (n,n'γ) |ref. Gi74| reactions. Spin assignments made on the basis of these experiments were 2^+, 2^+, and 0^+ respectively. As fig. 23 shows, the angular distribution for the 1283 → 513 keV transition is consistent with initial state spins of 0, 1, 2, and 3.

Angular distribution measurements for the 1381 → 513 keV transition are consistent with a spin assignment of 0^+ for the level at 1381 keV excitation. The angular distribution is shown in fig. 24. An assignment of $J^\pi = 0^+$ for this level has been made in previous works (Ca73).

4.2.2 The 1644 keV level.

In the present work, we have observed a level at 1644 keV de-excited by γ-rays of 1644 and 1130 keV to the ground and first excited states respectively. The results for these transitions are shown in figs. 25 and 26. The 1644 → 0 keV transition allows possible spin assignments for this state of 2 and 3. Values of arctan δ for the

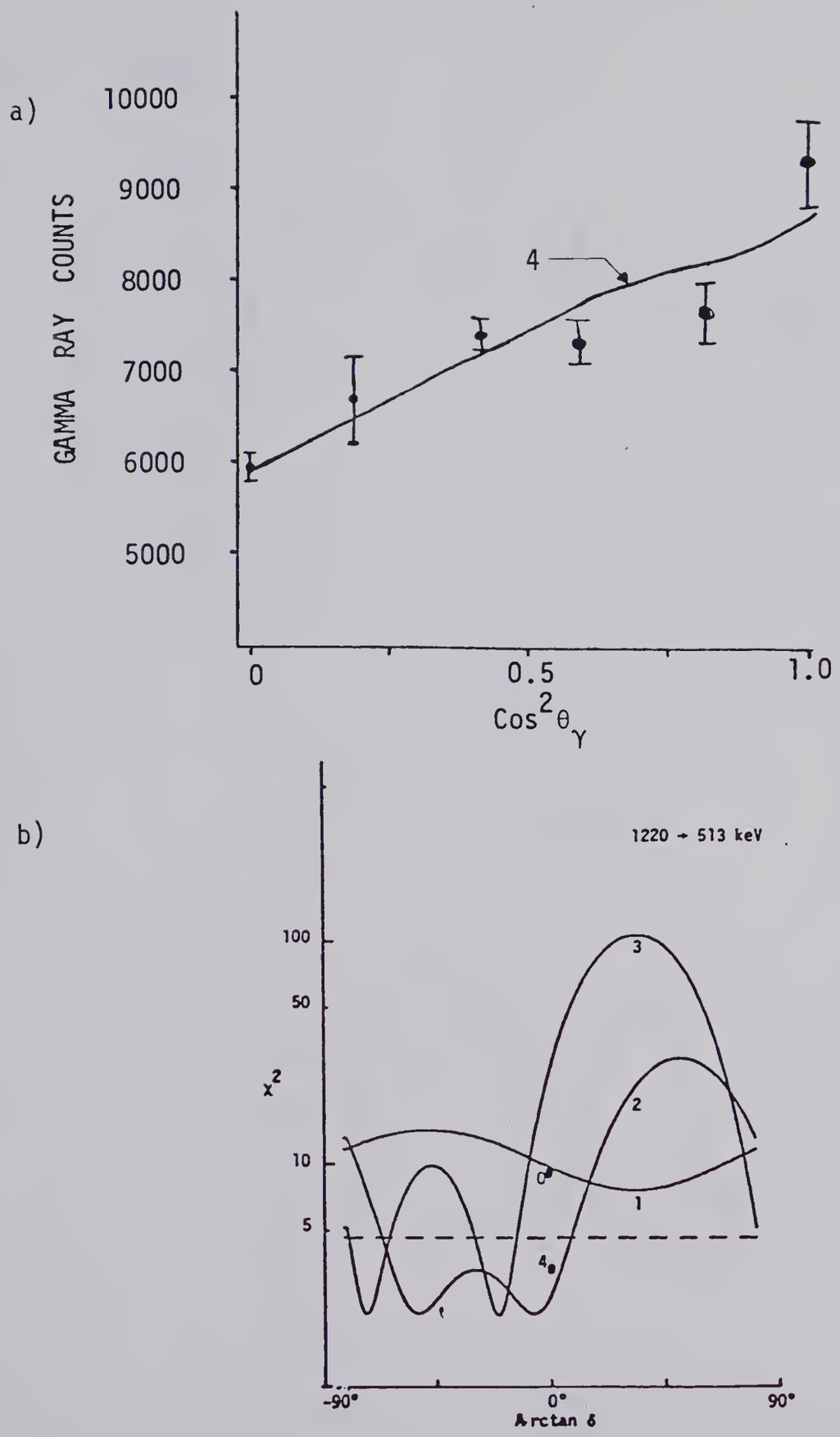

Figure 22. The 1220 keV level: a) angular distribution for the 706 keV γ-ray, and b) χ^2 curves.

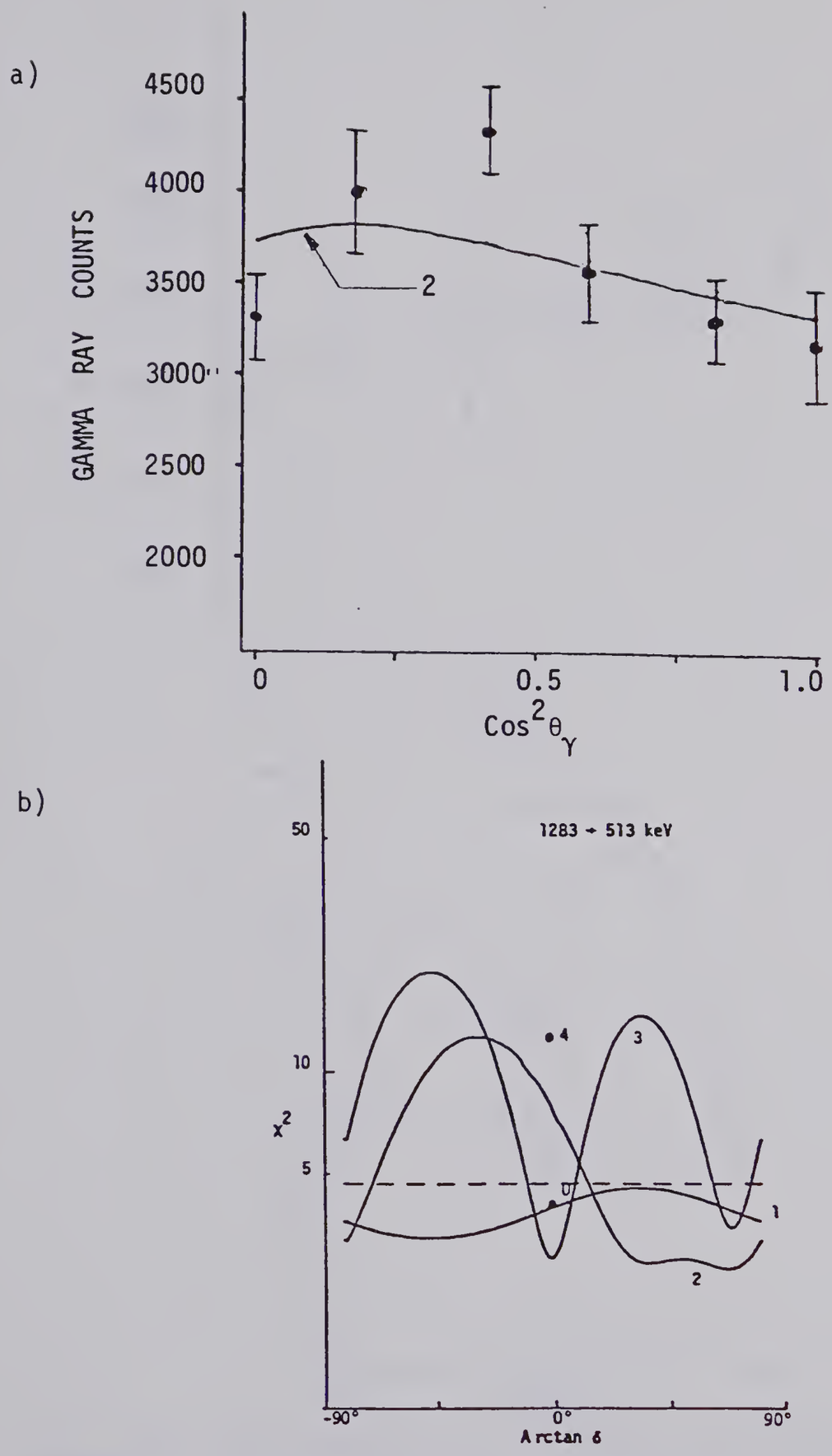

Figure 23. The 1283 keV level: a) angular distribution for the 769 keV γ-ray, and b) χ^2 curves.

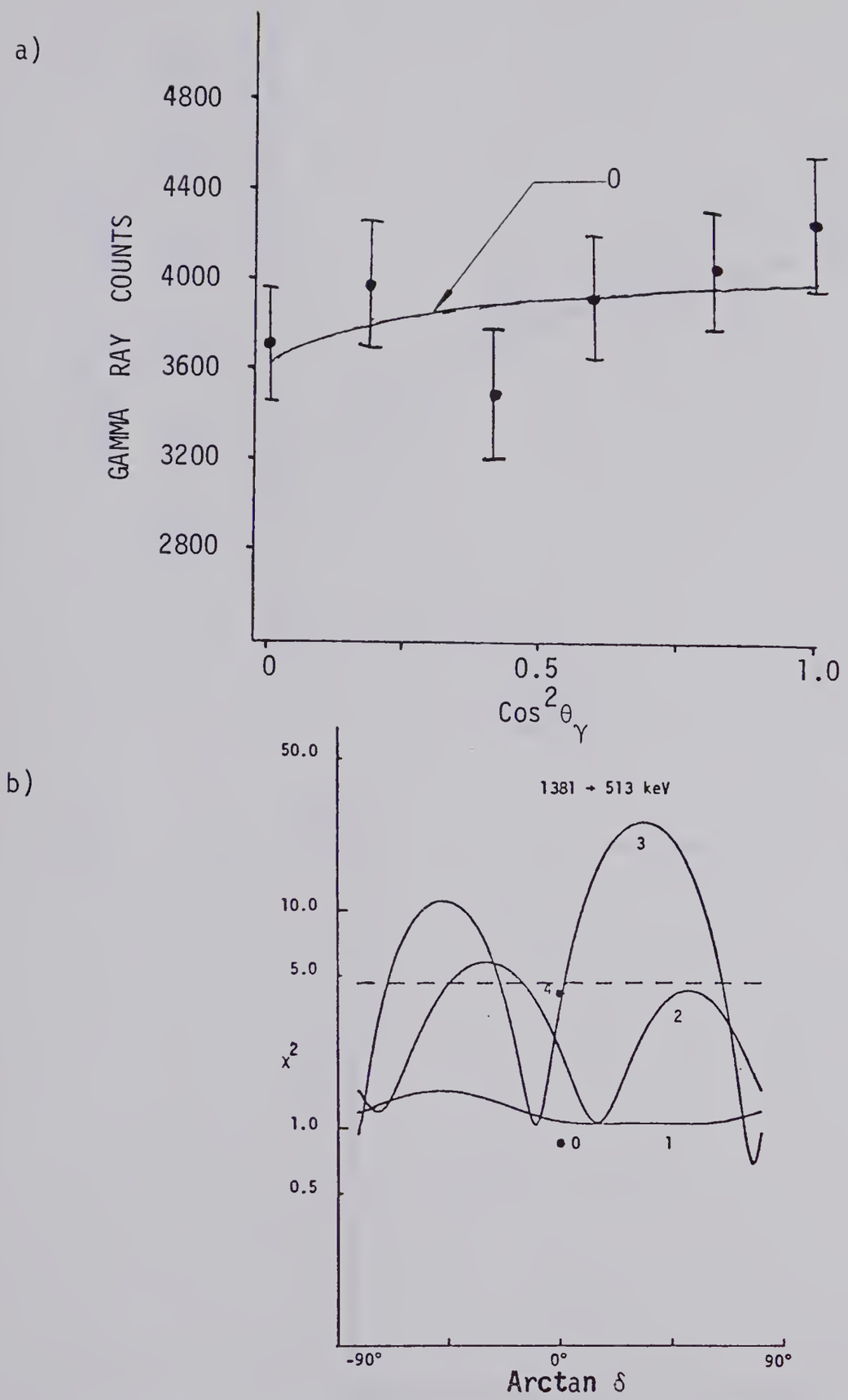

Figure 24. The 1381 keV level: a) angular distribution for the 867 keV γ-ray, and b) χ^2 curves.

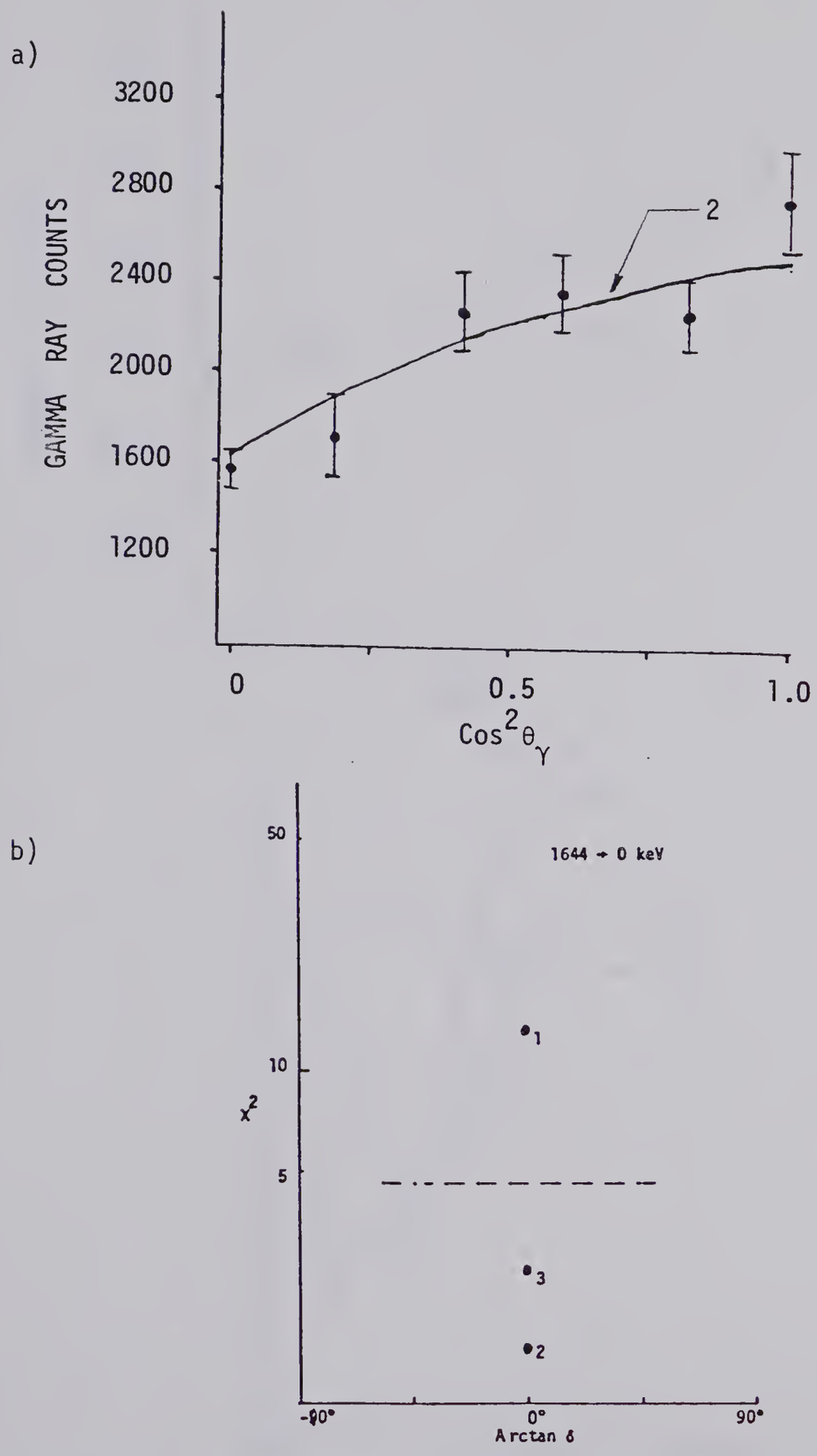

Figure 25. The 1644 keV level: a) angular distribution for the 1644 keV γ-ray, and b) χ^2 curves.

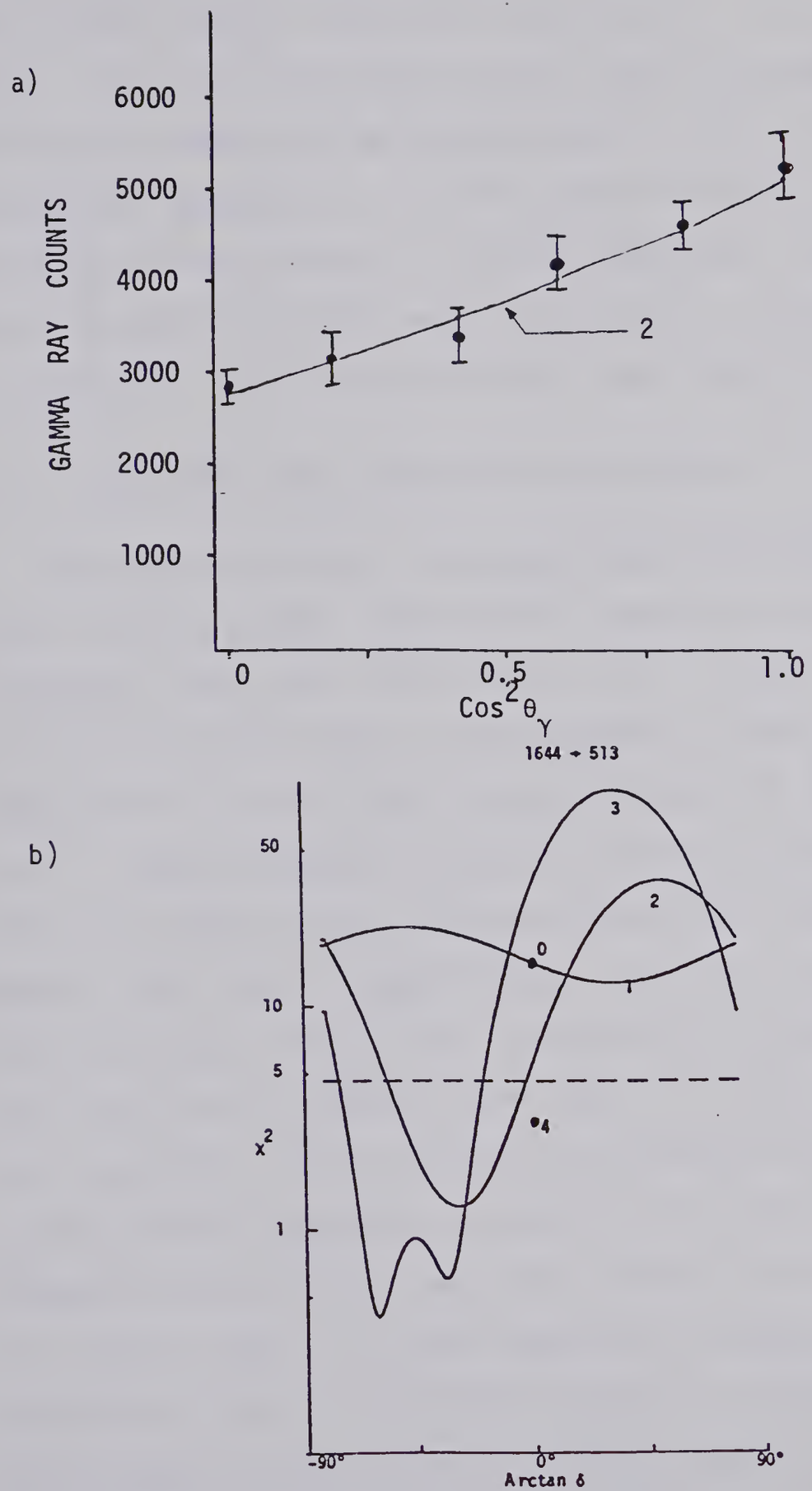

Figure 26. The 1644 keV level: a) angular distribution for the 1130 keV γ-ray, and b) χ^2 curves.

1644 → 513 keV transition ($J_i^\pi \rightarrow 2^+$) further limit the initial state spin-parity to 2^+ or 3^+. If this state is 3^+, then the decay of the 1644 keV state to the ground state will be by M3 radiation only. This is relatively improbable as the Weisskopf estimate for the lifetime of this state is 5 μsec. Therefore, we deduce that the 1644 keV level has a spin of 2^+. A tentative assignment of (2,3) has previously been made (Gi74).

4.2.3 The 1917, 1923, and 1930 keV levels.

The states at 1917, 1923, and 1930 keV excitation occur, within errors, where the 3^- octupole state was originally identified [ref. Ko69, De72]. These states all have reported (Gi74) γ-ray branches to the 513 keV first excited state, which has an established spin-parity of 2^+. Sample angular distribution data and plots of $\chi^2(\delta)$ for these three γ-ray transitions are shown in Figs. 27, 28, and 29, respectively. For the 1917 → 513 keV transition, minima occur below the 0.1% confidence level only for an initial state spin of 3, in disagreement with a previous (Gi74) tentative assignment of 0. The large quadrupole strength ($\arctan\delta = 38° \pm 20°$) for this transition makes it unlikely that the 1917 keV state is 3^-. For the 1923 → 513 keV transition, minima in $\chi^2(\delta)$ occur below the 0.1% confidence limit for initial spins of 1, 2, and 3. The value of $\arctan\delta$ of $-8° \rightarrow 8°$ deduced

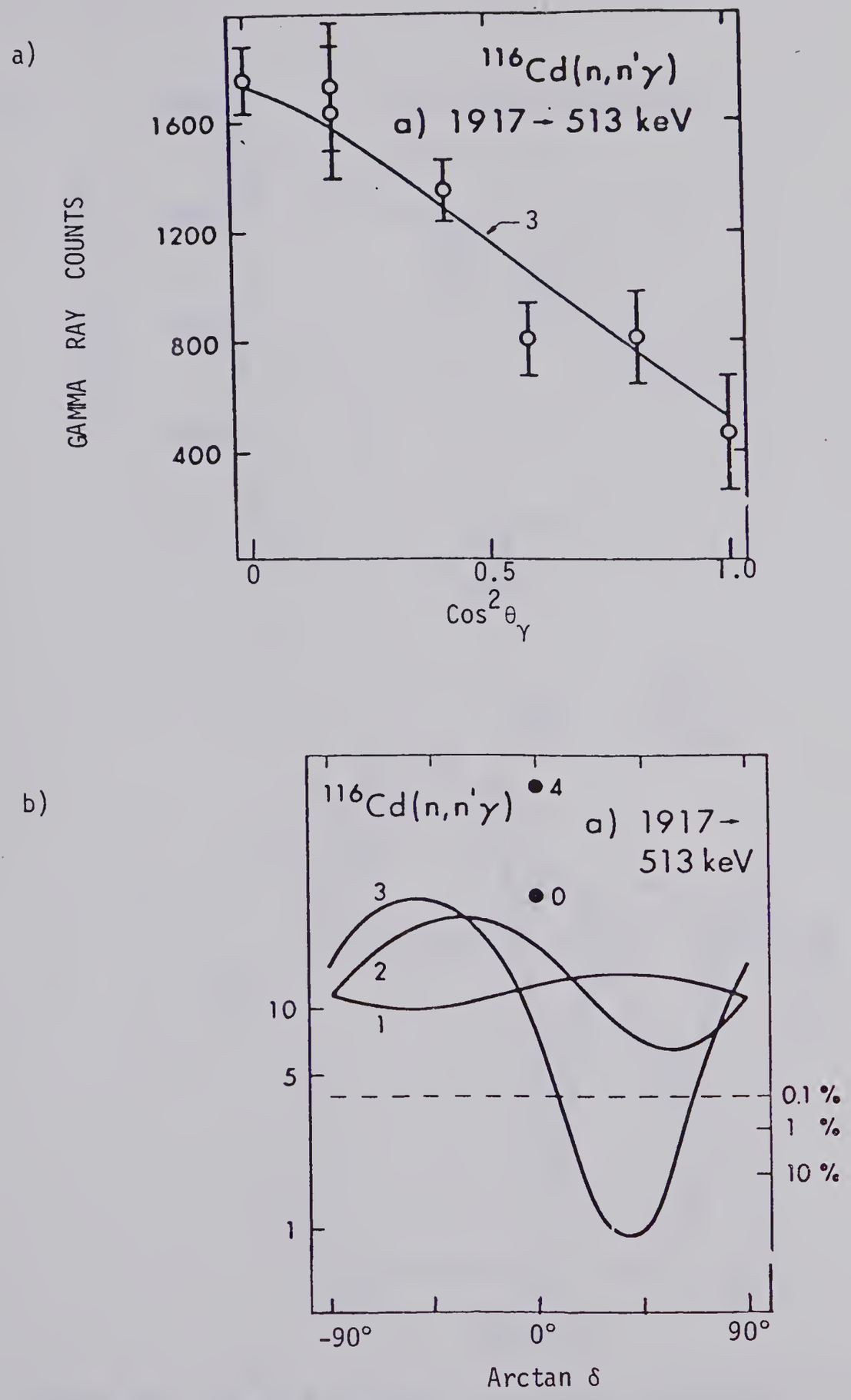

Figure 27. The 1917 keV level: a)angular distribution for the 1404 keV γ-ray, and b) the χ^2 curves.

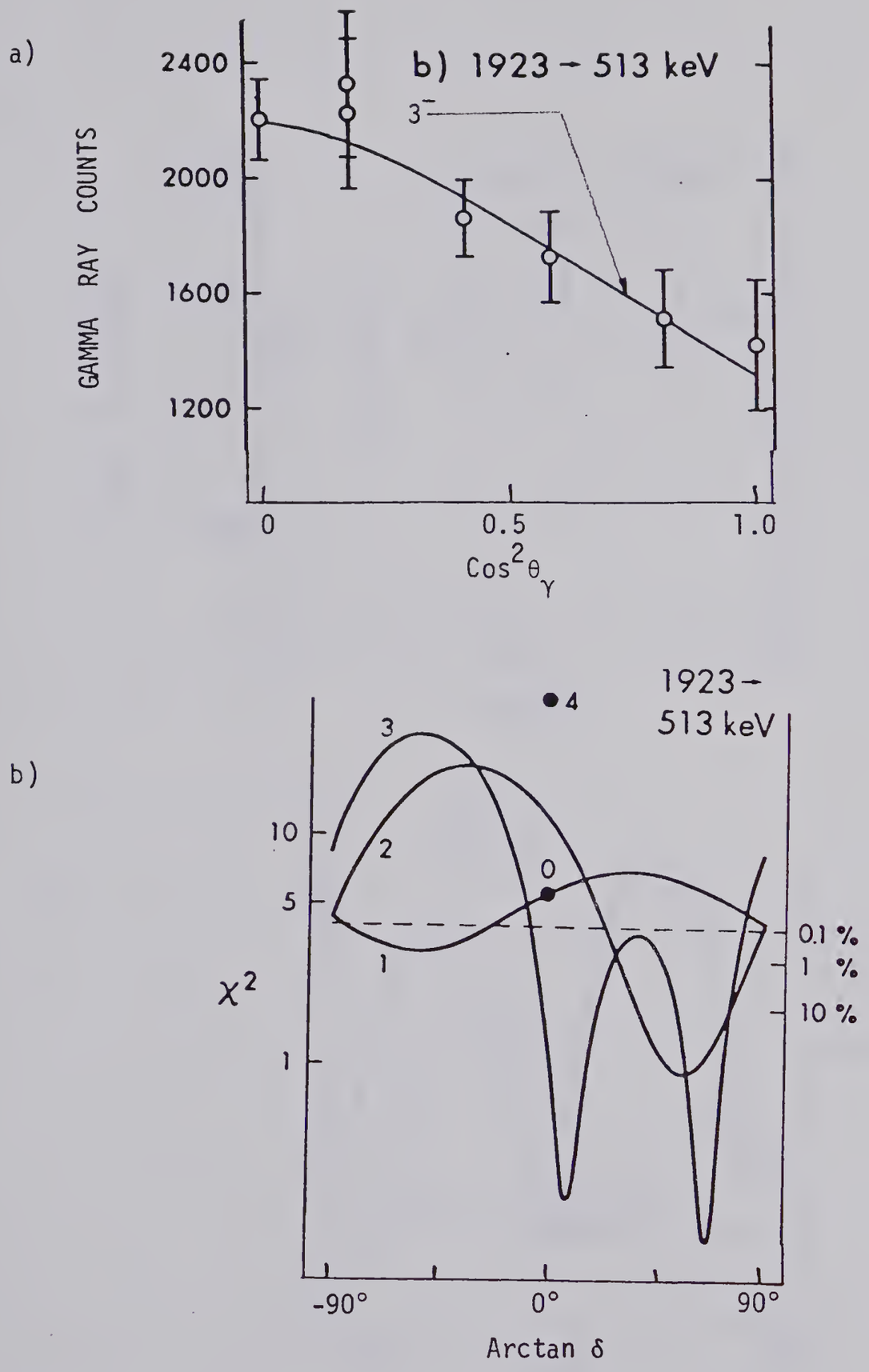

Figure 28. The 1923 keV level: a) angular distribution for the 1409 keV γ-ray, and b) χ^2 curves.

a)

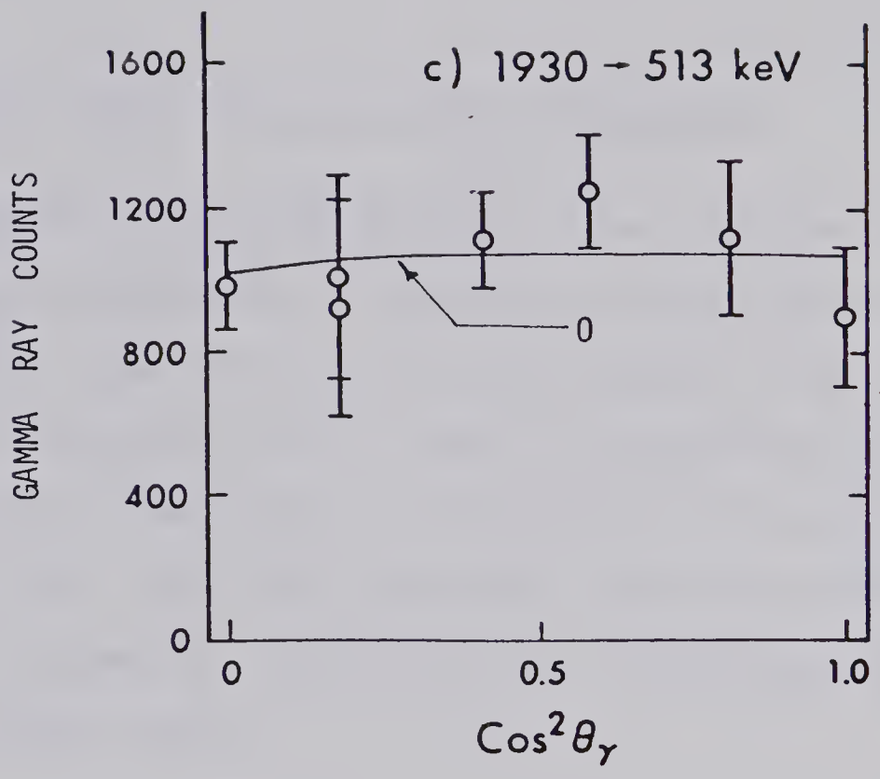

b)

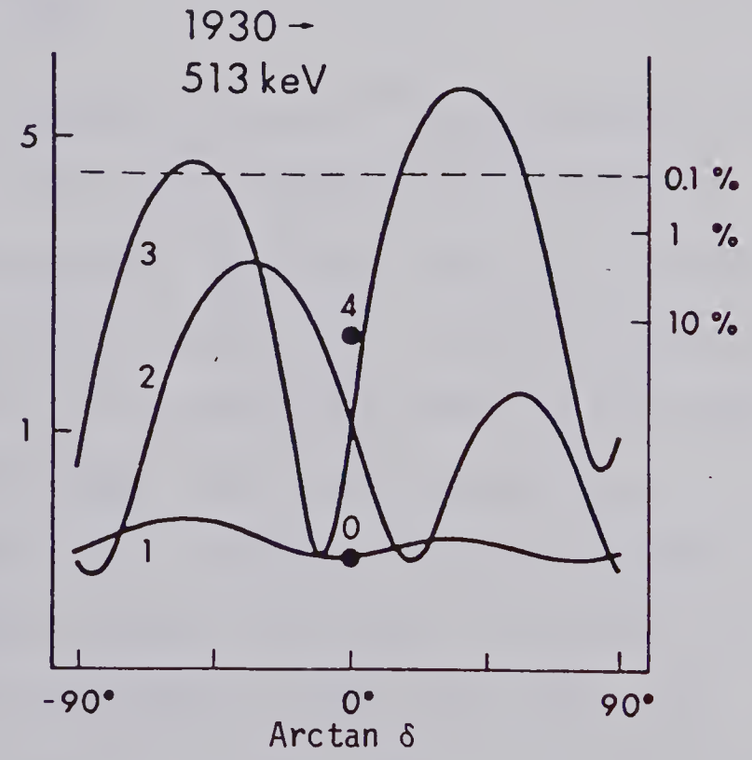

Figure 29. The 1930 keV level: a) angular distribution for the 1416 keV γ-ray, and b) χ^2 curves.

for an initial spin of 3 is consistent with an assignment of 3^- for the 1923 keV state. The data for the 1930 → 513 keV transition place no restriction on its spin-parity.

4.2.4 The 1953, 2044, and 2120 keV levels.

The 1953 → 513 keV transition was observed, but the large background in the forward angles prohibited any useful information from being deduced. The 2044 → 513 keV transition was too weak to provide any useful information. The angular distribution measurements, for the 2120 → 513 keV transition, which are shown in fig. 30, placed no restriction on the spin-parity of the 2120 keV state.

4.3 Results for ^{146}Nd.

Typical γ-ray spectra for the ^{146}Nd experiment are shown in fig. 31. The γ-ray transitions between the levels in ^{146}Nd are labeled by their energies, in keV. The energies determined in this work, with the exception of the level at 1377 keV, previously given as 1372 keV, are in excellent agreement with those adopted by Burrows (Bu75). The level and decay scheme is shown in fig. 32. This scheme differs from that of Burrows in that a new level is proposed at 1787 keV, while the previously adopted levels at 1515, 1538, 1751, 1837, and 1913 keV are absent as they were not observed in this

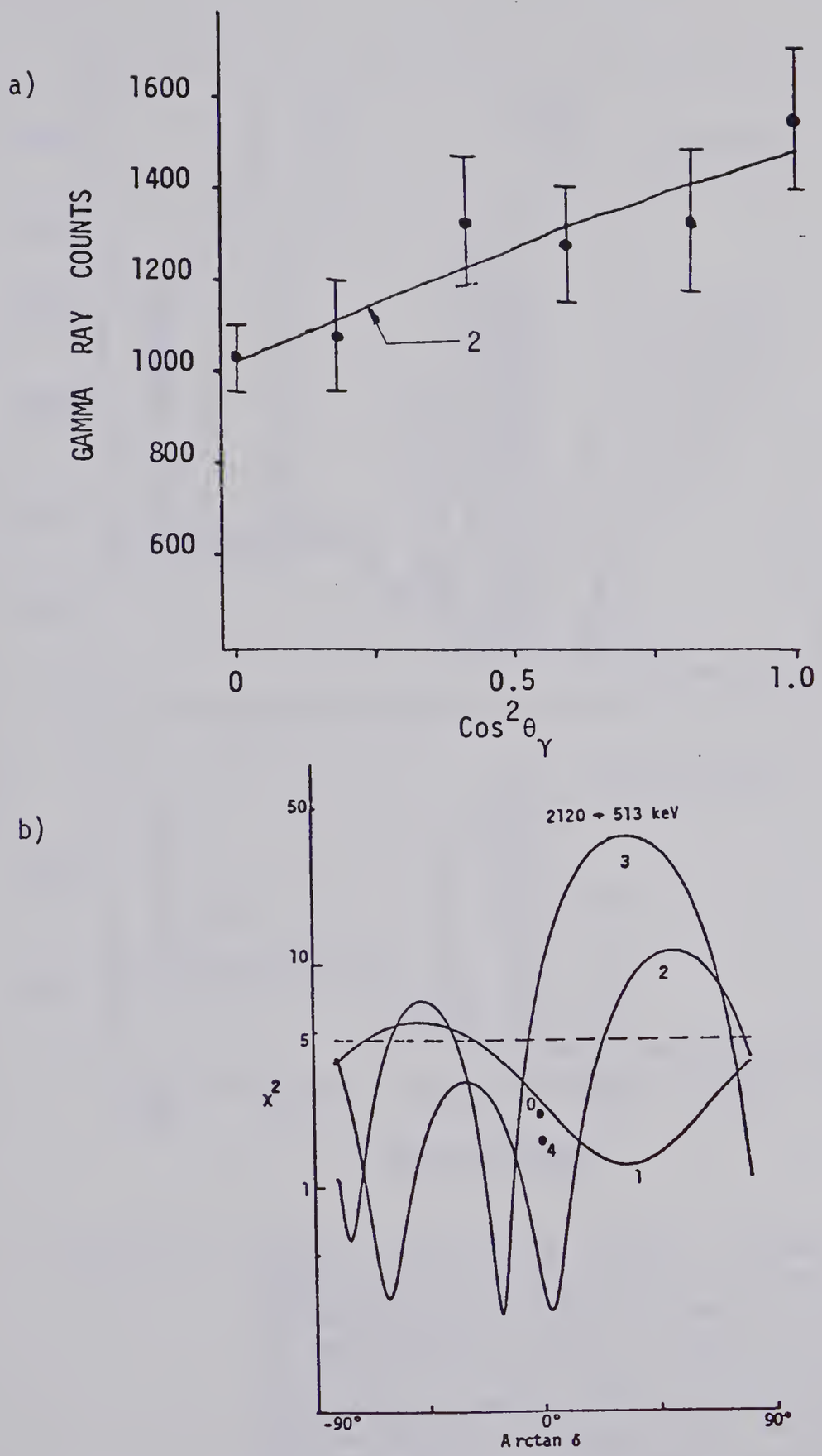

Figure 30. The 2120 keV level: a) angular distribution for the 1607 keV γ-ray, and b) χ^2 curves.

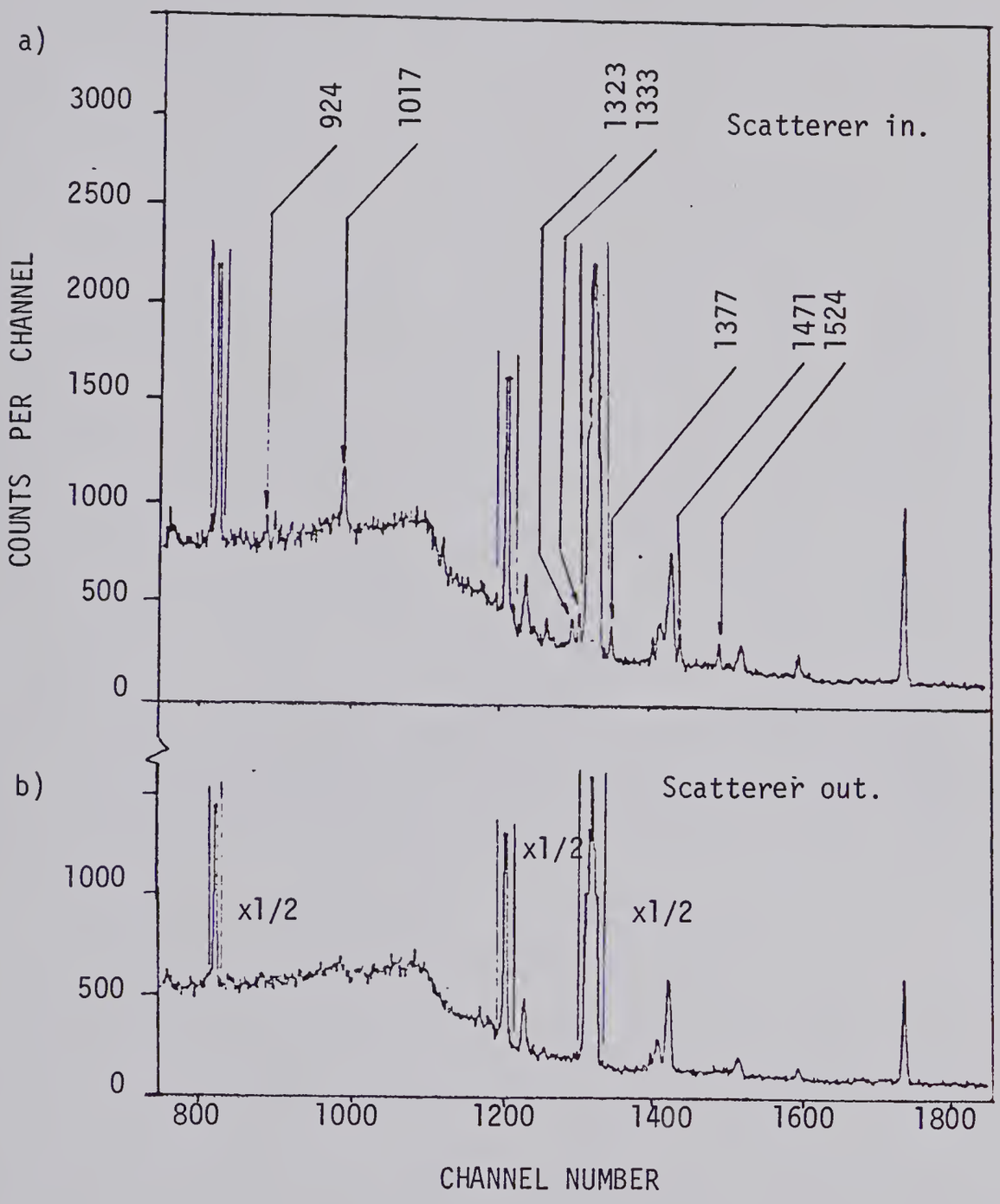

Figure 31. Typical γ-ray spectra for the ^{146}Nd experiment, taken at En$\leq$2.67 MeV, θ=90°. a) The scatterer in spectrum. The numbers above each peak refer to the energies, in keV, of the γ-ray transitions in ^{146}Nd. The three peaks that have lines on each side are drawn at 1/2 of the observed strength. b) The scatterer out spectrum. The data collection time for this spectrum was approximately 1/2 of the time taken for the spectrum shown in a).

Figure 32.

The deduced level and decay scheme of ^{146}Nd. The dotted lines refer to transitions that were observed, but were too weak to provide useful information. The spin-parity assignments are the result of the present and previous works.

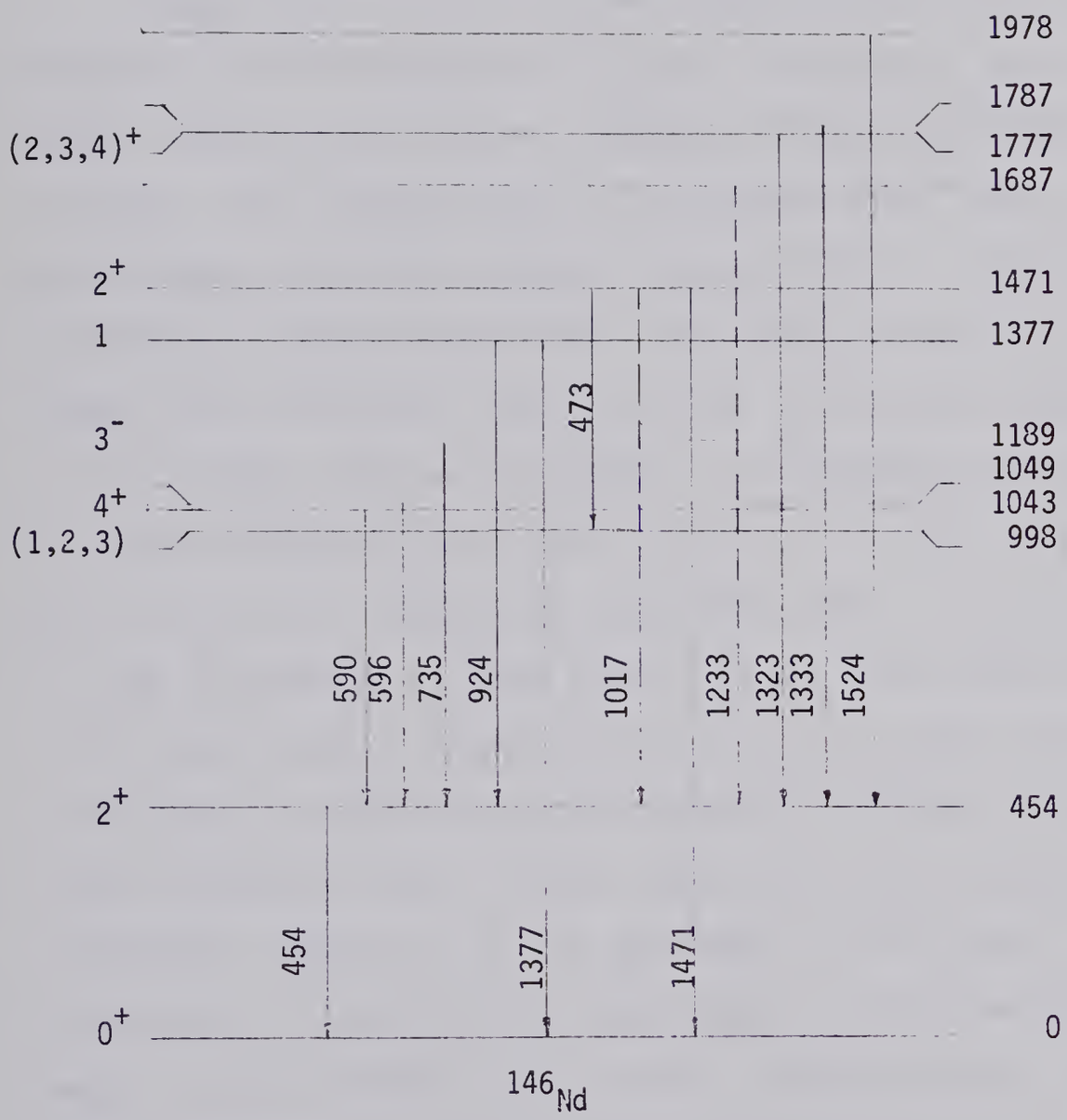
1978
1787
(2,3,4)+
1777
1687
2+
1471
1
1377
473
3-
1189
1049
4+
1043
(1,2,3)
998
590
596
735
924
1017
1233
1323
1333
1524
2+
454
454
1377
1471
0+
0
146Nd

work. The spin-parity assignments and multipole mixing ratios deduced in this work are summarized in Table VII. The one phonon 2^+ state at 454 keV was not studied in this work.

4.3.1 The 998, 1043, and 1049 keV levels.

These three states lie at approximately twice the energy of the one-phonon 2^+ state. Therefore, one might expect that they are members of the two-phonon triplet. The 998 keV has two reported decay modes; to the ground and first excited states (Gr68). Although neither of these transitions was seen in this work, a gamma ray transition from the state at 1471 keV excitation to this level was observed. The angular distribution for this transition is shown in fig. 33. This data was put through the computer program EVA with J_i^π fixed at 2^+ and J_f^π allowed to vary from 0 to 4. The resultant $\chi^2(\delta)$ plot allowed possible spins of 1, 2, and 3 for this state. The results for the 1043 → 454 keV transition, shown in fig. 34, are consistent with the previous assignment (Bu75) of 4^+ for the level at 1043 keV excitation. The 1049 keV level has one reported decay mode; to the 454 keV level (Gr68). Unfortunately, the large background in the γ-ray spectrum due to the $^{74}Ge(n,n'\gamma)$ reaction prohibited any useful information from being deduced.

Table VII. The Gamma Ray Mixing Ratios and Spin-Parity Assignments for ^{146}Nd Determined in This Work.

Level Energy[a]	γ-ray energy	$J_i^\pi \rightarrow J_f^\pi$	Arctanδ
998	474	$2^+ \rightarrow 1$	10 → 60
		$2^+ \rightarrow 2$	37 → 73
		$2^+ \rightarrow 3$	-77 → -23
1043	590	$4^+ \rightarrow 2^+$	0[b]
1189	735	$3^- \rightarrow 2^+$	5 $\underline{5}$
1377	1377	$1 \rightarrow 0^+$	0
	924	$1 \rightarrow 2^+$	-90 → 90
1471	1471	$2 \rightarrow 0^+$	0
1777	1323	$2^+ \rightarrow 2^+$	-32 $\underline{18}$
		$3^+ \rightarrow 2^+$	-81 → -25
		$4^+ \rightarrow 2^+$	0[b]
1778	1333	$0^+ \rightarrow 2^+$	0
		$1 \rightarrow 2^+$	-90 → 90
		$2 \rightarrow 2^+$	-81 → 27
		$3 \rightarrow 2^+$	-16 $\underline{11}$
		$4^+ \rightarrow 2^+$	0[b]
1978	1524	$0^+ \rightarrow 2^+$	0
		$1^+ \rightarrow 2^+$	±(90 → 45)
		$2 \rightarrow 2^+$	-75 → 14

(continued....)

Table VII (continued).

	3	2^+	-90	-70
			-35	-13
	4^+	2^+	$0^{b)}$	

a), b) notation is as in Table V.

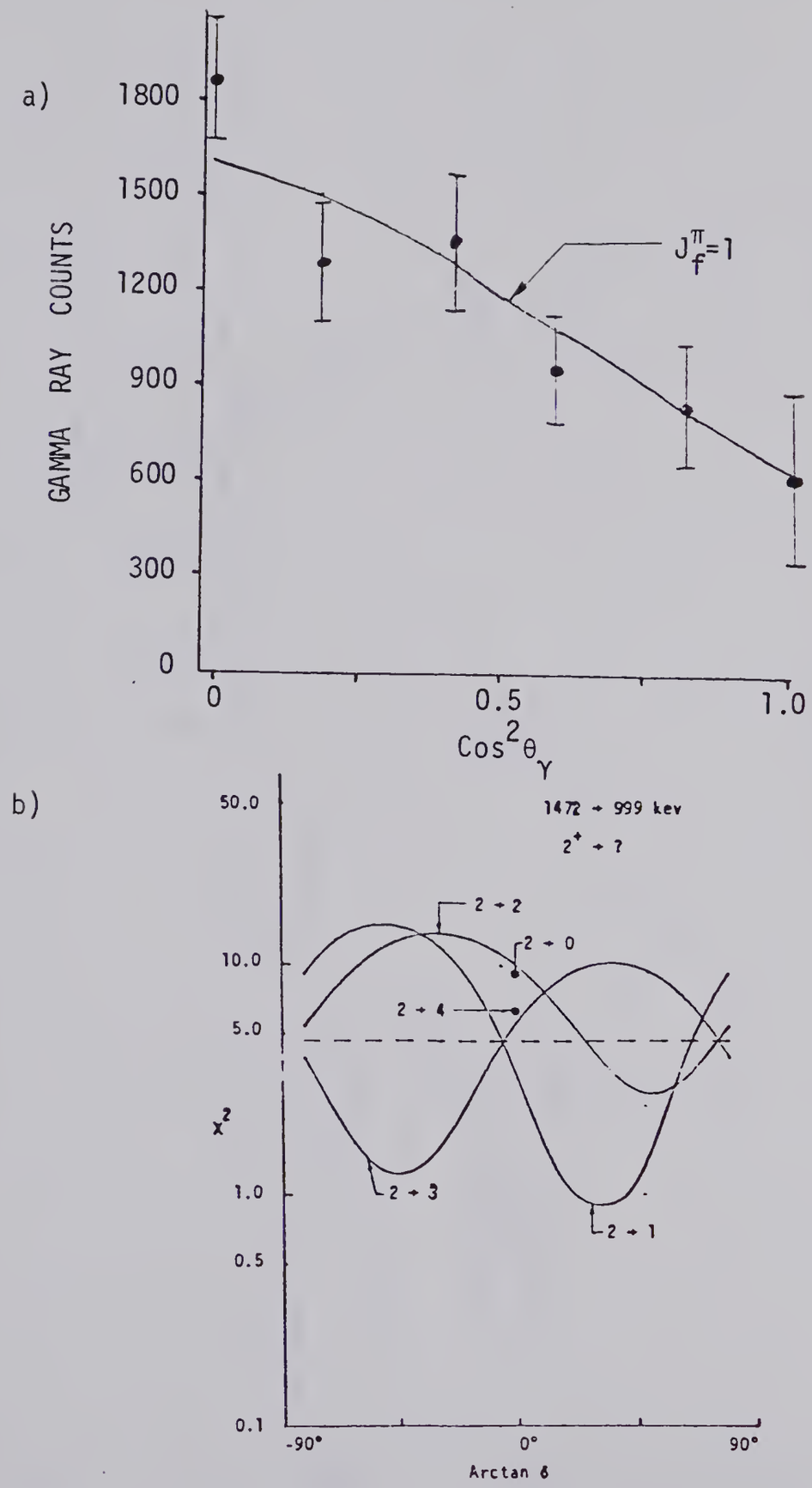

Figure 33. The 999 keV level: a) angular distribution for the 474 keV γ-ray, and b) χ^2 curves.

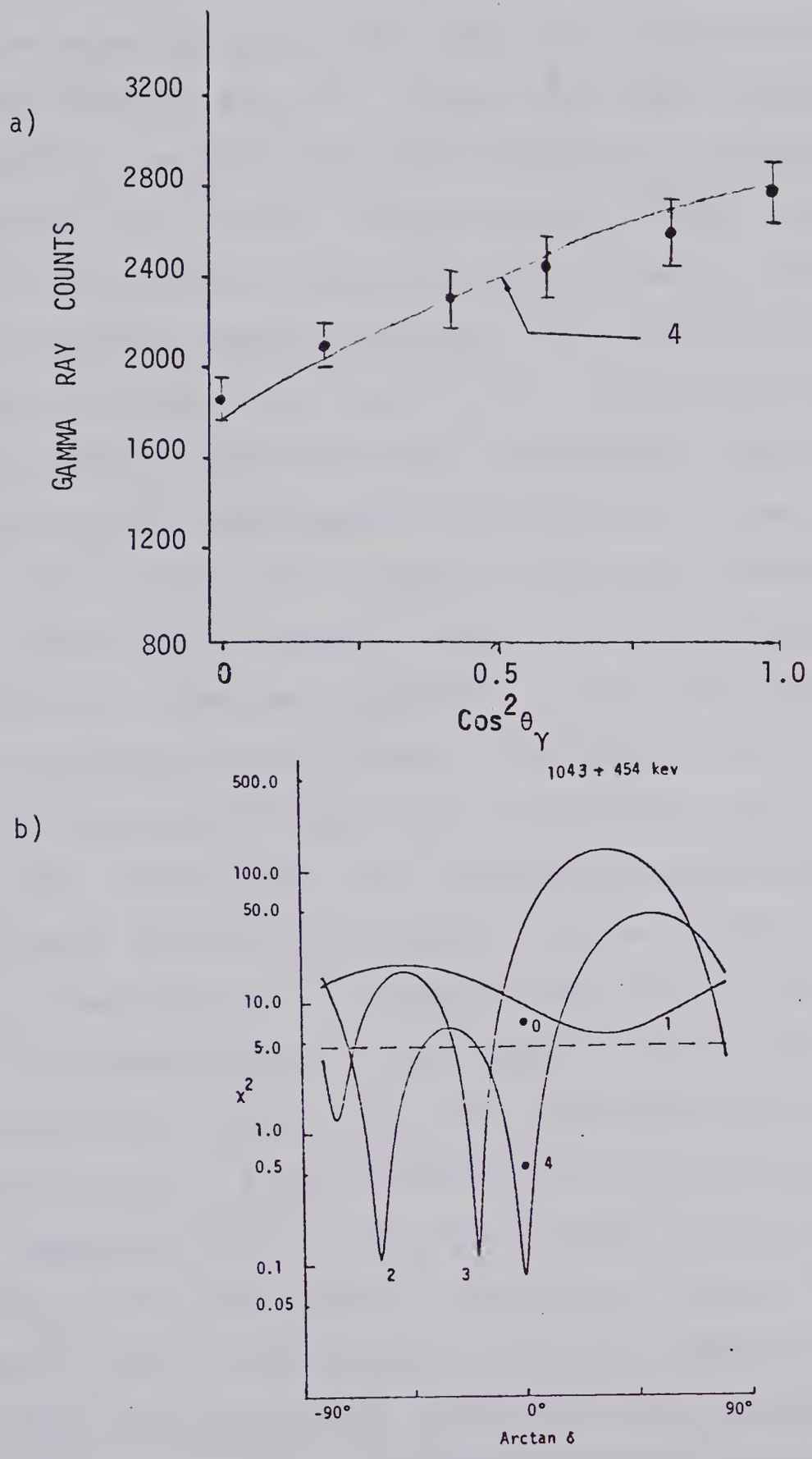

Figure 34. The 1043 keV level: a) angular distribution for the 590 keV γ-ray, and b) χ^2 curves.

4.3.2. The 1189, 1377, 1471, and 1687 keV levels.

The data and results for the 1189 → 454 keV transition are shown in fig. 35. As the $\chi^2(\delta)$ plot illustrates, the results are consistent with the previous spin-parity assignment of 3^- (Bu75). Therefore, for ^{146}Nd, the octupole state occurs at approximately the energy predicted by the harmonic vibrational model. The level at 1377 keV was seen to decay *via* γ-rays of 1377 and 924 keV to the ground and first excited states respectively. The angular distribution measurements for the 1377 → 0 keV transition, shown in fig. 36, allowed a unique spin assignment of 1. The deduced values of the multipole mixing ratio for the 1377 → 454 keV transition (see fig. 37) did not limit the parity of this state. The level at 1471 keV excitation was seen to decay *via* γ-rays of 474, 1017, and 1471 keV. The 474 keV γ-ray has already been discussed in the context of the 999 keV level. In the forward angle runs, we were not able to resolve the 1017 keV γ-ray from the ^{27}Al background peak. The results for the 1471 → 0 keV transition, shown in fig. 38, permit initial state spins of 2 or 3. A spin assignment of 2^+ has previously been suggested (Bu75). The level at 1687 keV was observed to decay to the one phonon 2^+ state by a γ-ray of 1233 keV. As can be seen in the scatterer out γ-ray spectrum (see fig. 31b) this is the same energy as a γ-ray transition in ^{19}F. The statistics for the ^{146}Nd 1233 keV γ-ray that

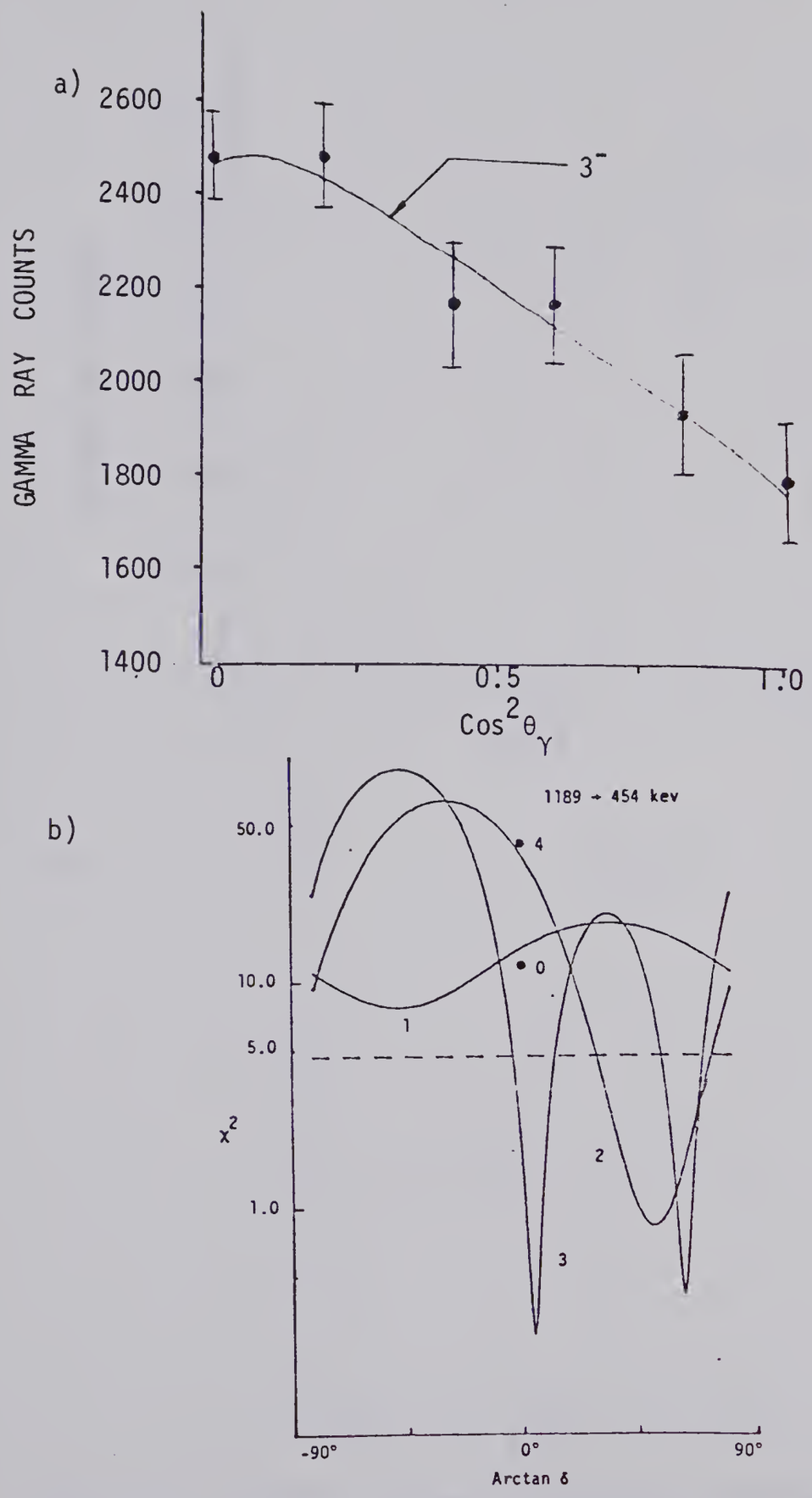

Figure 35. The 1189 keV level: a) angular distribution for the 735 keV γ-ray, and b) χ^2 curves.

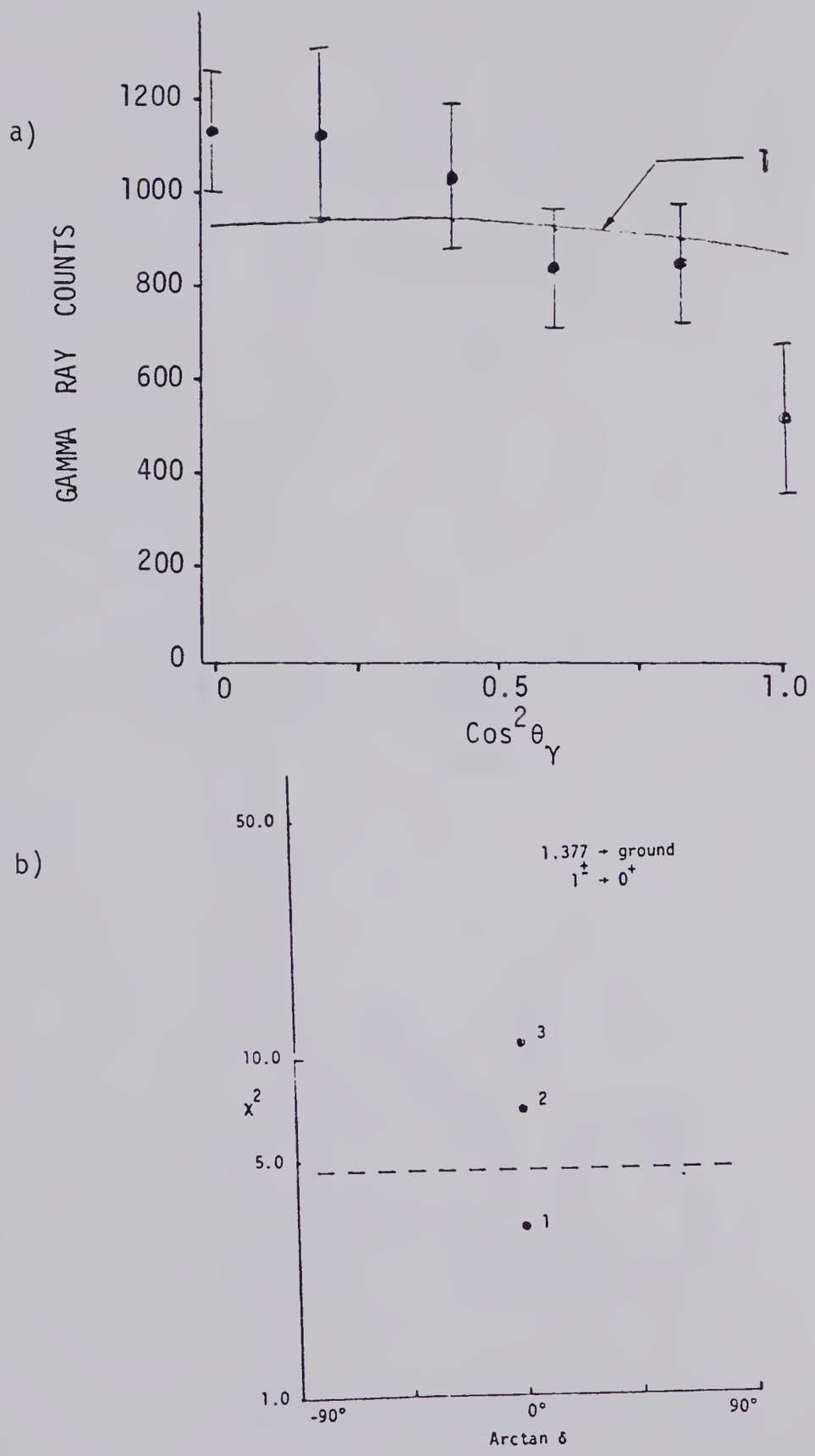

Figure 36. The 1377 keV level: a) angular distribution for the 1377 keV γ-ray, and b) $\chi^2(\delta=0)$.

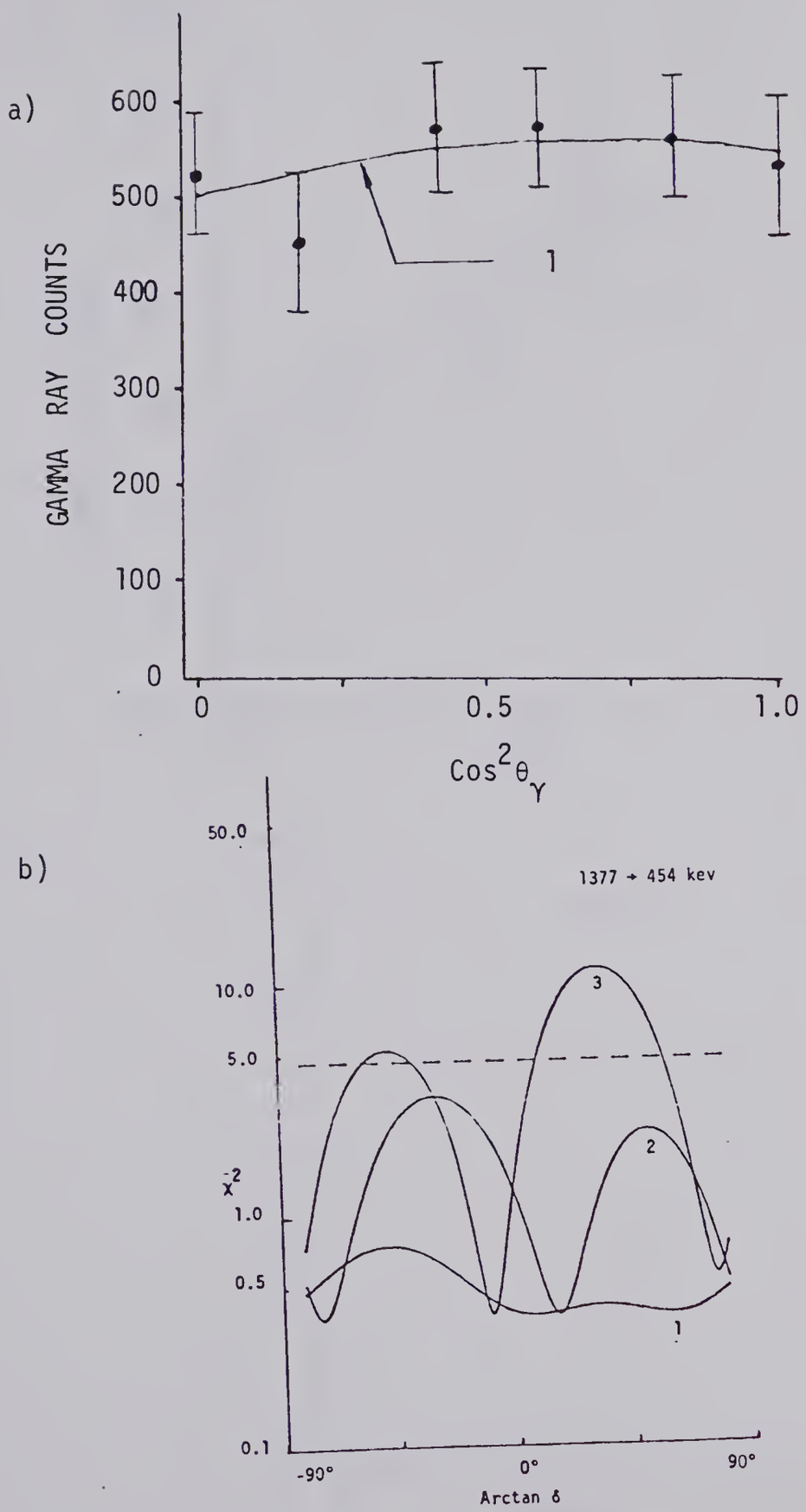

Figure 37. The 1377 keV level: a) angular distribution for the 924 keV γ-ray, and b) χ^2 curves.

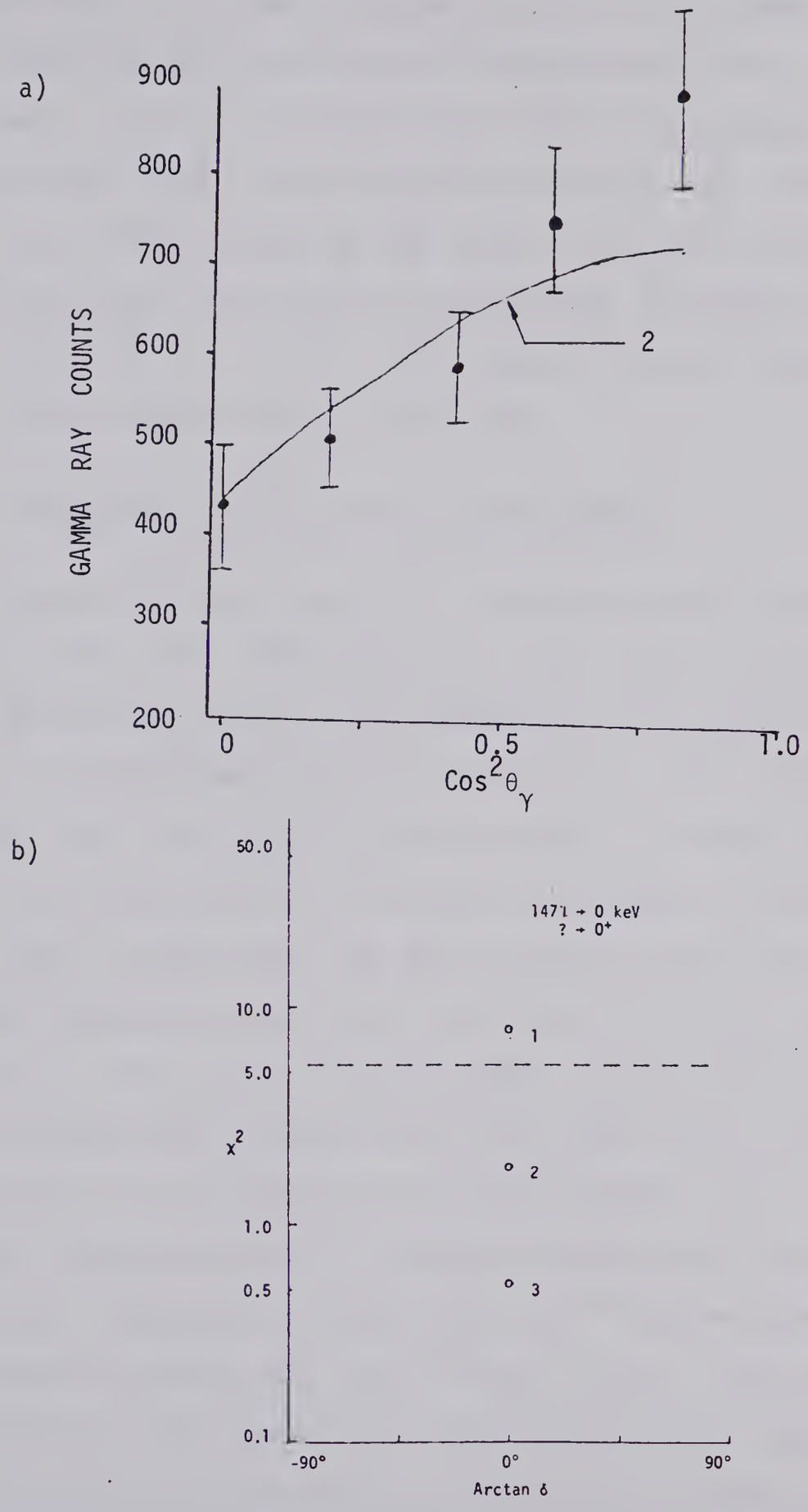

Figure 38. The 1472 keV level: a) angular distribution for the 1471 keV γ-ray, and b) $\chi^2(\delta=0)$.

results from a scatter-in minus scatterer-out spectrum were too poor to allow any information to be deduced. In (n,γ) capture work (Gr68), an observed γ-ray of 1687 keV was attributed to this level. This was later contradicted by the results from the (d,d') reaction (Ch70) which gave a spin-parity assignment of 0^+ to the 1687 keV level. No γ-rays of energy near 1687 keV were observed in this work.

4.3.3 The 1777, 1787, and 1978 keV levels.

The results for the 1777 → 454 keV transition are shown in fig. 39. The values of the initial state's spin that are below the 0.1% confidence level are 2, 3, and 4. The deduced values of arctanδ for these spins further limit the parity to be positive. No spin assignment for this level has previously been made. The 1333 keV γ-ray, as with the 1323 keV γ-ray from the 1777 → 454 keV transition, was seen only during the E_p = 3.60 MeV runs. As a γ-ray of this energy was not observed in the scatterer-out spectrum, the 1333 keV γ-ray must be the result of a transition in the Nd target. No γ-rays of this energy have been reported for the other Nd isotopes. Therefore, a new level for ^{146}Nd has been proposed to account for the 1333 keV γ-ray. The angular distribution measurements for this transition, shown in fig. 40, place no restriction on the spin of this state.

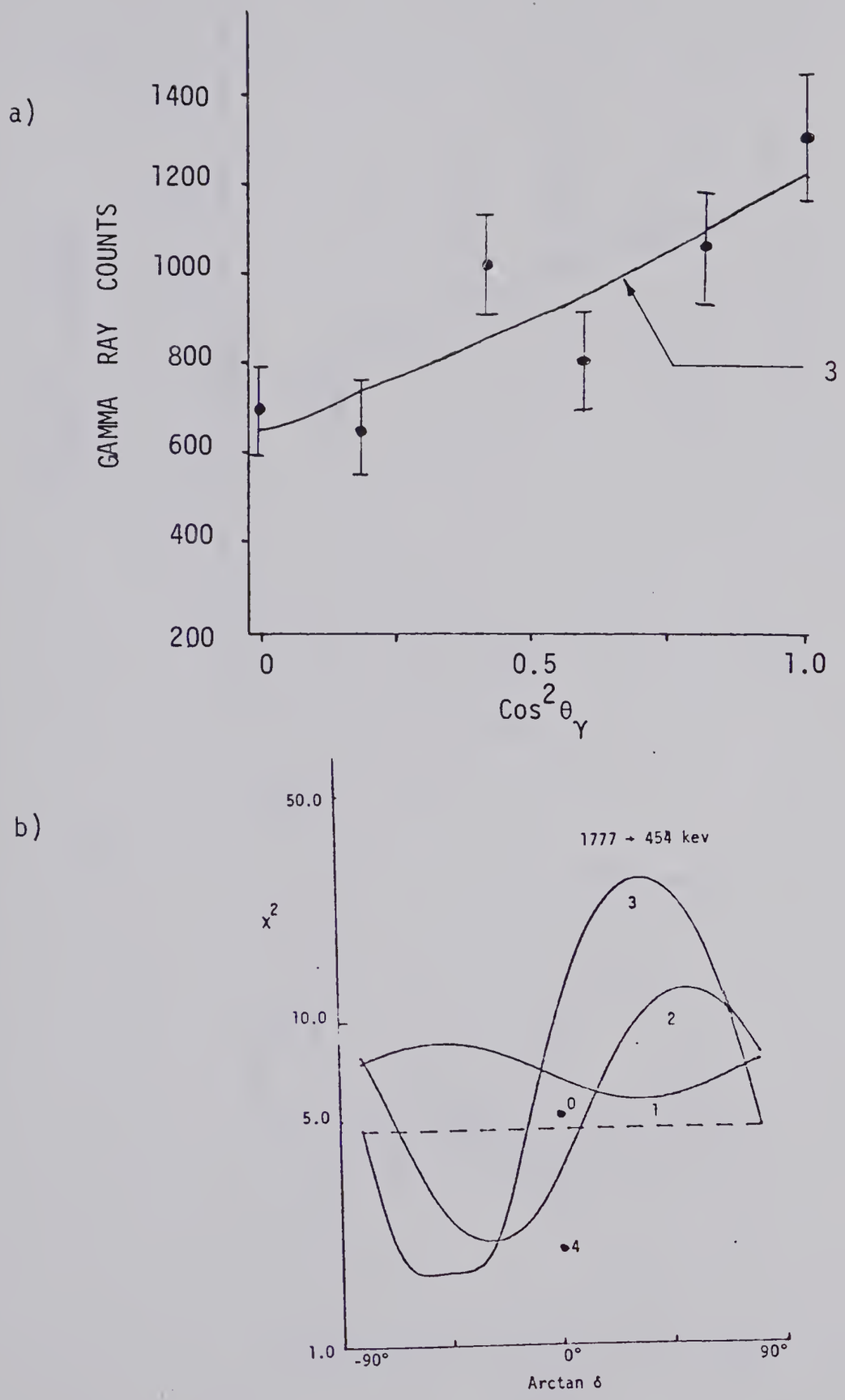

Figure 39. The 1777 keV level: a) angular distribution for the 1323 keV γ-ray, and b) χ^2 curves.

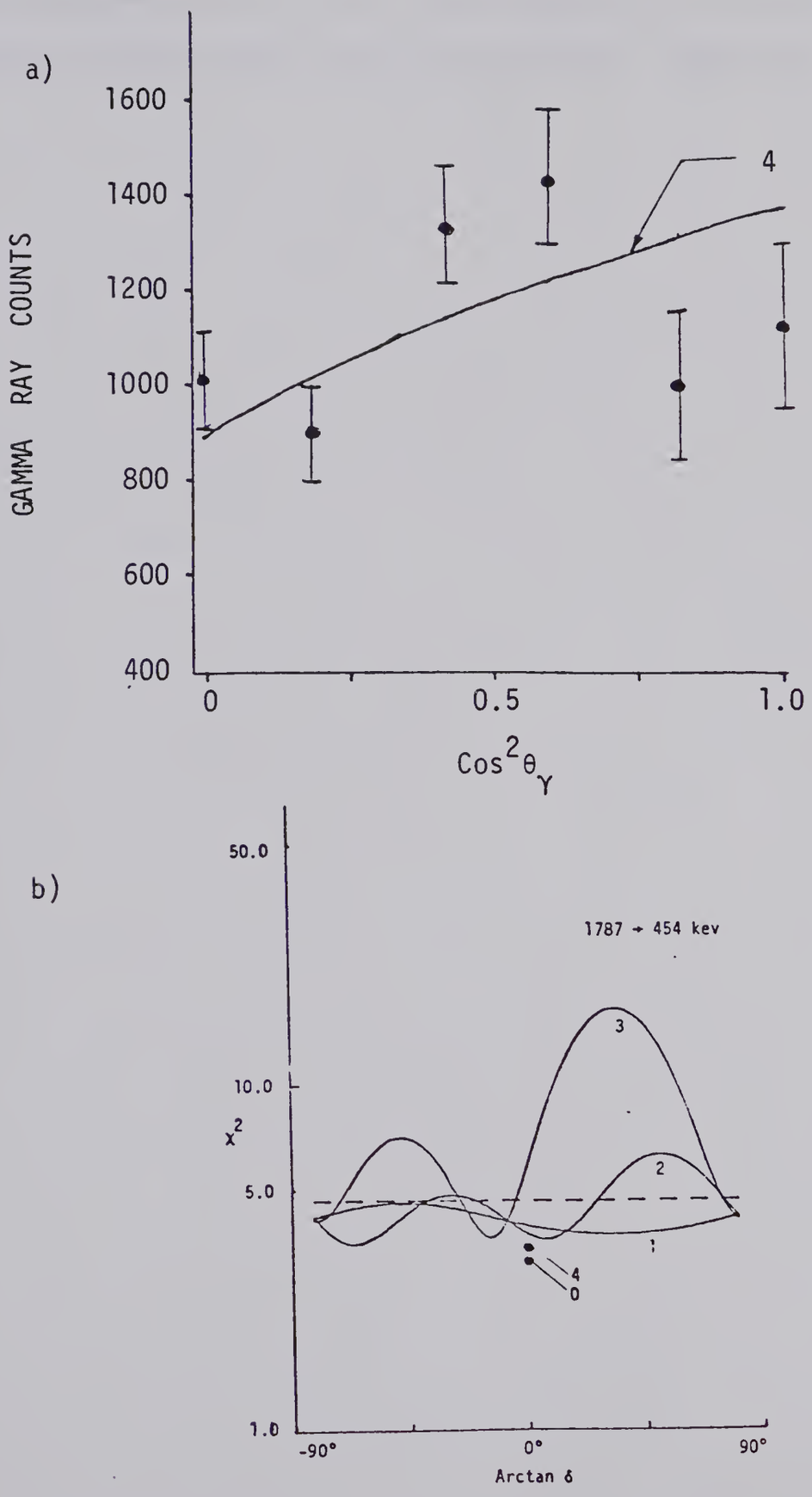

Figure 40. The 1787 keV level: a) angular distribution for the 1333 keV γ-ray, and b) χ^2 curves.

The data and results for the 1978 → 454 keV transition are shown in fig. 41. No information concerning the spin of the 1978 keV level has been deduced.

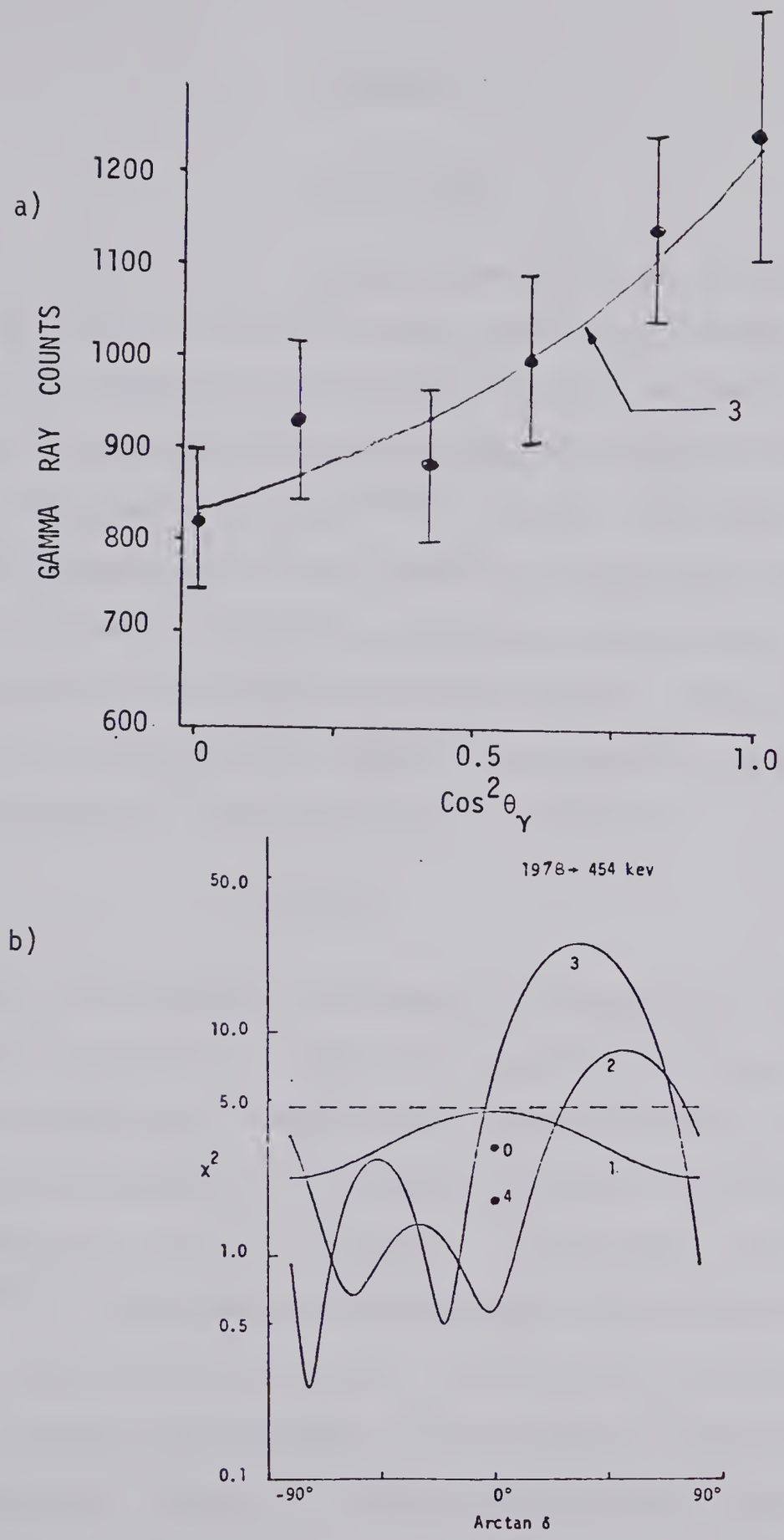

Figure 41. The 1978 keV level: a) angular distribution for the 1524 keV γ-ray, and b) χ^2 curves.

CHAPTER 5

DISCUSSION

As noted in the introduction, Scharff, Goldhaber and Weneser (Sc55) pointed out the vibrational nature of the first and second excited states of many even-even nuclei. It is my intention here to discuss the nature of the higher excited states of ^{114,116}Cd and ^{146}Nd with respect to the predictions of the harmonic vibrational model.*

Considering only the quadrupole and octupole modes of vibration, the spectrum of an harmonic vibrational nucleus is composed of highly degenerate and equally spaced levels. The levels can be denoted by

$$| \lambda,N,JM > \qquad (20)$$

where λ corresponds to the mode of vibration, N the number of phonons, J the total angular momentum, and M it's z-projection. States that are the result of the coupling of phonons of different modes of vibration are denoted by $| \lambda = \lambda_n + \lambda_m,N,JM >$. The levels of ^{114,116}Cd and ^{146}Nd that have been tentatively characterized as

---

* The harmonic vibrational model assumes a Hamiltonian of the form $H = T(\alpha_\lambda,\pi_\lambda) + V(\alpha_\lambda)$ where T and V are the kinetic and potential energies. Only second order terms of α_λ and π_λ are used. For a more detailed description of the vibrational model, see Appendix A.

vibrational states are summarized in Table VIII. The bases for these assignments are the observed energies and deduced spins and parities of the levels in question.

It should be noted that these three nuclei all possess a 0^+ ground state and a 2^+ first excited state. Also, the two phonon triplet occurs at an energy close to twice the energy of the one phonon 2^+ state. Taking an average of the triplet energy to that of the first excited state yields the ratios of 2.17 for ^{114}Cd, 2.41 for ^{116}Cd, and 2.29 for ^{146}Nd. The triplet is not degenerate and in ^{146}Nd two of the members of the triplet are not positively identified, while in the Cd isotopes, additional states occur in the neighborhood of the triplet. The fact that members of the triplet are missing may be due to experimental shortcomings. Two theories have been put forward to account for the additional states. Sakai and Tamura (Sa64a) postulated that these additional states may be thought of as single particle states while Eisenberg and Greiner (Ei70) suggested that they were members of a rotational band built on a deformed excited state.

The identification of the three phonon states is very sparse for ^{146}Nd. For ^{114,116}Cd, the situation is clearer, but the $|\ 2,3,6M >$ state is still not identified. In this work, a state with $J^\pi = 6^+$ would probably not be observed as the transmission coefficients are too

Table VIII. Vibration Levels of ^{114,116}Cd and ^{146}Nd.

$\|\lambda, N, JM\rangle$	^{114}Cd (keV)	^{116}Cd (keV)	^{146}Nd (keV)
$\|0,0,00\rangle$	0	0	0
$\|2,1,2M\rangle$	558	513	454
$\|2,2,0M\rangle$	1134	1283	-
$\|2,2,2M\rangle$	1210	1213	-
$\|2,2,4M\rangle$	1283	1220	1043
$\|2,3,00\rangle$	(1865)	(1930)	-
$\|2,3,2M\rangle$	1843	1644	(1471)
$\|2,3,3M\rangle$	1861	1917	-
$\|2,3,4M\rangle$	1733	-	-
$\|2,3,6M\rangle$	-	-	-
$\|3,1,3M\rangle$	(1959)	(1923)	1189
$\|2+3,2,JM\rangle$	-	-	(1377)
Other States	1306 (0^+)	1381	999
Observed in	1365 (2^+)	1953	1049
This Work	2049 (3^+)	2044	1777
	2246	2120	1787
			1978

small to sufficiently populate the level. The assignment of the 1865 keV and 1930 keV levels as the $|\ 2,3,0M\ >$ states in ^{114}Cd and ^{116}Cd respectively, is tentative only.

For ^{114}Cd and ^{116}Cd, the levels at 1959 keV and 1923 keV respectively were assigned as the octupole states. As the multiplet of $|\ 2+3,2,JM\ >$ states is therefore expected at approximately 2500 keV, they were not observed. This was not the case for ^{146}Nd as the octupole state was seen at 1189 keV. The state at 1377 keV, with a spin of 1, is therefore at approximately the energy (454 + 1189 keV) that one would expect a quadrupole-octupole state.

Nevertheless, the splitting of the two phonon states and also their deviation from the predicted energy spacing are indications of anharmonic terms (higher order terms in α_λ) in the Hamiltonian. The harmonic approximation seems to be a zero-order approximation for these nuclei.

In summary, the measurement of the angular distributions of γ-rays from the ^{114,116}Cd, ^{146}Nd $(n,n'\gamma)$ reactions enable spin-parity assignments to be made for these nuclei as tabulated in Tables V, VI, and VII.

In ^{114}Cd, the states at 1843 and 1861 keV have been assigned spin-parities of 2^+ and 3^+ respectively, in disagreement with previous work (6:74). The state at 2049 keV has been assigned a spin of 3^+. While the state at 1959 keV excitation cannot be rigorously limited to 3^-,

it has been shown that the previous assignment of 1 (6.74) is unlikely.

In ^{116}Cd, the spin of the state at 1644 keV, previously given a tentative assignment of (2,3) has been shown to be 2^+. A new spin assignment has been shown to be consistent with an assignment of 3^+.

In ^{146}Nd, the states at 1377 and 1471 have been assigned spin-parities of $1^\pm$ and 2^+ respectively. In previous work, these assignments were tentative only. A new level at 1787 keV has been proposed.

REFERENCES

(Bä66) A. Bäcklin, N.E. Holmberg, and G. Bäckström, Nucl. Phys. 80, (1966) 154.

(Be67) I. Ben Zvi, P. Gilad, G. Goldring, R. Erber and R. Kalish, Nucl. Phys. A96, (1962) 138.

(Bj58) F. Bjorklund and S. Fernbach, in *Proceedings of the Second United Nations International Conference on the Peaceful Use of Atomic Energy* (United Nations, Geneva, 1958), Vol. 14, p. 24.

(Bl52) J.M. Blatt and V.F. Weisskopf, *Theoretical Nuclear Physics* (J. Wiley and Sons, New York, 1952) p. 394.

(Bu67) G.A. Burginyon, J.S. Greenberg, D.A. Bromley and R.K. Kasten, Bull. Am. Phys. Soc. 12, No. 1, B64 (1967) 36.

(Bu75) T.W. Burrows, Nucl. Data Sheets 14, (1975) 413.

(Ca75) G.H. Carlson, W.L. Talbert Jr., and S. Raman, Nucl. Data Sheets 14, (1975) 247.

(Ch70) P.R. Christensen, G. Lovhoiden and J. Rasmussen, Nucl. Phys. A149, (1970) 302.

(Ch72) R. Chapman, W. McLatchie and J.E. Kitching, Nucl. Phys. A186, (1972) 603.

(Co65) J.A. Cookson and W. Darcey, Nucl. Phys. 62, (1965) 326.

(Cr56) L. Caranberg and J.S. Levin, Phys. Rev. 103, (1956) 343.

(Da76a) J.M. Davidson, H.R. Hooper, D.M. Sheppard and G.C. Neilson, Nucl. Instr. and Method, 134, (1976) 291.

(Da76b) J.M. Davidson, Internal Report No. 79, Nuclear Research Centre, University of Alberta (1976).

(De72) J.A. Deye, R.L. Robinson and J.L.C. Ford Jr., Nucl. Phys. A180, (1972) 449.

(De73) J.A. Deye, R.L. Robinson and J.L.C. Ford Jr., Nucl. Phys. A204, (1973) 307.

(Di72) J.K. Dickens, Nucl. Instr. and Method, 98, (1972) 451.

(Ei70) J.M. Eisenberg and W. Greiner, in *Nuclear Theory*, North Holland Publishing Company, 1970, Chap. 3.

(El71) S.A. Elbakr, I.J. van Heeden, W.K. Dawson, W.J. McDonald and G.C. Neilson, Nucl. Instr. and Method, 97, (1971) 283.

(En74) P.M. Endt and C. van der Leun, Atomic Data and Nucl. Data Tables 13, (1974) 67.

(Gi74) D.R. Gill, N. Ahmed, W.J. McDonald, G.C. Neilson, S.A. Elbakr, I.J. van Heerden and W.K. Dawson, Nucl. Phys. A229, (1974) 397.

(Go56) M.D. Goldberg, S.F. Mughabhab, S.N. Purohit, B.A. Magurno and V.M. May, Report BNL 325, Brookhaven National Laboratory (1956).

(Gr68) L.V. Groshev, B.A. Bartholomew, A.M. Demidov, A. Doveika, V.I. Palekhov, K.M. Eastwood, L.L. Sokolovskii and S. Monaro, Nucl. Data A5, (1968) 42.

(Gr71) P.W. Green, Internal Report No. 27, Nuclear Research Centre, University of Alberta (1971).

(Gr72) P.W. Green, G.C. Robertson and D.M. Sheppard, Nucl. Instr. and Method, 98, (1972) 45.

(Ha62) O. Hansen and O. Nathan, Nucl. Phys. 37, (1962) 177.

(Ha63) O. Hansen and O. Nathan, Nucl. Phys. 42, (1963) 197.

(Ki75) J.J. Kim, Nucl. Data Sheets 16, (1975) 107.

(Ko69) M. Koike, I. Nonaka, J. Kokame, H. Kamitsubo, Y. Awaya, T. Wada and H. Nakamura, Nucl. Phys. A125, (1969) 161.

(Mc65) F.K. McGowan, R.L. Robinson, P.H. Stelson and J.L.C. Ford Jr., Nucl. Phys. 66, (1965) 97.

(Mi69) W.T. Milner, F.K. McGowan, P.H. Stelson, R.L. Robinson and R.O. Sayer, Nucl. Phys. A129, (1969) 687.

(Ni65) K. Nishimura, K. Okano and S. Kikuchi, Nucl. Phys. 70, (1965) 421.

(Pe60) J.E. Perry Jr., E. Haddad, R.L. Henkel, G.A. Jarvis and R.K. Smith, referenced by J.D. Seagrave in *Nuclear Forces and the Few Nucleon Problem* (eds. T.C. Griffith and E.A. Dower, Pergamon Press, 1960) p. 583.

(Pe62) F. Perey and B. Buck, Nucl. Phys. 32, (1962) 353.

(Pi70) A.A. Pilt, D.M. Sheppard, W.C. Olsen, T.P.G. Carola and P.J. Twin, Nucl. Phys. A150, (1970) 439.

(Ro65) L. Rosen, J.G. Beery, A.S. Goldhaber and E.H. Aurebach, Ann. Phys. (N.Y.) 34, (1965) 96.

(Ro67) H.J. Rose and D.M. Brink, Rev. Mod. Phys. 39, (1967) 306.

(Ro75) D.W.O. Rogers, Nucl. Instr. and Method, 126, (1975) 253.

(Sa64a) M. Sakai and T. Tamura, Phys. Lett. 10, (1964) 323.

(Sa64b) M. Sakai, H. Ikegami, Y. Nakgima, K. Yagi, H. Ejiri, and G.R. Satchler, Phys. Lett. 8, (1964) 197.

(Sc55) G. Scharff, A.S. Goldhaber and J. Weneser, Phys. Rev. 121, (1955) 212.

(Sh76) H.S. Sherif and T.M. Newton, Internal. Report No. 83, Nuclear Research Centre, University of Alberta (1976).

(St67) E. Storm and H.I. Isrial, Report LA-3753, Los Alamos Scientific Laboratories (1967).

(St68) P.H. Stelson, J.L.C. Ford Jr., R.L. Robinson, C.Y. Wong and T. Tamura, Nucl. Phys. A119, (1968) 14.

(Wi64) D. Wilmore and P.E. Hodgson, Nucl. Phys. 55, (1964) 673.

(Vo73) E. Vogt in *Advances in Nuclear Physics*, Vol. 1 (eds. M. Baranger and E. Vogt, Plenum Press, New York, 1973).

APPENDIX A

THE HARMONIC VIBRATIONAL MODEL FOR EVEN-EVEN NUCLEUS

Many models have been formulated to explain the energy level schemes of nuclei. The hydro-dynamic, or liquid drop, model is a collective formalism that visualizes the dynamics of the nucleons in the nucleus as molecules undergiong motion in a liquid drop. In a liquid drop, the lowest possible energy is achieved when the drop has spherical symmetry. An excited state is said to exist when the surface of the drop undergoes deformation. The deformation of the surface can be expressed as

$$R(\theta,\phi,t) = R_o[1 + \sum_{\lambda\mu} \alpha_{\lambda\mu}(t)\ Y_\lambda^\mu(\theta,\phi)];\ |\mu| \leq \lambda \qquad \text{(A-1)}$$

where R_o is the undeformed radius and λ and μ refer to the mode of vibration. The lowest mode of surface deformation corresponds to the $\lambda = 2$ mode. For a nucleus, the largest mode of suface deformation corresponds to $\lambda \simeq A^{1/3}$. For higher modes, the vibrations of the nuclear surface are less than the internucleon separation, which implies a discontinuity of the nuclear surface. As this is unrealistic, all higher modes of vibration are excluded.

The total deformation energy of a harmonic charged liquid drop is (Ei70)

$$H = \frac{1}{2} \sum_{\lambda\mu} B_\lambda |\dot{\alpha}_{\lambda\mu}|^2 + \frac{1}{2} \sum_{\lambda\mu} C_\lambda\ |\alpha_{\lambda\mu}|^2 \qquad \text{(A-2)}$$

where B_λ represents the moment of inertia of the drop

with respect to changes in deformation and C_λ is the deformability coefficient which measures the resistance of the drop to deformation. Introducing the variable canonically conjugate to $\alpha_{\lambda\mu}$

$$\pi_{\lambda\mu} = B_\lambda \dot{\alpha}^*_{\lambda\mu}$$

gives $$H = \frac{1}{2} \sum_{\lambda\mu} \left[\frac{1}{B_\lambda} |\pi_{\lambda\mu}|^2 + C_\lambda |\alpha_{\lambda\mu}|^2 \right] \quad \text{(A-3)}$$

This is in the same form as the Hamiltonian for an harmonic oscillator. The solution is

$$E = \sum_\lambda h\omega_\lambda \left(\sum_\mu n_{\lambda\mu} + \frac{1}{2} \right) = \sum_\lambda h\omega_\lambda N_\lambda + \frac{1}{2} \sum_\lambda h\omega_\lambda (2\lambda + 1) \quad \text{(A-4)}$$

where $n_{\lambda\mu}$ is the number of oscillators in the $\lambda\mu$ mode,

N_λ is the number of oscillators in the λ mode;

$N_\lambda = \sum_\mu n_{\lambda\mu}$ and

ω_λ is the characteristic frequency of vibration for the λ mode. The last term in Eq. (A-4) is taken as the zero point energy. The characteristic frequency ω_λ is given by

$$\omega_\lambda = C_{\lambda/B_\lambda} = \left\{ \lambda(\lambda-1) \left[(\lambda+2) - \frac{10\gamma}{2\lambda+1} \frac{4\pi\alpha}{3MA} \right]^{1/3} \right\} \quad \text{(A-5)}$$

(BI52)

where γ is the ratio between the Coulomb and surface tension energies. It is given by $\gamma \approx 0.0474\ Z^2/A$.

α is the surface tension coefficient,

M is the mass of a single nucleon,

and A is the atomic number.

By neglecting the Coulomb energy term, one can obtain a rough estimate of the ratios of the characteristic frequencies. For example, the ratio of the frequency of the octupole ($\lambda = 3$) mode to that of the quadrupole ($\lambda = 2$) mode is approximately 2. As $\omega_{4/\omega_3} \simeq 2.4$, the $\lambda = 4$ mode can be ignored when only the low-lying states are of interest.

A $\lambda\mu$ mode phonon is a boson with a spin of λ, a z-component of angular momentum of μh, and an intrinsic parity of $(-1)^{\lambda}$. When there are two or more phonons present, the individual angular momenta can be coupled to form eigenstates of J^2 and J_z. For example, two $\lambda = 2$ phonons, corresponding to the $N_2 = 2$ state, form a triplet of states with spin-parities of 0^+, 2^+, and 4^+. Considering only the quadrupole and octupole modes of vibration, a highly degenerate, equally spaced level structure is predicted (see fig. 42). Small corrections to the energy levels are thought to be due to the fraction of the nuclear matter involved in the surface deformations undergoing rotation.

Since this formulism deals with a spherical liquid drop, one would expect it to be valid only for nuclei that have a spherically symmetric ground state. These nuclei are usually found where N or Z is close to a magic number. Because of this, the level scheme should exhibit marked shell effects. That is, there should be

Figure 42.

The level scheme predicted by the harmonic vibrational model. The degeneracy of the levels has been removed to facilitate identification. The states are denoted by

$|\lambda, N, JM>$ where

λ = mode of vibration
N = the number of phonons
J = the total angular momentum
M = it's Z projection

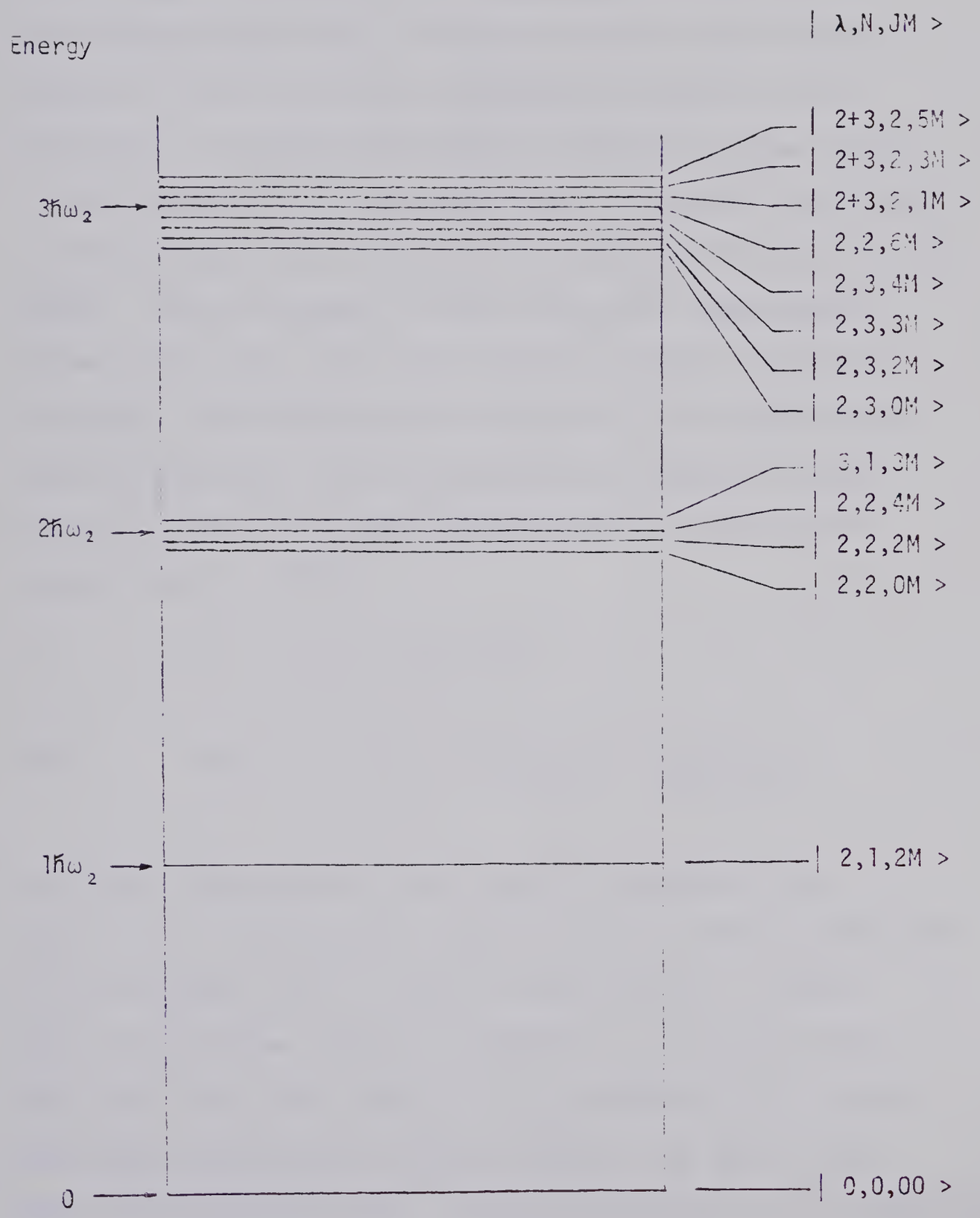
Energy
| λ,N,JM >
3ħω2
2ħω2
1ħω2
0
| 2+3,2,5M >
| 2+3,2,3M >
| 2+3,2,1M >
| 2,2,6M >
| 2,3,4M >
| 2,3,3M >
| 2,3,2M >
| 2,3,0M >
| 3,1,3M >
| 2,2,4M >
| 2,2,2M >
| 2,2,0M >
| 2,1,2M >
| 0,0,00 >

a mingling of the collective excited states of the vibrational model with the intrinsic shell model states.

In the liquid drop model, the parameters B_λ and C_λ are evaluated classically by assuming an irrotational and incompressible drop. The particles in the nucleus, however do not form such a homogeneous system as the particles in closed shells behave differently than those in unfilled shells. The vibrational energy of the nucleus is mainly due to the motion of the nucleons in the unfilled shells. This is readily evident when the experimental values of B_2 and C_2 are obtained for a large assortment of nuclei. The values can be obtained from a consideration of the energy and the reduced E2 transition probability B (E2; 0 → 2) for the excitation of the first excited state (Ei70).

$$\omega_2 = (C_2/B_2)^{1/2}$$

and
$$B(E2;\ 0 \rightarrow 2) = (3ZeR^2_{o/4\pi})^2 \frac{5h}{2(B_2C_2)^{1/2}} \qquad \text{(A-6)}$$

The values obtained for the inertial parameters B_2 obtained are consistently higher than the values predicted by irrotational flow. While in the region of closed shells the surface tension parameter C_2 is much larger than the liquid drop value, the C_2 parameters for nuclei with many particles in unfilled shells are much lower than the predicted values. This corresponds to the approach

to instability of the spherical shape.

When the instability of the nucleus is such that it takes only a small amount of energy to break apart the nucleus, induced fission is expected. The vibrational model gives the limit of stability against fission. In equation A-5, it can easily be seen that the frequency for vibration because imaginary when the ratio between the Coulomb energy and the surface energy approaches a critical value γ_c. When this occurs, the negative Coulomb energy exceeds the surface energy and the nucleus is no longer stable against surface deformation. As quadrupole is the lowest mode of vibration, the limit for stability predicted by the vibrational model is

$$Z^2/_A = 42.2 \qquad \text{(A-7)}$$

Nuclei approaching this limit have a small deformation frequency ω_2. Therefore the amplitude of oscillation becomes large, resulting in the breaking up of the nucleus.

Other fundamental characteristics of vibrational excitations are an enhanced E2 transition from the first excited state to the ground state as compared to single particle estimates and a small static electric quadrupole moment. The vibrational model also imposes certain restrictions on the type of γ decay that can occur. As the second 2^+ excited state results from the coupling of two $\lambda = 2$ phonons, the decay of this level to the ground

state is forbidden. The decay can proceed only *via* a cascade to the first excited state. In this cascade, M1 radiation, which is preferred by single particle motion, is strictly forbidden; the transition taking place only through E2 radiation.